ELSEVIER
Available online at www.sciencedirect.com
SCIENCE DIRECT®
Coordination Chemistry Reviews 248 (2004) 493–532
COORDINATION
CHEMISTRY REVIEWS
www.elsevier.com/locate/ccr

Review

Novel group 14 nitrides

Edwin Kroke*, Marcus Schwarz

FB Chemie, Chemische Materialwissenschaft, Universität Konstanz, 78457 Konstanz, Germany

Contents

1. Introduction 494
2. Binary C/N-compounds—carbon nitrides 495
  2.1. Motivation: properties and applications of C/N/(H) compounds 495
  2.2. Molecular CN_x compounds 496
  2.3. “Traditional" CN_x polymers 497
  2.4. Carbon(IV) nitrides C_3N_4 and related materials 497
    2.4.1. Historical work (till 1990) 497
    2.4.2. Theoretical work concerning C_3N_4 phases 499
    2.4.3. Postulated C_3N_4-phases 500
      2.4.3.1. α-C_3N_4 ($P3_1c$) 500
      2.4.3.2. β-C_3N_4 ($P6_3/m$) 500
      2.4.3.3. “Pseudo-cubic” or “(defect) zincblende”-C_3N_4 ($P\bar{4}2m$) 502
      2.4.3.4. “Cubic” or “willemite-II” C_3N_4 ($I\bar{4}3d$) according to Teter and Hemely 502
      2.4.3.5. Spinel-C_3N_4 according to Mo et al. (Fd3m) 503
      2.4.3.6. λ-C_3N_4 according to Kroll and Hoffmann ($P4_322$) 503
      2.4.3.7. “α-$C(NCN)_2$” according to Greiner, Kroll and Hoffmann ($P4_12_12$) 503
      2.4.3.8. “β-$C(NCN)_2$” according to Greiner, Kroll and Hoffmann ($I\bar{4}2d$) 503
      2.4.3.9. “Graphitic” C_3N_4 according to Teter and Hemley ($P\bar{6}m2$) 503
      2.4.3.10. “Graphitic” C_3N_4 according to Liu and Wentzkovitch (R3m) 504
      2.4.3.11. “Graphitic-orthorhombic” C_3N_4 according to Alves et al. (P2mm) 504
      2.4.3.12. “Polydi(triazine)tri(carbodiimide)-structures” according to Greiner 504
      2.4.3.13. “Heptazine-based, graphitic” C_3N_4-phases 505
      2.4.3.14. Further “carbodiimide- and cyanamide-based” C_3N_4-phases 505
      2.4.3.15. s-Triazine based 3D-C3N4-phases “3D-srs” and “3D-ths” according to Vodak et al. 505
      2.4.3.16. Tri-s-triazine-3D-C_3N_4-phases “3D-srs-$[(C_6N_7)(N)]_n$” and “3D-ths-$[(C_6N_7)(N)]_n$” 505
      2.4.3.17. Amorphous C_3N_4-phases 505
      2.4.3.18. Summary: comparison of postulated C_3N_4 phases 505
    2.4.4. Thin films by vapour phase deposition 506
    2.4.5. Bulk synthesis approaches for CN_x solids (since 1990) 507
  2.5. Summary and outlook 511
3. Silicon nitrides 512
  3.1. α- and β-Si_3N_4 512
  3.2. Spinel-Si_3N_4 513
    3.2.1. Discovery: DAC-syntheses 513
    3.2.2. Nomenclature 513
    3.2.3. Structure 513
    3.2.4. MAP-syntheses 514
    3.2.5. Shock synthesis 515
    3.2.6. Properties of spinel silicon nitride 516
      3.2.6.1. General properties 516
      3.2.6.2. Hardness 516
      3.2.6.3. Fracture toughness 518
      3.2.6.4. Elastic properties 518
      3.2.6.5. Thermal stability 519

---

*Corresponding author. Tel.: +49-7531-884415; fax: +49-7531-884406.
E-mail address: edwin.kroke@uni-konstanz.de (E. Kroke).

0010-8545/$ – see front matter © 2004 Published by Elsevier B.V.
doi:10.1016/j.ccr.2004.02.001

3.2.6.6. Coefficient of thermal expansion 519
3.2.6.7. Further thermal and thermodynamic properties 520
3.2.6.8. Vibrational spectroscopic properties 520
3.2.6.9. NMR spectroscopic properties 520
3.2.6.10. Electronic properties 520
3.3. Amorphous SiN_x 521
3.4. Post-spinel nitrides 521
3.5. Silicon sub- and hypernitrides 521
4. Novel germanium nitrides 522
5. Tin nitrides 522
6. Lead nitrides 522
7. Theoretical work on spinel nitrides 523
8. Multinary phases 523
8.1. Si/C/N 523
8.2. Oxide nitrides and sialons 524
9. Summary and conclusions 524
References 525

Abstract

In recent years, a lot of work has been focused on the synthesis of novel carbon nitrides, especially crystalline C_3N_4 phases. Numerous attempts to synthesise the theoretically predicted solids have been published. This review summarises the theoretical work as well as the attempts to prepare carbon(IV) nitrides by chemical and physical vapour deposition, and in particular on the concepts and results of bulk synthesis routes. Although very interesting materials have been obtained, a comprehensive characterisation of a crystalline C_3N_4 phase is still missing. In 1999, a novel class of nitrides, which posses the spinel structure, has been discovered. The synthesis and properties of the high pressure phases γ-M_3N_4 with M = Si, Ge and the first tin nitride γ-Sn_3N_4 are reviewed. Related oxide nitride spinel compounds, other ternary phases such as Si/C/N as well as subnitrides, sialons and amorphous phases are mentioned briefly.

Keywords: Binary nitrides; C_3N_4; Si_3N_4; Synthesis; Properties; Structures

1. Introduction

For most elements of the periodic table, significantly fewer nitrogen compounds as compared to oxygen compounds are known. This also holds true for the fourth main group, i.e. group 14 (Table 1). Nevertheless, among the nitrides of group 14 elements C, Si, Ge, Sn and Pb there are some very interesting materials, and recently exciting discoveries have been made. This review article is focused on these new developments, which include the prediction and preparation of CN_x compounds as well as the discovery of spinel nitrides. The former represents a group of materials, including postulated crystalline phases, which are expected to possess diamond-like mechanical, optical and electrical properties as well as a number of non-stoichiometric amorphous solids which are most frequently synthesised by chemical or physical vapour deposition (CVD and PVD) techniques. This field of research was initiated and propelled by speculations that saturated (sp^3-hybridised) carbon(IV) nitride phases should be as hard or even harder than diamond, causing excitement in the scientific community.

Table 1
Comparison of the number of results of data base researches for binary oxygen compounds with the number of binary nitrogen compounds of group 14 elements

	CAS-registry file [427]					ICSD-database [428]				
	C	Si	Ge	Sn	Pb	C	Si	Ge	Sn	Pb
Oxygen	3582	15832	114	103	78	14	323	25	20	50
Nitrogen	1601	441	28	4	9	13	45	3	1	5

Accordingly, during the 1990s the number of publications—especially concerning CVD and PVD synthetic approaches to C_3N_4—has increased exponentially. Due to the fact that several review articles [1–4] have been published discussing the major results, this review mainly deals with *chemical* and *bulk routes* to CN_x-phases, which so far have not been treated to the same extent. High pressure/high temperature (HP/HT) attempts to generate a crystalline C_3N_4 phase led to the discovery of a novel high-density Si_3N_4 phase. Silicon nitride is without doubt, the most important and most investigated material of the binary nitride compounds of group 14 elements [5,6]. The synthesis, structure, properties of the α- and β-modifications have been investigated in detail. Si_3N_4-based ceramics are used in various applications, e.g. as cutting tools, for bearings and other extremely demanding structural components or as an amorphous film material in electronic devices. Their development still continues. Due to this background, the discovery of a novel high pressure form of Si_3N_4 with a 25% higher density was surprising. It initiated the synthesis of spinel germanium nitride (γ-Ge_3N_4) as well as the first spinels within the system Si/Al/O/N (*spinel-sialons*). These spinel sialons may be the first members of a new class of high pressure-derived nitride oxide compounds and have the potential to become relevant for applications as functional and structural ceramics.

2. Binary C/N-compounds—carbon nitrides

In principle, all binary carbon–nitrogen compounds can be considered as carbon nitrides. There are on the one hand molecular carbon nitrides similar to the well known carbon oxides CO_2, CO and other C_xO_y species. On the other hand, solid state C/N-phases have been described, which are usually not very well characterised (see Sections 2.3 and 2.4). Carbon(IV) nitrides, especially crystalline phases, have been predicted to be stable. They are comprised of an alternating arrangement of carbon and nitrogen atoms, i.e. they do not contain any C–C and/or N–N bonds (with very few exceptions). Why could these compounds be interesting? And what is known about the classes of molecular and polymeric C/N compounds? These questions are addressed in the following sections.

2.1. Motivation: properties and applications of C/N/(H) compounds

Many nitrogen-rich organic compounds are characterised by very good oxidative as well as thermal stability. For example, the molecular compound melamine $C_3N_6H_6$. Melamine resins and related materials are known to be of low flammability. Therefore, they are used in fire protection applications. Reasons for this property are the relatively high bond dissociation energy of C–N-single and multiple bonds, as well as the relatively high electronegativity of nitrogen atoms, since it causes a partial oxidation of the carbon atoms. Oxidation reactions are therefore less likely for nitrogen rich C/N/(H) compounds compared to other organic compounds such as hydrocarbons.

The C/N materials described in the literature show in part highly interesting chemical, mechanical, tribological and other functional properties, independent of the preparative procedure, the chemical structure and the composition. CN_x-coatings, for example, synthesised by laser-ablation exhibited thermoluminescence with two maxima at 150 and 290 °C [7]. The authors suggest use of this material for applications in thermoluminescence dosimeters.

A PVD technique (ion beam sputtering) was also used to deposite CN_x-coatings, which were successfully applied as functional layers in ITO/a-CN_x/Al thin film-Schottky-solar cells [8]. A comparison of amorphous CN_x-coatings, which contained 23% nitrogen, with amorphous carbon indicated that field emission of electrons starts at lower electric field strength and yields higher current densities [9].

Recently, nitrogen-rich carbon nitride coatings were utilised as functional layers in humidity sensors and microelectromechanical (MEM) gas detectors [10]. Also, an ion-sensitive field effect transistor has been patented with a gate consisting of a carbon nitride layer [11].

Examination of the optical and electrical properties of C/N-coatings indicated that these materials can be completely transparent, which corresponds well with the theoretically predicted large band gap [12,13]. Furthermore, a high electrical resistance and a low dielectric constant were measured for amorphous C/N-films [14].

Many carbon nitride coatings are characterised by good corrosion resistance, low coefficient of friction and excellent resistance to wear [15,16]. The mechanical and tribological properties, including the hardness, were determined as a function of several different parameters such as elemental composition, film thickness and deposition conditions (see Section 2.4.4). In some studies, very high hardness values of >40 GPa were measured [17–21]. It was reported, that the H/E-ratio (hardness/elastic modulus), which is an indicator for the wear resistance, exceeds the value of other tribologically relevant materials. In some cases H/E was found to be 0.18, while sapphire, tungsten, quartz and diamond show $H/E = 0.06$, 0.08, 0.12 and 0.1, respectively [22]. This observation may be explained by the formation of partially graphitic C/N-networks, which contain fullerene- or nanotube-like structures, that are known to sustain extreme strains via buckling of the graphitic layers without any plastic deformation [23]. As a matter of fact, several authors have described the successful deposition of CN_x-nanotubes and CN_x-fibres [24–26].

CN_x-polymers with low nitrogen content ($x < 0.5$), which were deposited by PVD and CVD techniques, showed properties similar to DLC-coatings. IBM and possibly other companies as well used C/N-coatings on computer hard discs due to the decreased surface roughness as compared to pure carbon films [27].

For many researchers, interest in C/N materials has been attracted by predictions on the properties of saturated, i.e. sp^3-hybridized, crystalline C_3N_4-phases. Such carbon nitrides were postulated by Sung and Sung, speculating that they could be harder than diamond ([28], see Section 2.4.2). This initiated further theoretical as well as experimental activities. The results have attracted attention [29–33], and an intense development is ongoing.

High pressure techniques have been proposed to transform suitable precursor compounds with high nitrogen content into a crystalline C_3N_4-phase [34,35,103]. However, in contrast to this *bulk-approach*, most of the experimental efforts (see below) as well as the numerous patent applications [11,36,37] are concerned with the preparation of thin C_3N_4-films by different vapour phase deposition routes (see Section 2.4.4). Although there have been many indications for the existence of crystalline carbon nitride phases, no pure single phase has been obtained [1–4]. This gives further motivation to search for a macroscopic bulk synthesis route in order to comprehensively characterise such a material, e.g. by a single crystal X-ray structure analysis. One way to reach this goal is to prepare a molecular or polymeric precursor with C_3N_4-stoichiometry. A successive high pressure transformation into a hard crystalline carbon nitride appears to be promising [34,35,38,103].

2.2. Molecular CN_x compounds

Relatively few binary molecular and polymeric (see Section 2.3) compounds are known that consist solely of carbon and nitrogen. This is demonstrated by a Chemical Abstracts Registry database search: 1601 hits are found for single component CN_x-compounds. In contrast, 3582 single component binary CO_x-compounds have been described, and an analogous search for CF_x-species gives even more hits.

The reason for this finding is probably the stability of the respective molecule-terminating groups: For oxygen–carbon—as well as for fluorine-carbon-compounds the C=O- and C–F-functions provide a stable saturation of terminal valences of the carbon atoms. CO_x-compounds may also be terminated by cyclic oxo- or peroxo-groups.

For C/N compounds there are many different functional groups known, e.g. cyano- (NC–), isocyano- (:CN–), azido- (N_3–) and diazo-(N=N=)-units, but these groups are generally more labile and reactive compared to carbonyl and C–F-groups. The most stable terminating C/N-function is certainly the cyano group. It may form oligomers or polymers due to the relatively reactive and polar C–N-triple bond.

Fig. 1 displays a small number of typical binary molecular carbon nitrides. Some of these species like the gaseous cyanogen NC–CN [39], or tetracyanoethylene, $(NC)_2C=C(CN)_2$ [40], have been examined in detail with respect to their chemical and physical properties.

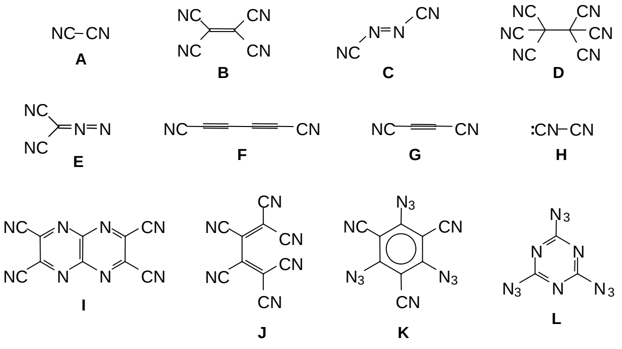

Fig. 1. Exemplary selection of some binary molecular CN_x-compounds. While cyanogen **A** and tetracyanoethylene (TCNE) **B** belong to the species that have been examined in detail, most of the other molecules have been described or mentioned in just one or very few publications. Dicyanodiazomethane **E** and 1,3,5-triazido-2,4,6-tricyanobenzene **K** exhibit $(C_3N_4)_n$ stoichiometry, but due to their structure and the formal oxidation number of the carbon atoms they cannot be described as carbon(IV) nitrides. Besides, the molecular carbon(IV) nitrides tricyanoamine and dicyanocarbodiimide have been mentioned in the literature, but are most (see text).

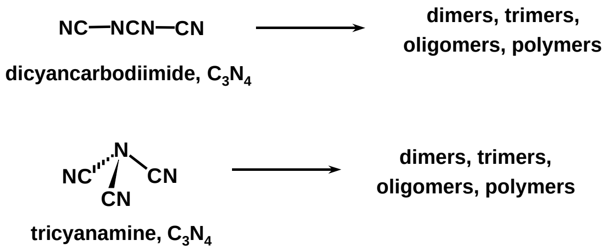

Fig. 2. Tricyanamide $N(CN)_3$ and dicyancarbodiimide NC–NCN–CN are the smallest molecular carbon(IV) nitrides. None of these isomers were experimentally shown to be isolable or stable. Formally, by a hypothetical oligomerisation via the C–N-triple and/or the C–N-double bond, numerous $(C_3N_4)_n$-species may be postulated. These structures contain alternating C- and N-atoms and can be considered as carbon(IV) nitrides.

By far the largest group of binary C/N compounds is the class of percyano compounds. Syntheses, structures and important chemical characteristics of binary pernitriles were summarised and discussed in several review articles (see e.g. [41]).

Most of the percyano-compounds like molecules B, D, F, G, I and J in Fig. 1 contain C–C bonds. They could be considered as subnitrides with oxidation numbers for the carbon atoms of <4.

The nitrogen-to-carbon ratio has a wide range. Stable, binary molecular C/N-compounds with the highest N-content are cyanoazide, CN_4, and its trimer tri-azido-s-triazine, C_3N_{12} (Fig. 1, L). Nitrogen-containing fullerenes like $N@C_{60}$ or $N@C_{70}$ are most likely the molecular species with the highest C:N-ratio [42].

A carbon(IV) nitride, C_3N_4, exhibits a nitrogen content of 40 wt.%. Dicyandiazomethane E and 1,3,5-triazido-2,4,6-tricyanobenzene K, which have been prepared and described in the literature, posses the carbon(IV) nitride $(C_3N_4)_n$-stoichiometry. However, due to the C–C bonds these molecules cannot be described as carbon(IV) nitrides.

The smallest “true” molecular carbon(IV) nitrides are tricyanamide and dicyanocarbodiimide (Fig. 2). Both molecules have been examined theoretically using ab initio calculations [43–45].

Interestingly, dicyanocarbodiimide was predicted to be the most stable isomer, because of its extended π-system. It is followed by the trigonal planar form of tricyanamide. A pyramidal conformation of tricyanamide is energetically disfavoured by 5.13 kcal/mol according to these calculations [44].

Tricyanamide was also mentioned in an earlier experimental study. It was described as a reactive intermediate [46]. A synthesis for this molecule is not known. $N(CN)_3$ is a very exothermic compound, i.e. thermodynamically stable, at least with respect to the elements, according to the calculations [43].

Very recently, dicyanocarbodiimide was photolytically generated from triazido-s-triazine at 20 K in a nitrogen matrix and identified using IR and UV-Vis spectroscopy [47].

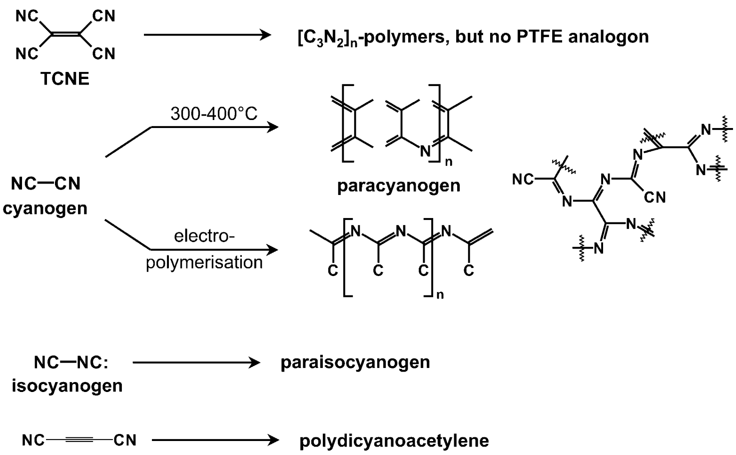

Fig. 3. Compilation of the most important hydrogen-free CN_x-polymers that have been synthesised in bulk. Further CN_x-materials were fabricated by CVD and PVD techniques (see also Section 2.4.4).

2.3. “Traditional” CN_x polymers

Very few hydrogen- and heteroatom-free CN_x-polymers that have been synthesised in bulk amounts have been described in literature (Fig. 3) [48]. Polymerisation of TCNE via the C=C bonds in analogy to the polymerisation of other ethylene derivatives like tetrafluorethylene forming PTFE has been attempted several times. However, the polymeric products were always formed by reactions of the cyano groups. They are usually characterised by a high degree of crosslinking rather than forming chains. No commercially used bulk TCNE polymers are known [48].

Cyanogen can be polymerised by different techniques furnishing products with different structures [48]. Thermally induced reactions at 300–400 °C provide a more or less ladder-like product which is generally called paracyanogen. Electropolymerisation gives polymers, where only one cyano group per cyanogen molecule reacts to form a chain-like structure. However, none of these materials has been fully characterised and it is likely that less regular and disordered network structures are also formed [39]. The result of a theoretical study is interesting as it suggests that paracyanogen is one of very few polymers exhibiting intrinsic metallic conductivity [49,50]. Isocyanogen and dicyanoacetylene were also transformed into polymers, but there is very little known about the structures and properties of these materials [41,48,51].

In addition to the pure C/N polymers there have been several reports about related materials with very small hydrogen content. Some authors incorrectly denote these structures as carbon nitrides (see below). An important example is melon, with an ideal composition $C_6N_9H_3$. Due to the low molecular mass of hydrogen atoms, the hydrogen weight fraction in melon is only 1.5%. Furthermore, there are a number of non-stoichiometric CN_x-polymers with various graphitic, amorphous or (partially) crystalline structures, which have been prepared by CVD, PVD and in some cases via bulk synthesis routes. These materials will be described briefly in the following sections.

2.4. Carbon(IV) nitrides C_3N_4 and related materials

2.4.1. Historical work (till 1990)

First attempts to prepare $(C_3N_4)_n$ were reported as early as in the 1830s [52]. It was not possible at that time to characterise the structure of these materials. In 1922, Franklin described the formation of an amorphous C/N material by thermolysis of mercury(II) thiocyanate [53]. The composition of the product was very close to a carbon(IV) nitride, C_3N_4, according to the elemental analysis results. This report is presumably the basis for the description of “a normal carbon(IV) nitride”, which is found in some inorganic chemistry textbooks from the 1950s [54]. However, no information about the chemical structure was given.

The C/N/H compounds melam, melem and melon, also described in the above mentioned publication, can be synthesised by calcination of melamine and several other compounds such as cyanamide or cyanoguanidine. Again these compounds were synthesised and studied almost a century earlier by Liebig as well as other authors [52,55,56]. The characterisation was very difficult due to the insolubility or very low solubility of melam, melem and melon in water and organic solvents. In the early literature possible formation mechanisms for C_3N_4 were discussed. In analogy to the (formal) dehydration of tertahydroxymethane via carbonic acid to carbon dioxide

$$C(OH)_4 \rightarrow H_2CO_3 \rightarrow CO_2$$

a similar, but more complicated reaction sequence may be suggested for carbon(IV) nitride starting from tetraamminomethane (Fig. 4). Due to the lack of knowledge about the structures of melam, melem, and melon, triazine-based cyclic and linear motives were discussed, which later turned out to be wrong [53,56]. Pauling and Sturdivant were the first to suggest, in a theoretical paper, that the heptazine

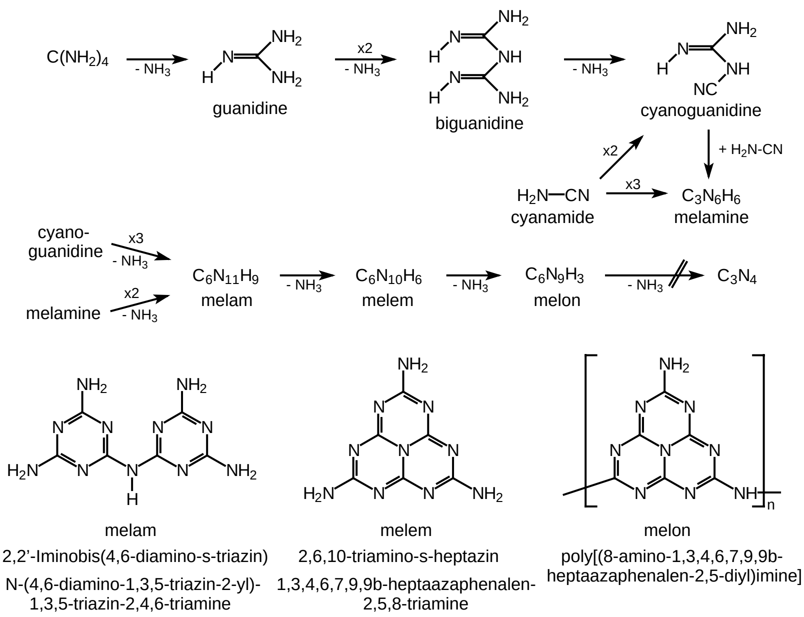

Fig. 4. Formal description of the formation of melam, melem and melon by oligomerisation and condensation starting from C/N/H-precursors, and the hypothetical generation of C_3N_4 from melon via separation of NH_3. The lower section displays the structures of melam, melem and melon and the corresponding systematic names according to the CAS-registry database.

unit (tri-s-triazine, C_6N_7) is the basic structural motif for melem and its derivatives [57]. In the following years, the first molecular heptazine-derivatives were synthesised and characterised [58]. Nevertheless, the pyrolysis of melamine was again examined by different authors. The structure of the products was a matter of controversial discussion [59–61]. None of the authors succeeded in transforming melon into C_3N_4 by separation of ammonia. It was found that melon decomposes into volatile C/N/H-fragments above 500 °C.

From the mid 1950s until the end of the 1970s, Finkel'shtein et al. performed extensive investigations on the synthesis and properties of hepatzin derivatives [60,62–65]. Based on a thorough analysis of the vibrational spectra and determination of important chemical properties, the theoretical postulate by Pauling and Sturdivant was confirmed experimentally. Up to date there are only very few heptazine compounds which have been analysed in detail using NMR, UV-Vis and MS or X-ray structural analyses. One of the exceptions is the hydrogen-substituted parent molecule tri-s-triazine $C_6N_7H_3$. This compound was synthesised via a three step route starting from an amino-s-triazine derivative. Tri-s-triazine was carefully examined with respect to physical and chemical properties [66–69].

Several papers of Russian authors describe the formation of carbon(IV) nitrides by thermal decomposition of thiocyanates and related sulphur-containing organic as well as inorganic compounds. According to a report from 1972 lanthanum(II) thiocyanate decomposes at 400 °C forming C_3N_4, La_2S_3 and CS_2 [70]. In the mid 1980s, studies on the pyrolysis of the sulphuric acid adduct of semicarbazide, $[(H_2N–CO–NHNH_2)_2\cdot H_2SO_4]$ were published. It was claimed that at 295 °C carbon(IV) nitride is formed in addition to other products [71], although others had previously described the thermolysis of thiosemicarbazide, $H_2N–CS–NHNH_2$, and certain derivatives of this substance. It was found that one mole thiosemicarbazide reacts at 400 °C quantitatively to form 1 mol hydrazine, 0.5 mol H_2S, 0.25 mol CS_2 and 0.25 mol C_3N_4 [72]:

$$4CH_5N_3S \rightarrow 4N_2H_4 + 2H_2S + CS_2 + C_3N_4$$

Since all products of this reaction are volatile except for the carbon nitride, pure C_3N_4 should be obtained. Later, this reaction was re-investigated [73]. It was found that significant amounts of sulphur are formed and that the reaction at 350 °C should be described as follows:

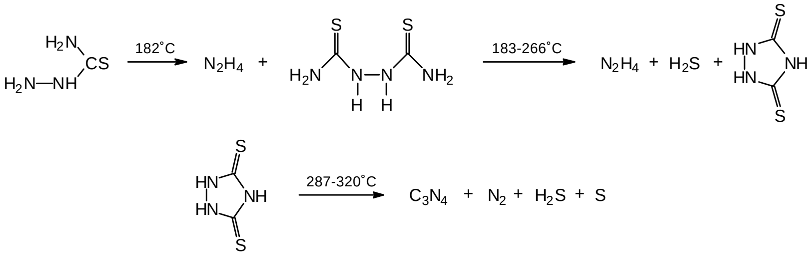

It is very likely that a pure carbon nitride phase is not produced by this pyrolysis and the product should be described as a multinary phase or a mixture of several phases, containing hydrogen and sulphur as well as carbon and nitrogen.

Synthesis of cyanoisocyanate (NC-NCO) from AgOCN and Cl-CN gave a polymeric substance, which formed carbon dioxide upon heating to 140–240 °C [46]:

$$2\text{NC-NCO} \rightarrow CO_2 + C_3N_4$$

The non-volatile polymeric residue should possess the composition of a carbon(IV) nitride, since other volatile products such as O_2, N_2, CO or C_2N_2 were not detected. However, these results have not been confirmed.

Attempts to prepare carbon nitrides by vapour phase deposition techniques were published (see Section 2.4.4) in the 1970s and 1980s, and theoretical work at the end of the 1980s caused an exponential increase of the number of publications on vapour phase deposition studies on carbon nitrides. A chemical abstracts search for the period from 2000 to 2002 gives approximately 600 hits for “carbon nitride” and “C_3N_4”.

2.4.2. *Theoretical work concerning C_3N_4 phases*

As already mentioned in Section 2.1, in 1984, Sung and Sung, by their own account, postulated that a carbon(IV)nitride, with a structure analogous to α- or β-Si_3N_4 (α-C_3N_4, β-C_3N_4), could be harder than diamond [28]. The basis of this speculation was provided by a well known relationship between the bond length d and the modulus of compression (or bulk-modulus) B_0 of a solid: As B_0 is given by the second volume-derivative of the energy $\partial^2U/\partial V^2$ and the volume may be expressed by the third power of the bond length ($V \sim d^3$), B_0 should scale as d^{-5}. This means that the smaller the bond length, the more *incompressible* the material. Typical bond lengths of 1.47 Å for a C–N single bond were known from organic, nitrogen-containing molecules, while the C–C distance in diamond is 1.54 Å. The theoretician M.L. Cohen developed a quantitative model in order to estimate the hardness of the postulated phase and in 1985 calculated a bulk modulus of 461–483 GPa for a “tetrahedral compound ... formed between C and N”, which “is significantly larger than diamond” [74]. This calculation was based on a semiempirical approach, and the effective correlation between bulk modulus and bond length was found to be $B_0 \sim d^{-3.5}$. In 1989/1990, Liu and Cohen specified their prediction to the discrete crystal structure of β-C_3N_4 and used pseudopotential calculations to determine the cohesive properties [75,76]. The result was $B_0 = 427$ GPa, and by comparison with the value for β-Si_3N_4, obtained by the same calculational method and experimental results, the authors judged that this might be slightly overestimated. It should be stressed here, that in none of the publications of Cohen and his co-workers, the terms “harder than diamond” appear [74–76]. The only statement that was made is that these materials are likely to be extremely incompressible, i.e. possess a bulk modulus “comparable to” or larger than that of diamond, and that they could be metastable at ambient conditions. Nevertheless, it appears that many researchers had already been infected by the “*harder-than-diamond fever*” which led to a large number of experimental attempts to prepare the postulated phase, but also gave motivation for further theoretical studies on carbon(IV) nitrides (see below). In a review article in 1998, Teter reminded the science community that the *shear modulus* G_0 rather than compressibility κ (=1/B_0) is a good predictor for hardness [77]. A fact that should not be surprising, since both, solids and fluids, have compressibilities, but the presence of a finite (and static) shear modulus is exactly the property that makes the difference between the solid and the liquid state. Teter backed his statement by a systematic comparison of experimental hardness values with experimental bulk and shear moduli of a large variety of materials. It can be concluded that all hard materials have a high bulk modulus, but not all materials with a very high bulk modulus are very hard. However, the theoretically estimated values for the shear modulus G_0 of 320–390 GPa for different C_3N_4 phases are still very high. These values are higher than all industrially important hard materials except for c-BN and diamond (Table 2).

Teter pleaded for the search of “materials that are more useful” than diamond, rather than harder. Carbon nitrides with unusual mechanical behaviour could be among these more useful materials: Backed by force field calculations, Guo and Goddard speculated that a single crystal of α-C_3N_4 would be *auxetic* (negative Poisson ratio) [78]: tensile stress would cause an expansion in the perpendicular direction. So far, only crystals that exhibit this property into one or two directions are known, e.g. α-cristoballite [79]. Auxetic behaviour into all directions of space in combination with a comparatively high elastic modulus would certainly be interesting for a number of applications.

In many other studies, the authors concentrated on the electronic structure and relative stabilities of different

Table 2
A comparison of Vickers hardness, bulk and shear moduli for different examples of hard materials and three postulated C_3N_4-phases (for a description of these and other carbon(IV) nitride phases see Section 2.4.3)

Material	Vickers hardness (GPa)	Bulk modulus B_0 (GPa)	Shear modulus G_0 (GPa)
Diamond	96	443	535
c-BN	63	400	409
“Zincblende-C_3N_4”	–	448	390
c-C_3N_4	–	496	332
β-C_3N_4	–	437	320
γ-Si_3N_4	43–30	300	264
r-SiO_2*	33	305	220
TiB_2	33	244	263
SiC	28	226	196
B_4C	30	247	171
β-Si_3N_4	21	249	123

* Stishovite.

carbon(IV) nitrides [80–84]. It was concluded that there are only small energy differences between carbon(IV) nitrides such as α- and β-C_3N_4 [85–87]. Some studies also included amorphous phases [81a,82] as well as hexagonal-graphitic [85,81b,83] modifications, which is very reasonable due to the tendency of C- and N-atoms to form multiple bonds. Moreover, a graphitic C_3N_4-phase with orthorhombic symmetry [88] and a *spinel*-C_3N_4 [89] analogous to the novel spinel-Si_3N_4 [90] (see below) were postulated. Furthermore, a new, dense, 3-4-linked C_3N_4-modification was proposed, which contains C–C and N–N-bonds [91].

C/N phases with higher nitrogen contents were also a matter of theoretical examinations, e.g. CN_2 in a pyrite-type structure [92], as well as carbon-rich materials with compositions such as $C_{11}N_4$ [93], CN [94], and C_3N [95] were studied recently. Some amorphous [96,97], fullerene-like [98] and crystalline [99] modifications with different nitrogen contents were taken into account by the theoreticians. The bulk modulus for non-graphitic highly cross-linked structures is usually found to be very high, which is due to the short and strong C–N (and C–C, N–N) bonds. For example, the very nitrogen-rich CN_2 pyrite-type material was predicted to have a bulk modulus of 405 GPa [92].

The electronic, optical, mechanical and thermodynamic properties of the postulated C_3N_4-phases were investigated with different calculational methods [28,78,100–105]. All structures are metastable with an energetic minimum located only slightly above the graphitic C_3N_4-forms, the three-dimensionally crosslinked, dense modifications posses a large electronic band gap. According to the calculations, amorphous phases are significantly less stable. Based on force field calculations (MM2) it was concluded that a layered graphitic C_3N_4-network comprised of triazine units linked via nitrogen atoms should have a curved structure [106]. Contrarily, more recent ab initio calculations show that the most stable conformation is completely planar [125]. Nevertheless, the formation of (metastable) curved structures should certainly be possible, as this is well known for graphite (fullerenes and carbon nanotubes) as well as many other layered materials [107]. Nanotubes with the exact C_3N_4 stoichiometry were examined theoretically with respect to their mechanical properties [108], but could not be synthesised so far [109].

Recently published DFT-calculations indicate that 3D structures consisting of non-coplanar s-triazine rings and connected via N-atoms are more stable than the corresponding graphitic analogues [110].

A detailed investigation of certain molecular, oligomeric and polymeric building blocks for carbon nitrides showed that a high pressure transformation of unsturated C_3N_4-polymers to (ultra) hard carbon(IV) nitrides should be possible [91].

There are a few theoretical publications focused on the gas phase deposition of carbon nitrides [111–115]. Some authors investigated the fragmentation of nitrogen-containing CVD precursors such as CH_3NH_2 [114], gas mixtures (C_2H_2/N_2 [113]) as well as single reactive species like C_2N and CN_2 [111,112].

In addition to the prediction of relative stabilities and the structural modelling of carbon nitrides, the simulation of spectroscopic properties was addressed by theoreticians. The results of such studies allow a facile comparison of experimental and theoretical data similar to the calculated XRD pattern for crystalline phases. Various publications were dedicated to the calculation of X-ray absorption- [104], ^{13}C NMR- [116], $^{14/15}N$ NMR- [116,117], FTIR and Raman [118,119] as well as ELNES [120] (electron-energy-loss near-edge spectroscopy) spectra and electronic [94b,115] or dielectrical [119] properties of CN_x-materials.

2.4.3. Postulated C_3N_4-phases

A number of carbon(IV) nitride phases has been theoretically predicted or intuitively suggested by several authors in the literature. In order to get an overview concerning these phases they are briefly described and compared in the following paragraphs and are listed in Table 3 (see also Figs. 5–7). None of the mentioned solids has been synthesised or unambiguously proved to exist experimentally.

2.4.3.1. α-C_3N_4 ($P3_1c$). After being postulated in an unpublished patent disclosure letter in 1984 by Sung and Sung [28], Guo and Goddard were the first to investigate a carbon(IV) nitride phase in analogy to the very well-known α-Si_3N_4 [78]. The structure can be described as an AB-stacking of undulated β-C_3N_4-layers (see also Section 3.1 and Fig. 7a). The C- (or Si-) atoms are tetrahedrally co-ordinated with N-atoms. The corner-sharing tetrahedra form a covalent network of three-, four- and six-membered rings. In contrast to the β-Si_3N_4 phenacite structure, where at least one half of the N atoms are constrained to a trigonal planar conformation by symmetry, the α-Si_3N_4 structure, in principle, allows all nitrogens to be pyramidal. Regardless of these additional degrees of freedom, N is found to be almost planar in both, α-Si_3N_4 and β-Si_3N_4. In the case of C_3N_4 however, the force field calculations of Guo and Goddard suggest that removing the constraint of a trigonal planar nitrogen conformation, α-C_3N_4 is 25.1 kcal/mol more stable than β-C_3N_4 and exhibits negative Poisson ratios between $\nu = -0.025$ to -0.053 in all three directions of space.

2.4.3.2. β-C_3N_4 ($P6_3/m$). As already mentioned above, Sung and Sung [28] recommended examination of a β-Si_3N_4-analogous β-C_3N_4 (see Fig. 7b). Liu and Cohen [75,76] used the same relative positions of the atoms in the silicon nitride phase and replaced the Si–N bond by the shorter C–N. A possible pyramidal arrangement around the nitrogen atoms was not taken into account. Similar to the α-phase, the silicon or carbon atoms are tetrahedrally co-ordinated by N-atoms. Guo and Goddard [78], Teter and Hemley [85], Ortega and Sankey [86] as well as others [87,102] re-calculated the same model β-C_3N_4 structure. Different methods of simulation were applied and several

Table 3
Postulated and theoretically modeled C_3N_4-phases (see also text and Figs. 5 and 6)

C_3N_4-phase	Space group	Hybridisation[a]		Network-topology[b]	δ^{c} (g/cm^3)	B_0 (GPa)	G_0 (GPa)	Literature[d]
		C-atom	N-atom					
α-C_3N_4	$P3_1c$ (159)	sp^3	sp^2	$^{3}_{\infty}[C^{[4]}_{3}N^{[3]}_{4}]$	3.58	198/425	–	[78,85]
β-C_3N_4	$P3$ (143)	sp^3	sp^2	$^{3}_{\infty}[C^{[4]}_{3}N^{[3]}_{4}]$	3.58	451	320	[78,85–87,102]
Pseudo-cubic-C_3N_4 (pc-C_3N_4)	$P\bar{4}2m$ (111)	sp^3	sp^3	$^{3}_{\infty}[C^{[4]}_{3}N^{[3]}_{4}]$	3.81	448	390	[85,87]
c-C_3N_4	$I\bar{4}3d$ (220)	sp^3	sp^3	$^{3}_{\infty}[C^{[4]}_{3}N^{[3]}_{4}]$	3.89	496	332	[85]
Spinel-C_3N_4	$Fd\bar{3}m$ (227)	sp^3d^2	sp^3	$^{3}_{\infty}[C^{[6]}_{2}C^{[4]}N^{[4]}_{4}]$	3.77; 3.92	369	–	[89,121]
λ-C_3N_4	$P4_322$ (95)	sp^3	sp^2 and sp^3	$^{3}_{\infty}[C^{[4]}_{3}N^{[3]}_{4}]$ (C–C and N–N-bonding)	3.02	–	–	[91]
α-$C(NCN)_2$	$P4_12_12$ (94)	sp^3 and sp	sp^2 (and sp)	$^{3}_{\infty}[C^{[4]}C^{[2]}_{2}N^{[2]}_{4}]$ or $^{3}_{\infty}[C^{[4]}(NCN)^{[2]}_{2}]$	1.05	–	–	[91,122]
β-$C(NCN)_2$	$I\bar{4}2d$ (122)	sp^3 and sp	sp^2 (and sp)	$^{3}_{\infty}[C^{[4]}C^{[2]}_{2}N^{[2]}_{4}]$ or $^{3}_{\infty}[C^{[4]}(NCN)^{[2]}_{2}]$	1.20	–	–	[91]
g-C_3N_4	$P\bar{6}m2$ (187)	sp^2	sp^2	$^{2}_{\infty}[C^{[3]}_{3}N^{[3]}N^{[2]}_{3}]$ or $^{2}_{\infty}[(C_3N_3)^{[3]}N^{[3]}]$	2.02	–	–	[85]
g-C_3N_4	$R3m$ (160)	sp^2	sp^2	$^{2}_{\infty}[C^{[3]}_{3}N^{[3]}N^{[2]}_{3}]$ or $^{2}_{\infty}[(C_3N_3)^{[3]}N^{[3]}]$	2.20	51	–	[87]
g/o-C_3N_4	$P2mm$ (25)	sp^2	sp^2	$^{2}_{\infty}[C^{[3]}_{3}N^{[3]}N^{[2]}_{3}]$ or $^{2}_{\infty}[(C_3N_3)^{[4]}N^{[2]}]$	2.48		–	[80a,88]
Amorphous C_3N_4	–	sp^2/sp^3	$sp/sp^2/sp^3$	–	2.9	113	–	[127,128]
g-$[(C_3N_3)(NCN)_{1.5}]_n$	–	sp^2 and sp	sp^2 (and sp)	$^{2}_{\infty}[C^{[3]}_{2}C^{[2]}N^{[2]}_{4}]$ or $^{2}_{\infty}[(C_3N_3)^{[3]}(NCN)^{[2]}_{1.5}]$	<2.5	–	–	[91,122,123]
g-$[(C_6N_7)(NCN)_{1.5}]_n$	–	sp^2 and sp	sp^2 (and sp)	$^{2}_{\infty}[C^{[3]}_{12}C^{[2]}_{3}N^{[3]}_{2}N^{[2]}_{18}]$ or $^{2}_{\infty}[(C_6N_7)^{[3]}(NCN)^{[2]}_{1.5}]$	–	–	–	[126]
3D-srs-C_3N_4	–	sp^2	sp^2 and sp^3	$^{3}_{\infty}[C^{[3]}_{3}N^{[3]}N^{[2]}_{3}]$ or $^{3}_{\infty}[(C_3N_3)^{[3]}N^{[3]}]$	1.59	–	–	[110]
3D-ths-C_3N_4	–	sp^2	sp^2	$^{3}_{\infty}[C^{[3]}_{3}N^{[3]}N^{[2]}_{3}]$ or $^{3}_{\infty}[(C_3N_3)^{[3]}N^{[3]}]$	1.65	–	–	[110]
3D-srs-$[(C_6N_7)(N)]_n$	–	sp^2	sp^2 and sp^3	$^{3}_{\infty}[C^{[3]}_{2}C^{[2]}N^{[2]}_{4}]$ or $^{3}_{\infty}[(C_6N_7)^{[3]}N^{[3]}]$	–	–	–	[e]
3D-ths-$[(C_6N_7)(N)]_n$	–	sp^2	sp^2	$^{3}_{\infty}[C^{[3]}_{2}C^{[2]}N^{[2]}_{4}]$ or $^{3}_{\infty}[(C_6N_7)^{[3]}N^{[3]}]$	–	–	–	[e]
$[(C_6N_4)(NCN)_6]_n$	–	sp^3 and sp	sp^3, sp^2 (and sp)	$^{3}_{\infty}[C^{[4]}_{3}C^{[2]}_{3}N^{[3]}_{2}N^{[2]}_{6}]$ or $^{3}_{\infty}[(C_6N_4)^{[12]}(NCN)^{[2]}_{6}]$	–	–	–	[e]
$[(C_2N_2)(NCN)]_n$	–	sp^2	sp^2	$^{1}_{\infty}[C^{[3]}_{2}C^{[2]}N^{[2]}_{4}]$	–	–	–	[e]
g-$[(C_6N_7)(N)]_n$	–	sp^2	sp^2	$^{2}_{\infty}[C^{[3]}_{3}N^{[3]}N^{[2]}_{3}]$	–	–	–	[126]
g/o-$[(C_6N_7)(N)]_n$	–	sp^2	sp^2	$^{2}_{\infty}[C^{[3]}_{3}N^{[3]}N^{[2]}_{3}]$	–	–	–	[126]
g-$[(C_3N_3)(C_6N_7)(NCN)_3]_n$	–	sp^2 and sp	sp^2 (and sp)	$^{2}_{\infty}[C^{[3]}_{9}C^{[2]}_{3}N^{[3]}N^{[2]}_{15}]$	–	–	–	[126]

[a] Idealised hybridisation states according to the valence bond model.

[b] In the denotation $^{x}_{y}[A^{[m]}N^{[n]}]$, x: network-dimensionality, y: degree of extension of the structure (degree of oligomerisation), m: co-ordination number of the atoms or fragments A, n: co-ordination number of the atoms or fragments B.

[c] Calculated density.

[d] Further literature is cited in the text.

[e] This paper.

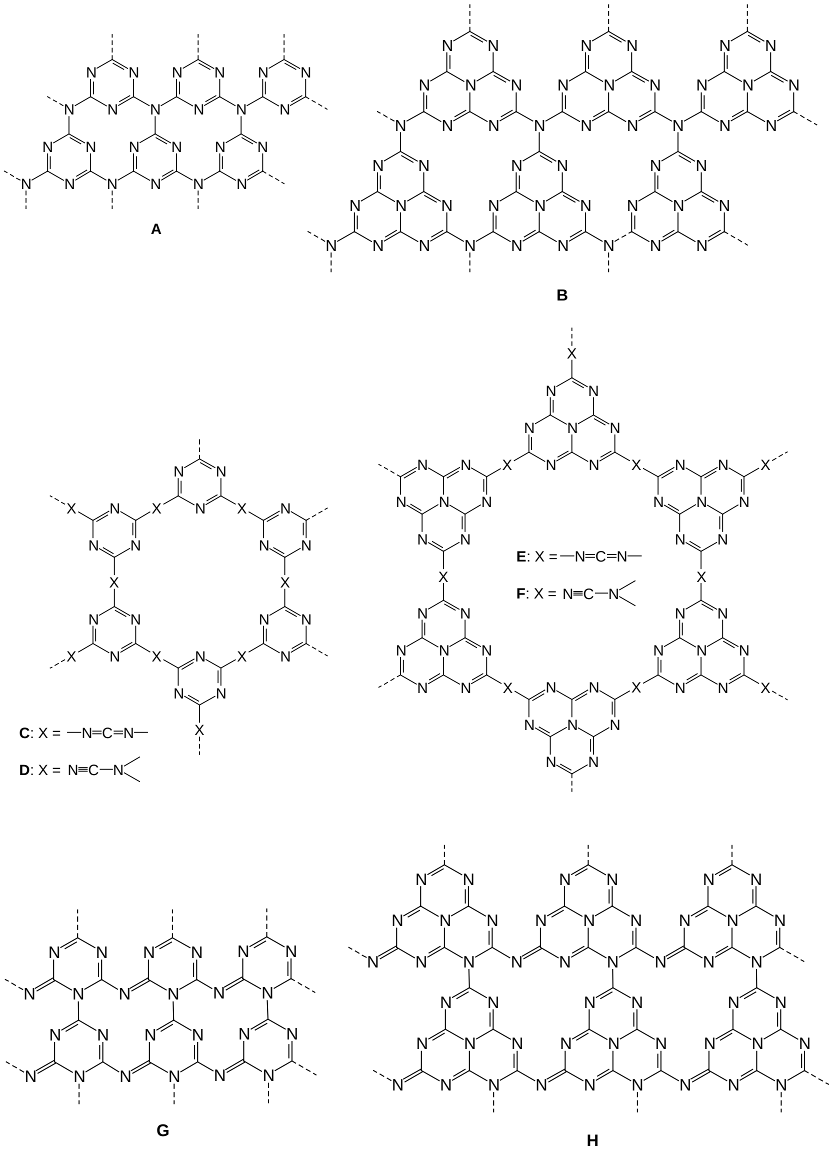

Fig. 5. Simple examples for (graphitic) carbon(IV) nitride networks with relative high symmetry, which are based on the s-triazin unit and the s-heptazine (tri-s-triazine) unit. Originally, it was found by theoretical studies that structure **A** should be the thermodynamically most stable C_3N_4-modification. Recently, it was shown that **B** is significantly more stable than **A**. Due to the lack of aromaticity within the heterocyclic rings the structures **G** and **H** are expected to be non-planar and destabilized.

aspects of the structure and its stability and properties were discussed. When a pyramidal environment of the nitrogen atoms was allowed, a more stable and more dense structure was obtained. However, in some cases the bulk modulus was found to be substantially lower than had been previously calculated. Guo and Goddard [78] concluded that the predicted diamond-like compressibilities of crystalline C_3N_4 phases were a result of the arbitrary assumption of planar nitrogen in these early calculations. A comprehensive discussion of the geometric differences between the nitrogen co-ordination in C_3N_4 and α- and β-Si_3N_4 is given in [3].

2.4.3.3. "Pseudo-cubic" or "(defect) zincblende"-C_3N_4 ($P\bar{4}2m$). Liu and Wentzkovitch [87] removed one quarter of the Zn-atom positions in the cubic ZnS-structure, which corresponds to the α-$CdIn_2Se_4$-structure type, and called the respective carbon nitride phase "cubic-C_3N_4" (see Fig. 7c). This structure contains C-atoms co-ordinated tetrahedrally to nitrogen, while the N-atoms are located in a trigonal pyramidal environment of C-atoms. In further studies this phase was again examined by theoreticians. They used the terms "defect-zincblende-C_3N_4" and "pseudocubic-C_3N_4" to designate this carbon nitride modification [85].

2.4.3.4. "Cubic" or "willemite-II" C_3N_4 ($I\bar{4}3d$) according to Teter and Hemely. A cubic C_3N_4-phase can be constructed on the basis of the high pressure modification of the mineral Willemite Zn_2SiO_4, by replacing the O-atoms with N-atoms and the Zn- and Si-atoms with C-atoms. This structural variant was first suggested by Teter and Hemely

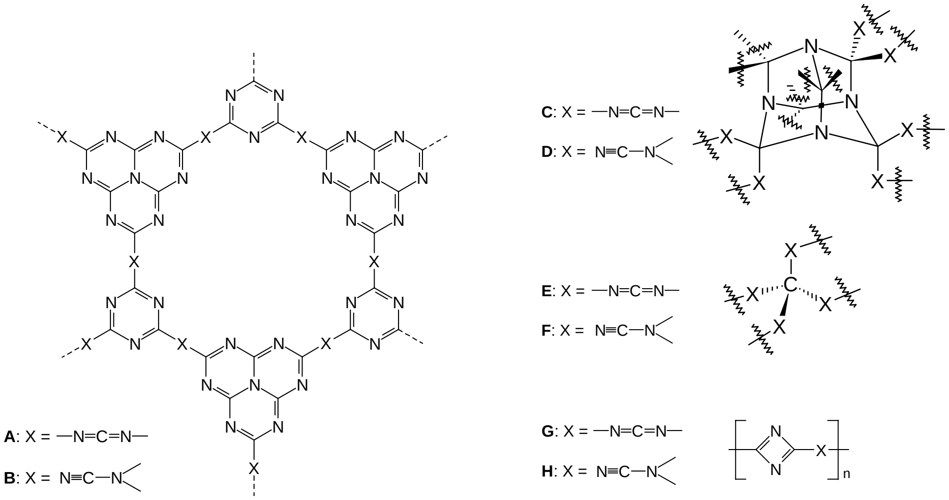

Fig. 6. Polymeric (graphitic) carbon(IV) nitrides, which are based on s-triazin a*nd* s-heptazine unit by connecting them via cyanoamide or carbodiimide bridges (structures **A** and **B**), as well as NCN-linked three-dimensional C_3N_4-networks, which can be constructed by combination with sp^3-hybridised C-atoms (structures **E** and **F**) or hexamethylenetetramine groups (structures **C** and **D**).

[85] (see Fig. 7d). The phase is characterised by an extremely high bulk modulus of 496 GPa. However, according to the simulations it is energetically less stable than both, the α- and the β-phase. But according to very recent results of a comparison and possible transformations between α-, spinel- and willemite-II E_3N_4-phases it is more favourable than the spinel modification at least at ambient pressure [121].

2.4.3.5. Spinel-C_3N_4 according to Mo et al. (Fd3m). After the discovery of a novel spinel-Si_3N_4-phase (see Section 3.2 and Fig. 7e) the possible existence of a cubic carbon(IV) nitride with spinel structure was discussed and theoretically investigated [89]. This structure contains carbon atoms octahedrally surrounded by nitrogen, which is energetically very unfavourable—even at extreme pressures. Furthermore, the calculations predict that the zero-pressure atomic density of spinel-C_3N_4 would be the same as diamond, but its bulk modulus notably *lower* ($B_0 = 369$ versus 442 GPa).

2.4.3.6. λ-C_3N_4 according to Kroll and Hoffmann ($P4_322$) [91]. Upon simulation of a compression of a hypothetical carbon dicarbodiimide (see below) Kroll and Hoffmann discovered a new and unusual C_3N_4-solid state structure. This phase consists of tetrahedrally co-ordinated C-atoms and both three-fold, planar and pyramidal co-ordinated nitrogen atoms. In contrast to the other phases mentioned here, this structure contains C–C– and N–N-bonds (Fig. 7f). Hence, based on the formalism of oxidation numbers this C_3N_4-modification cannot be considered as a carbon(IV) nitride. Nevertheless, the solid could be an interesting hard material just like the C_3N_4-modifications with alternating C/N-atom arrangement.

2.4.3.7. "α-$C(NCN)_2$" according to Greiner [122], Kroll and Hoffmann [91] ($P4_12_12$). Carbon atoms may be connected via carbodiimide units (–N=C=N–) forming an unsaturated, three-dimensionally cross-linked carbon(IV) nitride network (Fig. 6, structure **E**). The structure can be derived from SiO_2-structures by replacing the Si-atoms by C-atoms and the O-atoms by NCN-groups. A variation of the bond angles at the silicon and carbon atoms has relatively small effects on the energy of this network. It is known from other carbodiimide compounds that the NCN-unit can form the tautomeric cyanamide group (Fig. 6, structure **F**) and that the Si–N-bond angle in silylcarbodiimides is very flexible [123]. Similar to the graphitic carbon(IV) nitrides (see below) this phase is to be considered as a very soft material, which may be used as a precursor for the high pressure synthesis of hard C_3N_4-phases.

2.4.3.8. "β-$C(NCN)_2$" according to Kroll and Hoffmann [91] ($I\bar{4}2d$). As with the hypothetical modification described in the preceding paragraph, this phase is a C_3N_4-variant of a crystalline carbon dicarbodiimide network (Fig. 6, structure E). Most important properties of both postulated solids α- and β-$C(NCN)_2$ such as thermodynamic stability, bulk modulus and density are similar.

2.4.3.9. "Graphitic" C_3N_4 according to Teter and Hemley [85] ($P\bar{6}m2$). When tri-s-triazine rings are connected via trigonal planar co-ordinated N-atoms layered structures can be designed, which are similar to graphite in the sense that they should be planar and aromatic with (at least partially) delocalised π-electrons (Fig. 5, network **A**). However, the layers contain "holes" "filled" by electrons in the non-bonding sp^2-orbitals of the N-atoms in the s-triazine rings. Such graphitic C_3N_4 structures have been mentioned in the literature together with the C/N/H-polymer melon (see above). In 1994, Kouvetakis et al. [124] attempted to synthesise bulk amounts of this phase. Later, several other attempts were published (see Section 2.4.5). An ABAB stacking of the graphitic C_3N_4-layers, results in a structure with the space

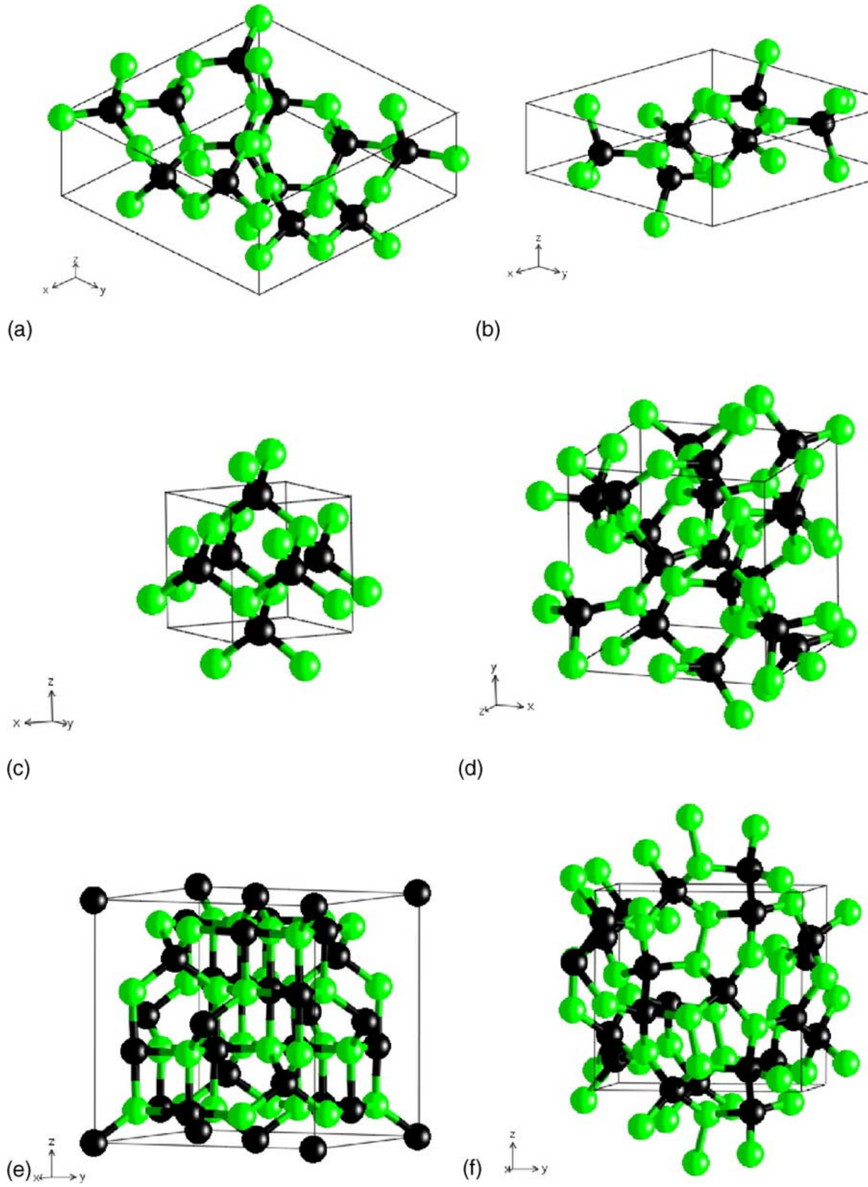

Fig. 7. Six of the carbon(IV) nitrides that have been proposed in literature and which were examined theoretically: (a) α-C_3N_4 ($P3_1c$), see e.g. [78]; (b) β-C_3N_4 ($P6_3/m$), see e.g. [75,76,78,85–87,102]; (c) "pseudo-cubic" or "(defect) zincblende"-C_3N_4 ($P\bar{4}2m$) [85,87]; (d) "cubic" or "willemite-II" C_3N_4 ($I\bar{4}3d$) [85,121]; (e) spinel-C_3N_4 ($Fd3m$) [89]; (f) λ-C_3N_4 ($P4_322$) [91].

group $P\bar{6}m2$. This was first calculated by Teter and Hemley in 1996. In addition to this graphitic (sp^2-hybridised) structure several other layered and/or unsaturated C_3N_4-phases may be postulated (see below).

2.4.3.10. "Graphitic" C_3N_4 according to Liu and Wentzkovitch [87] (R3m). In addition to the AB-stacking described above, the graphitic C_3N_4-layers (Fig. 5, network **A**) can adopt alternative stacking. Liu and Wentzkovitch suggested a rhombohedral ABCABC-stacking, which leads to a crystalline network with the space group $R3m$.

2.4.3.11. "Graphitic-orthorhombic" C_3N_4 according to Alves et al. [88] (P2mm). Layered, sp^2-hybridised C_3N_4 phases may also be constructed by connecting s-triazine rings via two-fold co-ordinated N-atoms (Fig. 5, network **G**). This unusual structure was proposed by Alves et al., and later examined theoretically in the simplest stacking variant AAA by Mattesini et al. [80a]. The electronic properties and the stability were calculated using a DFT method. Due to the non-existing aromaticity of the six-membered rings the most stable conformation of this structure should be most likely non-planar [125].

2.4.3.12. "Polydi(triazine)tri(carbodiimide)-structures" according to Greiner [122,123]. Connecting s-triazine rings via carbodiimide groups provides a C_3N_4-structure with alternating C–N-atom arrangement (Fig. 5, network **C**). These unsatutrated C_3N_4-networks may form layered (graphitic) structures. Nevertheless, due to the flexibility and large 'mesh size', a number of interpenetrating phases could exist. Kroll and Hoffmann [91] examined model structures in the space groups $I4_1/amd$ (141), $P4_2/n$ (86) and $C2/m$ (12). Furthermore, the isomeric cyanamide form may by postulated (Fig. 5, network **D**).

2.4.3.13. "Heptazine-based, graphitic" C_3N_4-phases. We proposed several carbon(IV) nitride structures, which contain the heptazine (tri-s-triazine) unit (see in Fig. 5, networks **B**, **E**, **F**, and **H** and Fig. 6, structures **A** and **B**) [126]. A graphitic network based on trigonal planar co-ordinated N-atoms g-$[(C_6N_7)(N)]_n$ is the so far most stable C_3N_4-phase according to ab inito calculations. Additionally, it is possible to formulate further tri-s-triazine containing carbon(IV) nitrides which are analogous to the above mentioned carbodiimide-bridged triazine network as well as the "graphitic-orthorhombic" triazine-C_3N_4-variant.

2.4.3.14. Further "carbodiimide- and cyanamide-based" C_3N_4-phases. In addition to the already described formation of carbon(IV) nitride structures by connecting sp^3-hybridised C-atoms, s-triazine-units (C_3N_3) and s-heptazine-units (C_6N_7) via NCN-groups, it is possible to interconnect 1,3-diazacyclobutadiene-rings (C_2N_2) or hexamethyleneteramine-units (C_6N_4) with carbodiimide (or cyanamide) groups (see Fig. 6, structures C, D, G and H) [126]. As mentioned above the networks $[C(NCN)_2]_n$ and $[(C_3N_3)(NCN)_{1,5}]_n$ have been calculated by Kroll and Hoffmann [91]. According to this study these phases should be less stable than the α-C_3N_4-structure by 80 and 180 kJ/mol, respectively. The bulk- and shear moduli are expected to posses very small values similar or even lower than those of the graphitic carbon(IV) nitrides.

2.4.3.15. s-Triazine based 3D-C_3N_4-phases "3D-srs" and "3D-ths" according to Vodak et al. [110]. In addition to graphitic C_3N_4-structures s-triazine units may be connected via N-atoms to form 3D-networks. Two recently investigated examples are "3D-srs" and "3D-ths". These hypothetical networks are derived from $SrSi_2$ and $ThSi_2$ structures, respectively. DFT-calculations indicate that the 3D arrangements are more stable than the layered systems. This is a consequence of the lone-pair repulsion of the non-bridging triazine nitrogens, which would be in close vicinity to each other in coplanar structures like those shown in Fig. 5a. However, the density of both investigated phases is much lower than the calculated density of the graphitic C_3N_4-structures. This might indicate that at higher pressures the graphitic phases are more stable. It is interesting to examine if the 3D-structures may form interpenetrating networks and how the stabilising effect due to the conjugation between the aromatic π-electron systems of the graphitic structures is compensated.

2.4.3.16. Tri-s-triazine-3D-C_3N_4-phases "3D-srs-$[(C_6N_7)(N)]_n$" and "3D-ths-$[(C_6N_7)(N)]_n$". By analogy with the above described s-triazine-based 3D-structures, it is possible to design the corresponding heptazine-based carbon(IV) nitride networks. To our knowledge, these novel structures have not yet been examined experimentally or theoretically.

2.4.3.17. Amorphous C_3N_4-phases. Generally, any number of amorphous C_3N_4-structures may be theoretically postulated. Nevertheless, numerous different amorphous CN_x-structures have been prepared experimentally depending on the synthetic method (see below). It is therefore very difficult to design a realistic model structure and very few theoretical studies on amorphous C_3N_4-phases have been published [127,128]. Trends counteracting the formation of a low-compressibility phase were found: "(i) N incorporation strongly catalyses C under-co-ordination, which in turn (ii) causes the nitrogens to develop paracyanogen-like (CN double and triple) bonding, and (iii) the most favourable densities for a-CN occur much lower than for the desired hard crystalline materials".

2.4.3.18. Summary: comparison of postulated C_3N_4 phases. In summary, several dense, i.e. hard, saturated or sp^3-hybridised carbon(IV) nitride structures have been postulated. Additionally, a large number of soft, unsaturated structural variants may be suggested, which are probably suitable precursors for the synthesis of a hard C_3N_4 phase. Especially the former hard phases have been examined with various theoretical approaches. Although the results with respect to the expected stability of the different modifications do not always agree quantitatively, it is possible to conclude a qualitative sequence of stability (under ambient conditions):

$$\begin{aligned}&\text{3D-ths-}C_3N_4 > \text{g-}[(C_6N_7)(N)]_n > \text{3D-srs-}C_3N_4\\&\quad > \text{g-}C_3N_4 > \alpha\text{-}C_3N_4 > \beta\text{-}C_3N_4\\&\quad > \text{g-}[(C_3N_3)(NCN)_{1,5}]_n > \lambda\text{-}C_3N_4\\&\quad > \text{c-}C_3N_4 > \alpha\text{-}C(NCN)_2 \sim \beta\text{-}C(NCN)_2\\&\quad > \text{pc-}C_3N_4 \gg \text{spinel-}C_3N_4\end{aligned}$$

Concerning the compressibility B_0 the following comparative sequence can be proposed based on the literature available up to date:

$$\begin{aligned}&\text{c-}C_3N_4 > \alpha\text{-}C_3N_4 \sim \beta\text{-}C_3N_4 \sim \text{pc-}C_3N_4\\&\quad \gg \text{g-}C_3N_4 \sim \text{g-}[(C_6N_7)(N)]_n\\&\quad \sim \text{g-}[(C_3N_3)(NCN)_{1,5}]_n \sim \alpha\text{-}C(NCN)_2\\&\quad \sim \beta\text{-}C(NCN)_2\end{aligned}$$

At this point, it should be stated once again, that the shear modulus G_0 correlates much better with the hardness of a material than its bulk modulus B_0. Provided that the phases are stable under ambient conditions, the following order of hardness is suggested:

$$\begin{aligned}&\text{pc-}C_3N_4 > \beta\text{-}C_3N_4 \sim \text{c-}C_3N_4 \sim \alpha\text{-}C_3N_4\\ &\quad \gg \text{g-}C_3N_4 \sim \text{g-}[(C_6N_7)(N)]_n\\ &\quad \sim \text{g-}[(C_3N_3)(NCN)_{1,5}]_n \sim \alpha\text{-}C(NCN)_2\\ &\quad \sim \beta\text{-}C(NCN)_2\end{aligned}$$

2.4.4. Thin films by vapour phase deposition

First attempts to prepare CN_x-coatings were published in the 1970s and 1980s [129,130]. After the above described theoretical work by Liu and Cohen in 1985, 1989 and 1990, which indicated that β-C_3N_4 should possess diamond-like properties and be metastable, there was an exponential increase in attempts to synthesise the postulated material via gas phase deposition techniques. Numerous papers have been summarised and analysed in several review articles [1–4], and a brief overview is given here.

Early studies published during the first half of the 1990s, used plasma-CVD with $NH_3/CH_4/H_2$- [131], CH_4/N_2- or NH_3/CH_4-gas mixtures as precursors [132] obtaining amorphous C/N-coatings. However, similar CVD-experiments gave products that contained α- and β-C_3N_4-crystallites [133] or exclusively α-C_3N_4-crystals [134] according to the XRD (XRD) analysis of the authors. Song et al. [135] reported the formation of microcrystalline C_3N_4-phases in an amorphous matrix by ammonia-enhanced ion beam deposition on graphite. Similar results were published by Zhang et al. [136], although this contribution was subject of a critical discussion published later [137]. Badzian and Badzian [138] obtained graphitic C/N-coatings with a turbostratic structure. Pulsed laser ablation of graphite under nitrogen ion beam irradiation allowed control of the nitrogen content of the products up to a maximum of 40%. The composition of the films was not homogenous, and electron diffraction analyses indicate that crystallites with high nitrogen content are present [139–141]. Sputtering techniques have been frequently used to generate C/N-films [142–148]. Again, it was reported that the nitrogen content of the coatings can be selectively adjusted. However, in most studies the maximum nitrogen content was 20% [144], 28% [143] or 50% [142], depending on the respective study, which is still below the required value of 57 at.% for a single phase material with C_3N_4 stoichiometry. At least two research groups claim to have reached this stoichiometry for a homogeneous material and reported nitrogen contents of 58% [148] and 60.87 wt.% (=57.1 at.%) [149], respectively. In both cases, the films were amorphous.

The implantation of N^+-ions with low energy (500 eV) [150] or high energy [151–154] (80–100 keV) in different carbon substrates provided various C/N-films. Some authors report the formation and detection of crystalline fractions in the products [151,153]. Ion beam PVD techniques, which involve the evaporation of carbon under simultaneous irradiation with nitrogen ions (0.1–50 keV), furnished interesting C/N-coatings [155,156]. C:N-ratios in the range between 0.5 and 3 were reported [156]. Those films with a C:N-ratio of 0.6–0.7 showed an extremely high Knoop-hardness (6500 N/mm^2 for 1 μm thick coatings).

In the second half of the 1990s as well as from 2000 to 2003. Most experimental efforts and patent applications [36] focused on the preparation of thin CN_x-coatings. Several research groups reported on the successful deposition of various, hard amorphous and (partially) crystalline C_3N_4-phases from the gas phase. As described for the first half of the 1990s CVD-techniques [10,12,15,18,22,24,157–202] and PVD-methods [7–9,13,14,203–268] were used. A few papers describe the formation of amorphous and mainly sp^2-hybridised carbon nitride phases (see e.g. [269–272]).

Practically all known variants of chemical vapour deposition techniques were applied to produce CN_x-coatings. These include thermal low-pressure CVD (see e.g. [12]), microwave- and RF-plasma-enhanced CVD (see e.g. [15,169b,178,182,186,188,189], laser CVD (e.g. [163,170]) or hot filament CVD (e.g. [171,179,180]).

Similar results were obtained from PVD syntheses. Here, the range of applied techniques goes from ion implantation (e.g. [220,252]) or ion beam deposition (e.g. [263]) to magnetron-, ECR- and other sputtering methods (e.g. [13,149,204,227,228,239,243,257,260–262]) to laser ablation (e.g. [205,213,230,240,241]) and vacuum arc deposition (e.g. [233a,273]) or laser-induced gas phase reaction (e.g. [264]).

The number of papers indicates that the CVD-approaches are dominated by plasma enhanced techniques, while in the PVD area predominantly various kinds of sputtering methods were used. Important deposition parameters like temperature, pressure, precursors and/or target materials were varied in a wide range. Silicon was frequently used as a substrate, but metals such as nickel and quartz glass were also utilised.

Independent of the respective vapour phase deposition methods and the applied apparatus or experimental techniques, a number of reports on the successful synthesis of partially or fully crystalline coatings was published (e.g. [37y,188,201]). Many authors believe that they proved the formation of β-C_3N_4-crystallites [167,170,171,173,207a, 208,209,215,217,218,220], α-C_3N_4-crystallites [15,168], α- *and* β-C_3N_4-crystallites [18,163,166,169,206,210a], cubic C_3N_4 [212], β-C_3N_4 *and* cubic C_3N_4 [219], graphitic C_3N_4 [176] or unknown crystalline C_3N_4-phases [210b] in their coatings. Other authors also found indications for crystalline materials in the deposition products, but are more careful with the interpretation of their results. This is reasonable since in many cases there are only very small crystallites formed, sometimes with various compositions or mixed with other (amorphous) phases. Most conclusions are based on XRD and TEM studies, but even when the possibility of C:N ratios different from that of C_3N_4 is neglected, the diffraction intensities and lattice constants match usually relatively poorly with the calculated values for the theoretically proposed modifications.

Matsumoto et al. [2] provided a detailed systematic analysis of the diffraction data published until 1999. They came to the conclusion that in all cases the reported X-ray and/or electron diffraction patterns may also be assigned to different crystalline carbon phases. Moreover, the determination of the elemental composition of the coatings is usually investigated with techniques such as EDX (or RFA), XPS (ESCA), RBS or EELS, which are in general not suitable to provide an exact and reliable quantification of the light elements C, H, N and O. Even the C:N-ratio is usually very difficult to be determined for a small single crystal. However, in some studies it was possible to obtain evidence through HR-TEM and EELS [212] that the crystallites as well as the surrounding amorphous matrix consist of carbon and nitrogen. In many cases it is clear from the vibrational spectra that a significant contamination with hydrogen is present in the coatings (see e.g. [207]). Many authors ignore the presence of the additional element hydrogen, discussing their results simply on the basis of the C:N-ratio. This is not sufficient, since molecular or polymeric crystalline C/N/H-phases may also be formed.

Amorphous non-stoichiometric CN_x-materials are nevertheless interesting from a fundamental as well as from a practical point of view, and much of the recent work in the field of carbon nitride coatings is focused on the synthesis and characterisation of amorphous, homogeneous materials [182,187,202,209,213,239].

Finally, it should be noted that extremely hard, ternary phases such as crystalline Si/C/N-modifications may be formed when silicon is used as a substrate material [274–276]. It is not unlikely, that many of the crystalline phases described in experimental reports contain significant amounts of oxygen, hydrogen or other elements. Nevertheless, it is relatively unlikely that the discussed techniques lead to a C:N-ratio which is *exactly* equal to 3:4.

2.4.5. Bulk synthesis approaches for CN_x solids (since 1990)

Several authors suggested use of bulk synthesis approaches in order to generate hard, ceramic carbon nitride materials in macroscopic amounts. According to the theoretical studies mentioned above, it is clear that high pressure techniques similar to the HP/HT-synthesis of diamond and c-BN should be applied to prepare C_3N_4 hard materials. This requires suitable precursors with high nitrogen content. Compared to the literature discussed in the preceding section there is a much smaller number of publications on this topic. In the following paragraphs these papers are summarised and discussed.

Wixom tried in 1990 to synthesise a carbon(IV) nitride by shock wave compression of a pyrolysed melamine-formaldehyde resin and a tetrazol derivative. Diamond was the only detectable crystalline phase in the product. Obviously, high peak temperatures during shock treatment caused a (partial) decomposition into nitrogen and carbon-rich materials [277].

Sekine et al. performed high pressure pyrolyses of tetracyanoethylen TCNE (C_6N_4) and 1,3,5-triazine ($C_3H_3N_3$) obtaining graphite-like products with low nitrogen contents (below 20%) [278]. In another study the following organic substances were pyrolysed at 700 °C/225 MPa: melamine ($C_3H_3N_6$), cyanoguanidine ($C_2H_4N_4$), 1,2,4-triazol ($C_2H_3N_3$), diaminomaleonitrile ($C_4H_4N_4$), polymerised HCN, dicyanoimidazol ($C_5H_2N_4$), tetracyanoethylene (TCNE, C_6N_4), TCNE with ammonia as well as hexaazatriphenylene hexacarbonitrile ($C_{18}N_{12}$). All starting materials provided pyrolysis products, which deviated from the ideal C_3N_4 composition. The authors concluded—primarily due to the fact that in almost all cases significant amounts of ammonia were formed—that an ideal precursor should contain no or at least the lowest possible hydrogen content [279].

Several attempts were published to synthesise graphitic C_3N_4 materials, especially the network **A** in Fig. 5. Kouvetakis et al. developed a single source precursor route to this structure [124,280]:

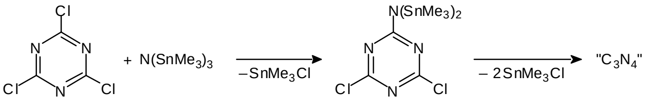

The pyrolysis products contained only small amounts of tin. According to Rutherford-back-scattering (RBS) they exhibited a nearly perfect elemental composition (e.g. $C_3N_{3.9}Sn_{0.07}$). In contrary, Purdy obtained a residue with an empirical formula $C_{6.9}N_{6.8}Sn$ after pyrolysis at 520 °C, while upon prolonged heating of **I** at ~50 °C, a metal-organic trimer $(SnN)_3$ six-membered ring was formed, which was identified by single-crystal XRD [430]. However, no crystalline material has been prepared based on this approach.

Martin-Gil et al. pyrolysed *N*,*N*-diethyl-1,4-phenylendiammoniumsulfate ($C_{10}H_{18}N_2O_4S$) in a nitrogen atmosphere and in the presence of SeO_2 as catalyst. A heterogeneous product was formed, which contained crystalline carbon nitride with zinc blende structure, according to HR-TEM-examinations [22]. The authors propose that this material is a carbon(IV) nitride C_3N_4, generated by incorporation of molecular nitrogen at 800 °C in the gas phase.

$$C_{10}H_{18}N_2O_4S + 8N_2 \rightarrow 3C_3N_4 + CO_2 + 6NH_3 + SO_2$$

The composition of the crystalline product could only be estimated with electron energy loss spectroscopy (EELS) because of the small crystallite size of 5–50 nm. The crystallites are surrounded by an amorphous matrix with a varying nitrogen content. It was possible to determine a micro-hardness H of about 35 GPa and an E-modulus of 190 GPa by AFM [22]. These values are significantly below the corresponding values found for diamond ($H \sim 100$ GPa,

$E \sim 1000$ GPa), but they are at least comparable with amorphous CN_x-coatings (see e.g. [281,282]).

Montigaud et al. tried to prepare the triazine-based structure **A** (Fig. 5) via solvothermal techniques at 250 °C/130 MPa starting from cyanuric chloride and melamine in the presence of ethyl-diisopropylamine [283]:

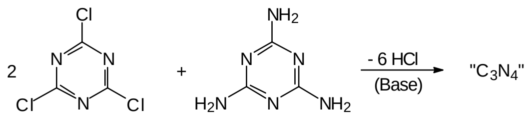

The orange-brown product was characterised using XRD, REM, EDX, Raman and XPS. The authors describe the material as a “novel graphitic C_3N_4”. Since no information about the hydrogen content was provided and the carbon-to-nitrogen-ratio was not determined by chemical (combustion) analysis, it is very likely that the C/N/H-polymer melon was formed (see above) [53].

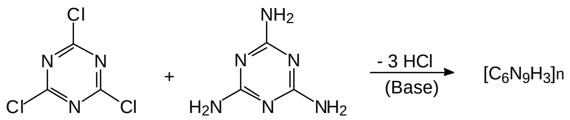

Melon, $C_6N_9H_3$, contains only 1.5 wt.% hydrogen, its composition is therefore very close to the carbon(IV) nitride stoichiometry. Recently, the same polymer was probably formed by a similar reaction of melamine with cyanuric chloride. Interestingly, the authors suggested to use the product as a new “host material” [284].

An alternative method to synthesise the graphitic C_3N_4 precursor A (Fig. 5) is based on reactions of cyanuric chloride with metal nitrides and/or amides. The major challenge of this approach is the separation of the side product, i.e. the metal chloride, from the polymer.

Kawaguchi et al. used lithium nitride and tried to remove the LiCl by extraction with water [285]:

$$C_3N_3Cl_3 + Li_3N \rightarrow \text{“}C_3N_4\text{”} + 3LiCl$$

Two different products were obtained, with the composition $C_3N_{4.5}O_{1.2}H_{4.1}$ and $C_3N_{3.6}O_{1.1}H_{4.2}$. The oxygen content indicates a hydrolysis reaction during the treatment with water. Remarkable is that the first material exhibited ferromagnetic properties: according to the authors it was possible to separate the product from the reaction mixture using a permanent magnet.

Lu et al. reduced chloroform with sodium amide and obtained a C/H/N-material with a N:C-ratio of 0.23 upon annealing under a flow of nitrogen [286]. The XRD pattern showed six peaks, which were assigned to α-C_3N_4. In order to provide a comprehensive characterisation of the crystalline phase further examinations such as TEM and elemental analysis are required.

Another synthesis of α-C_3N_4 and β-C_3N_4 crystals in 1997 is reported by a Chinese research team. He et al. subjected 3-amino-1,2,4-triazine ($C_3N_4H_4$) to a pressure of 7 GPa and 1400 °C:

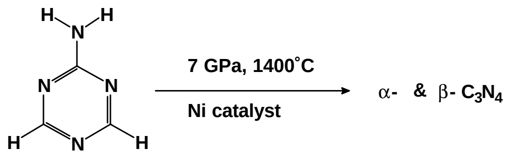

Under these conditions, the bulk of the material was converted to graphite, but a layer of “rod-like crystals with size of several micrometers” was found at the interface with Ni–Mn–Co alloy plates, which had been introduced as catalyst at the top and at the bottom of the pressure cell. According to XRD studies, most of the *d*-values showed good agreement to those calculated for α- and β-C_3N_4. The nitrogen content—measured by EDX—varied from 47 to 62%, but the authors admitted the experimental error of this method to be large. It is interesting that the formation of C_3N_4 could also be observed if pure cobalt was used as catalyst. Urea and NH_4HCO_3 did not lead to the formation of the crystalline layer, neither did Fe, Ni and Pd as catalysts. In spite of these promising results, it appears that these authors published no further work on this issue.

In continuation of the above described works, Todd et al. [280] published further attempts to prepare a carbon (IV)nitride-related ternary phases such as C_3N_3P [287]:

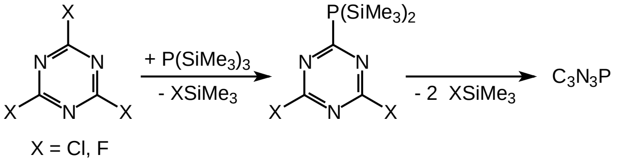

The polymers formed by pyrolysis were air sensitive and reacted spontaneously to form C_3N_3PO. Experiments to prepare sp^3-hybridised C_3N_3P-hard phases via HP/HT routes are planned [287].

In 1998, Nesting et al. were the first who reported the formation of nitrogen-rich carbon nitrides in diamond anvil cells [288]. TCNE (C_6N_4) was transformed at 2500 °C/42 GPa into a carbon nitride, which was free of any cyano groups. However, the material decomposed to form molecular nitrogen, diamond and nitrogen-depleted carbon nitride phases. A more interesting product was generated by high pressure pyrolysis at 2500 °C/115 GPa using a 2:1-mixture of TCNE with cyanuric triazide (C_3N_{12}, Fig. 1L). However, in the preliminary proceedings contribution, only an XRD-diagram was published. A detailed analysis of the diffractogram was not possible since it contained strong signals of the metal used as a gasket for the diamond anvil cell. No information was given on the elemental composition or spectroscopic properties of the product. It seems that no full paper on this study has appeared up to date.

However, support that the synthesis of a crystalline Carbon (IV) nitride phase still remains possible, comes from a recent success on the corresponding carbon (IV) oxide. Obviously, sufficient pressure can convert even the volatile CO_2 into a polymeric solid. In 1999, Lota et al. reported on a quartz-like, sp^3-hybridised CO_2-modification, prepared in a diamond anvil cell at 1800 K/40 GPa. The substance can be quenched down to 1 GPa at room temperature [289]. Also 1999, a carbon nitride phase with high nitrogen content was prepared by anodic deposition of a cyanoguanidine solution in acetone. The material was deposited on silicon and polished graphite substrates. The reaction was performed by applying a voltage of 1000 V at $T = 50\,^\circ C$. XPS and FTIR were used to characterise the products. C–C, C–N, C=N, CN and N–H-bonds were detectable. Annealing at 600 °C increased the fraction of C–N-bonds [290].

Four articles, which appeared almost at the same time, describe solvothermal approaches to C_3N_4 materials. Melamine was treated in a belt-apparatus at 800 °C/3 GPa, using hydrazine as a de-hydrogenating agent. The authors report on the formation of the graphitic C_3N_4-form with orthorhombic structure (see Fig. 5, network **G**) under evolution of ammonia [88,291]:

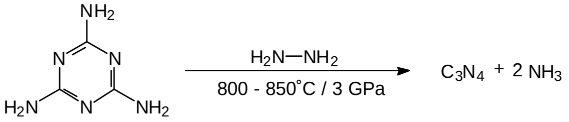

The product was characterised with XRD, SEM, XPS, electron microprobe analysis (EMPA), elemental analysis and IR-spectroscopy. A hydrogen content of 2 wt.% was reported. This is a significant amount of hydrogen indicating the presence of a C/N/H-phase, possibly a crystalline form of melon, which has the molecular formula $(C_6N_9H_3)_n$ and contains 1.5 wt.% hydrogen. This problem was discussed above and it is encountered in many publications. Very recently, Ma et al. obtained similar results upon melamine pyrolysis [292].

Similar solvothermal conditions (∼800 °C/3 GPa) were applied to test two further triazine derivatives for their suitability to prepare a C_3N_4-precursor: 2-amino-4,6-dichloro-1,3,5-triazine **A** and 5-azacytosin **B** [293].

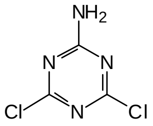

A

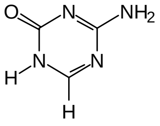

B

Compound **A** was supposed to evolve HCl and compound **B** was expected to form H_2 and H_2O thus forming a carbon(IV) nitride as the solid residue. Nevertheless, **A** was reacted with CaO in order to prepare C_3N_4 according to the following equation:

$$C_3N_4H_2Cl_2 + CaO \xrightarrow{800\text{–}1100\,^\circ C/3\,GPa} C_3N_4 + CaCl_2 + H_2O$$

All reactions with compounds **A** and **B** formed products with relatively high hydrogen contents and/or significant oxygen impurities [293].

A further solvothermal synthetic route for carbon(IV) nitride phases was applied to the above described reaction of cyanuric chloride ($C_3N_3Cl_3$) with lithium amide [294]. Similar conditions, i.e. 350 °C/<5 MPa in benzene, had been used before by Kawaguchi et al. (see above) forming a ferromagnetic material with the composition $C_3N_{4.5}O_{1.2}H_{4.1}$ [285]. In a short communication, an XRD pattern is discussed, which shows only three signals. An electron diffraction image indicates the presence of a polycrystalline sample. The authors concluded that β-C_3N_4-crystallites were formed. However, except for an XPS measurement no detailed analysis of the elemental composition of the crystallites was reported. Furthermore, the IR spectrum indicates that large amounts of hydrogen are present in the sample, which is most likely due to the treatment of the raw product with HCl, HNO_3 and HF.

Recently, Lu et al. tried to reproduce the solvothermal carbon nitride synthesis using cyanuric chloride with lithium amide as reactants in benzene solution at 350 °C/5–6 MPa [295]. They claimed the formation of α- and β-C_3N_4. Solvothermal reaction of CCl_4 with NH_4Cl at 400 °C was reported to provide graphite-like C_3N_4 nanocrystals [296]. Due to the small crystallite size of ∼11 nm, a comprehensive characterisation was not possible. A Russian publication from 1999 reports the high pressure synthesis of hexagonal α-C_3N_4 at 6 GPa [297]. The presented XRD-diagram shows ten signals located at 2Θ-values, which are in good agreement to the calculated data. The IR-spectrum is problematic, showing strong bands for C–H and N–H or O–H vibrations. Moreover, an elemental analysis of the products was not reported.

A shock-synthesis of β-C_3N_4 is described in a proceedings contribution [298]. Two mixtures of sodium cyanamide ($NaN(CN)_2$), tetracyanoethylene (TCNE), sodium azide and tetraiodomethane with an excess of copper were precompressed in steel capsules. These capsules were shock compressed for 1.8–3.6 μs at 20–40 GPa. The following reactions were proposed:

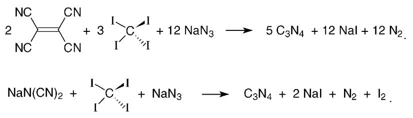

However, the products were only characterised by IR spectroscopy. Comparison with the IR-spectrum of β-Si_3N_4 led the author to conclude that β-C_3N_4 had formed.

High-energy ball mills may also be used to generate high pressures up to >5 GPa as well as high temperatures. The high p/T conditions occur at very localised spots in the reaction mixture. Fahmy et al. [299] tried to react pure graphite with liquid ammonia in a high-energy ball mill. The products were examined with XRD, EELS, FTIR, XPS, HR-TEM and elemental analyses. A nano-crystalline phase was detected, which could be β-C_3N_4.

In another mechano-chemical-synthesis approach using high-energy ball mills, CN_x-phases are reported by reacting graphite with elemental nitrogen [300]. The authors found evidence for the formation of C–N bonds using IR and XPS spectroscopy. However, the overall nitrogen content was determined to be about 1–10%, which is rather low. The products contained hydrogen and iron (wear debris from the ball mill).

Recently, further reports on the mechano-chemical-synthesis of nano-sized β-C_3N_4 were published by a Chinese group [301]. Graphite nanopowder was reacted with ammonia in a high-energy ball mill. The product was characterised by XRD, FTIR and TEM, but no clear evidence for the correct composition of the crystallites was provided. In another communication HRTEM, XPS and EELS were used to analyse crystalline nanorod-shaped products [302]. The results seem to support the above interpretation of β-C_3N_4 formation. However, although a very nice powder diffractogram is depicted in the publication, no Rietveld analysis was performed and the true elemental composition of the products remains unclear (especially the hydrogen and oxygen content). Since it is stated that the high-energy ball mill synthesis route provides a “convenient, well-repeatable, mild, low-cost, effective and large yield (on a 20 g synthesis scale)” way to β-C_3N_4 nanorods, a bulk combustion chemical analysis should be performed.

Graphitic C_3N_4-hollow spheres have been reported to be formed upon reacting cyanuric chloride or fluoride with lithium amide [106]. One year earlier, the authors had described the formation of amorphous carbon nitrides using the same starting materials [303]. In this paper, the successful synthesis of C_3N_4-materials in a Monel-reactor is reported. While solid state reactions between both starting materials did not give a positive result, an interesting product was obtained using a solvent. Similar results had been described before (see above) as well as in a recent review article [304]. Interestingly, the addition of materials such as glass wool to the educts seems to have a catalytic effect resulting in the formation of hollow spheres with diameters from 30 nm to 20 μm [106]. SEM, TEM, FTIR, XRD and solid-state-NMR-examinations indicated the presence of spherical CN_x-particles with graphitic structure. The authors supported their interpretation with force-field calculations (MM2), which indicate that triazine-based C_3N_4-structures crosslinked with nitrogen atoms (structure **A** in Fig. 5) tend to form curved layers. However, recent ab initio calculations show that the energetically most favoured conformation is completely planar [125]. Nevertheless, metastable curved structures similar to carbon fullerenes and nanotubes are certainly also quite stable.

One further attempt to synthesise triazine-based graphitic C_3N_4-structures from melamine and cyanuric chloride was reported by Zhang et al. in 2001 [305]. At 1–1.5 GPa and 500–550 °C, a crystalline phase was obtained, which contains stoichiometric amounts of HCl. The phase can be considered as a C_3N_4-derivative. The same product is formed when the single source precursor 2-amino-4,6-dichloro-1,3,5-triazine is used:

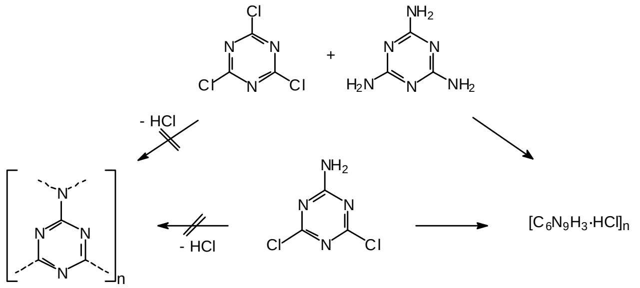

The crystal structure of this phase was determined by powder XRD. The material consists of a N–H-group bridged network of s-triazine rings, which possess the composition of the polymer melon $C_6N_9H_3$ (see above). The “voids” in this structure are filled with chloride anions, a corresponding number of protonated N–H-units is also present in the network. Furthermore, the described results are confirmed by elemental analyses, EELS-studies as well as IR- and ^{13}C NMR-measurements.

The high pressure synthesis of β-C_3N_4 was described in a brief communication [306]. The authors reported that carbon(IV) nitride crystallites were deposited on silicon wafers by laser evaporation of graphite in a nitrogen plasma. These crystals were used in a second step as a seed to crystallise an amorphous CN_x-precursor in a high pressure experiment. The latter precursor material was synthesised by decomposition of mercury(II) thiocyanate according to older literature (see above).

$$\mathrm{Hg(SCN)_2} \xrightarrow{180\,^{\circ}\mathrm{C}} \mathrm{C_3N_{4,2}} \xrightarrow[\mathrm{CN}_x-\text{beschichtetes Si}]{7\,\mathrm{GPa}/550\,^{\circ}\mathrm{C}/2\,\mathrm{h}} \beta-\mathrm{C_3N_4}$$

It is reported that macroscopic amounts of a C_3N_4 phase are formed in a 30 mm^3 high pressure cell at 7 GPa/550 °C/2 h. However, again the product was not comprehensively characterised, only X-ray and electron diffraction as well as XPS were used [306]. Another short communication describes the high pressure synthesis of a hexagonal C_4N phase at 6–7 GPa/300 °C [307]. The product was investigated using IR- and AES as well as XRD, but the structure could not be solved.

Much more analytical data is available for nitrogen-rich CN_x-networks which were prepared by slow thermal decomposition tri-azido-s-triazine, $C_3N_3(N_3)_3$ (=C_3N_{12}) [308]. A few years before we had used the same molecular precursor C_3N_{12} attempting to prepare a carbon nitride by a “detonative synthesis”, but the formation of carbon nanotubes (CNTs) and nanoparticles was observed instead [309]. Detonating of C_3N_{12} in ambient atmosphere yields only gaseous products [310].

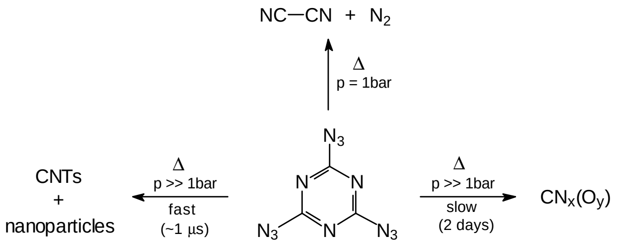

Table 4
Elemental composition of the products of slow thermal decomposition of triazido-s-triazine $C_3N_3(N_3)_3$ (=C_3N_{12}).

	C (wt.%)	N (wt.%)	H (wt.%)	O (wt.%)	$C_3N_xH_yO_z$
185 °C/1 bar[a]	38.0	57.5	1.53	3.08	$C_3N_{3.9}H_{1.4}O_{0.2}$
185 °C/6 bar[a]	33.2	60.3	1.17	5.38	$C_3N_{4.7}H_{1.3}O_{0.4}$
185 °C/6 bar[b]	34.45	61.78	<0.05	2.34	$C_3N_{4.6}O_{0.2}$

[a] Washed with dry toluene.
[b] Unwashed sample.

The *slow* decomposition under pressure provides amorphous materials with C:N-ratios between C_3N_4 and C_3N_5. Thermal analyses (TGA), IR-, UV-Vis- and ^{13}C MAS-NMR-spectroscopy as well as XRD, elemental analyses and electron microscopy indicated that a C/N-network based on s-triazine rings is formed. The rings are crosslinked primarily via N-atoms and diazo groups. Due to a washing treatment after synthesis and probably due to contact with air, the products contained hydrogen and oxygen as impurities (Table 4).

Nevertheless, these materials have been proposed to be promising precursors for high pressure transformations using e.g. multi-anvil- or diamond-anvil-presses. We have performed compression experiments with C_3N_{12} as a starting material in laser-heated diamond anvil cells at pressures up to 45 GPa. Unfortunately, only amorphous carbon nitride materials were obtained [311].

In another high pressure synthesis approach a 1:6 molar mixture of hexachlorobenzene and sodium azide was compressed in a tantalum cylinder at 7.7 GPa/1000 °C for 0.5 h [312]. The obtained products were characterised by XRD, SEM and IR-spectroscopy. No clear evidence was found for the presence of a carbon(IV) nitride phase in the reaction product. In a later study, the same starting materials were heated for 50–70 h in the presence of a sodium flux [313]. An amorphous material was formed, which contained carbon and nitrogen in a ratio close to the C_3N_4 stoichiometry.

Preparation of graphitic C_3N_4 -materials based on the tri-s-triazine nucleus C_6N_7 by chemical synthesis at ambient pressure was reported in 2001 by Komatsu et al. [314]. This is a very interesting approach since it has been demonstrated by ab initio calculations that the structure **B** in Fig. 5 is the most stable C_3N_4 modification [126]. In contrast to this result most authors have discussed their experimental (and theoretical) data with respect to triazine-based graphitic carbon(IV) nitride structures (see above). In a first attempt Komatsu tried to synthesise C_3N_4 by pyrolysis of tricyanomelamine at 800 °C [314a]. This experiment generates the C/N/H-polymer melon, as discussed above. The IR- and MS-spectrometry data as well as the C/H/N-analyses published in the paper clearly support this interpretation. Similar results were obtained upon pyrolysis of mixtures of melamine with metal halides like $ZnCl_2$ [314b]. Much more promising are the reactions of potassium melonate $K_3[(C_6N_7)(NCN)_3]$, with heptazinetrichloride, $C_6N_7Cl_3$ [314c]. In order to separate the side product KCl from the C/N-polymer, the reaction residue was washed with boiling aqueous HCl (35%) and hot water. This purification step probably causes a partial hydrolysis of the product, since small amounts of hydrogen were detected. The chlorine, oxygen and potassium content of the products were not determined. On the basis of IR- and MS-examinations as well as XRD and analysis of the C:N-ratio determined by combustion chemical analysis the author describes the product as a “prototype carbon nitride”. Komatsu suggested a network structure like that shown in Fig. 5B, but according to the starting materials, networks like **C** or **D** should have formed. The presented data do not show that a single phase, heteroatom free, graphitic carbon(IV) nitride has formed. Nevertheless, the approach to prepare a heptazine-based graphitic C_3N_4-polymer appears to be very promising.

2.5. *Summary and outlook*

All theoretical studies indicate that dense saturated carbon(IV) nitrides should be very hard materials. However, the calculated shear moduli clearly suggest hardness values well below diamond. What is more important, both carbon and nitrogen are well known alloying elements for steel. Hence, cutting of ferrous alloys—one of the commercially most important fields of metal working—may be prohibitive for carbon nitrides just as it is for diamond. Nevertheless, the relatively large structural variety among C_3N_4 phases remains an interesting academic challenge. The most stable phase so far considered is a 3-dimensional network of nitrogen-bridged triazine units with $ThSi_2$ topology, followed a heptazine-based graphitic structure, while for the hard phases, α-C_3N_4 is predicted to be the most stable modification.

Numerous attempts to prepare C_3N_4-films via CVD and PVD have been performed. There are many hints from different groups that crystalline C/N-phases are obtainable, but no unambiguous prove for the existence of such a phase is available. Also amorphous and (semi)crystalline carbon nitride coatings have been shown to be very hard materials, sometimes with interesting functional properties.

A detailed analysis of the bulk synthetic approaches shows that many nitrogen-rich materials have been generated, but similar to the gas phase routes, no unambiguous characterisation of a carbon(IV) nitride network is available. The sophisticated tools of preparative organic and inorganic chemistry should however allow design of a precursor which is suitable for a transformation into a C_3N_4-phase.

From a fundamental point of view there is still a lot of work necessary to gain a comprehensive understanding of the relations between synthetic parameters (for each method), composition (i.e. C:N-ratio), chemical structure and properties of C/N-materials. This kind of understanding would also be very useful for the development of industrially relevant materials and their optimisation.

3. Silicon nitrides

Silicon carbide [315,319] and silicon nitride [5] form the basis of the most important non-oxide ceramics. At least six different crystalline polymorphs of Si_3N_4 have been described in the literature: In addition to the well known hexagonal α- and β-forms, which have almost the same density of 3.2 g/cm^3, a novel high pressure form with spinel structure (c-Si_3N_4 = γ−Si_3N_4) was discovered in 1998/1999 [90] and will be described in detail in Section 3.2. High pressure experiments on β-Si_3N_4 at room temperature led to the formation of a so-called δ-Si_3N_4 with tetragonal symmetry in 2001 [316]. It is most likely a metastable intermediate between β- and γ-Si_3N_4 (see Section 3.4). In 2002, Cai et al. found crystallites of a novel hexagonal silicon nitride formed during pyrolysis of an Si/B/C/N precursor-derived ceramic at nitrogen pressures between 1 and 10 MPa [317a]. By subsequent TEM investigations, the space group of this phase was identified as *P*-62*c* [317b,317c]. Most likely a defecteous non-stoichiometric silicon nitride with space group $P4_22_12$ that occurred during nitridation experiments of silicon was reported in 1986 by Saha et al. [318]. To our knowledge, these results have not been reproduced. There is little known about (crystalline) silicon subnitrides (Section 3.4) in general. *Amorphous* silicon nitride in contrast is an important material for barrier coatings in electronic devices (Section 3.3). Amorphous Si_3N_4 powder also occurs as an intermediate in the synthesis of α-Si_3N_4 via the diimide-route (see next section).

3.1. α- and β-Si_3N_4

A comprehensive treatment of the syntheses and properties of α- and β-Si_3N_4 is well beyond the scope of this review article. These issues have been addressed in several books and review articles, e.g. [5,319,320] to name only the most recent ones. Hence, only a few remarks on the structure, properties and significance of the classical silicon nitride phases will be presented here.

α- and β-Si_3N_4 contain distorted SiN_4-tetrahedra and trigonal planar NSi_3-units. All silicon atoms are sp^3- and the nitrogen atoms sp^2-hybridised. The SiN_4-tetraedra are interconnected via common vertexes. The planarity of these connecting nitrogen atoms in these low pressure modifications has been comprehensively reviewed in [3]: Electronic interactions between the Si an N orbitals, such as (d–p)π or (n–σ*)π were considered as possible explanations.

Most commercial silicon nitride products are prepared by different sintering techniques starting from powders. There are basically four different synthetic routes for these powders, which differ in purity, morphology and sintering activity: (i) in 1910, a direct synthetic method of stoichiometric silicon nitride was found. The reaction of elemental silicon with nitrogen gives relatively coarse products, which have to be milled prior to further processing; (ii) carbothermal reduction utilises a fine mixture of carbon- and SiO_2-powders in a flowing N_2-atmosphere at 1500 °C; (iii) the so-called diimide-process is a liquid- or gas-phase route to Si_3N_4-powders, which was discovered as early as in 1830. $SiCl_4$ is reacted with NH_3 at ∼0–20 °C to form amorphous, polymeric silicon diimide ($[Si(NH)_2]_n$) which transforms into amorphous silicon nitride upon annealing at >1000 °C, before it crystallises to α-Si_3N_4; (iv) CVD techniques using volatile silicon compounds such as $SiCl_4$, SiH_4 or related molecular compounds yield Si_3N_4-powders upon gas phase reaction with ammonia. Due to the predominantly homogenous nucleation, very fine powders can be produced with specific surface areas of 2–20 m^2/g and high sintering activity. In addition to these classical routes to Si_3N_4, several variants and alternatives have been suggested. These include, for example, plasma- or laser-enhanced techniques or the so called SHS-process, which is based on very exothermic reactions directly forming ceramic bodies [319]. The pyrolysis of silicon-containing polymers, especially polysilazanes gives amorphous as well as crystalline silicon nitride, depending on the pyrolysis temperature [321]. Independent of the synthetic method, the resulting Si_3N_4-powders primarily contain the α-modification and only small amounts of the β-form.

In comparison to other non-oxide ceramics like SiC, B_4C, diamond and c-BN, the processing and sintering of Si_3N_4 is better understood. With few exceptions, Si_3N_4-ceramics are prepared by liquid phase sintering: At typical temperatures ≥1700 °C, oxidic sintering additives (e.g. $MgO+SiO_2$) form a melt, which dissolves the α-Si_3N_4 crystallites. β-Si_3N_4-nuclei grow by reprecipitation. The in situ grown β-Si_3N_4 is characterised by a rod-like crystal morphology. These elongated crystals build effective bridges in the wake zone of a crack, leading to a high fracture toughness of Si_3N_4-ceramics. In combination with the high intrinsic thermal conductivity of β-Si_3N_4, this results in a very good thermal shock resistance.

Compared to most oxide ceramics, Si_3N_4-ceramics are characterised by relatively high tensile and shear strength. By carefully controlling type and amount of the sintering additives, high temperature stability and chemical inertness have been attained [5]. Due to this property profile, silicon nitride ceramics are increasingly used for cutting tools as well as special machine parts such as bearings, seals or turbo charger rotors [322]. The quality of silicon nitride ceramics (SN) depends strongly on many factors, including the starting material, amount and type of sintering additives as well as the method of production. So called SSN, GPSN, HPSN, HIP-SSN, HIP-SN, RBSN, SRBSN and HIP-RBSN silicon nitride ceramics are available, denoted depending on the processing which may be standard sintering (S), gas pressure sintering (GP) (uniaxial), hot pressing (HP), hot isostatic pressing (HIP) or reaction bonding (RB), respectively.

3.2. Spinel-Si_3N_4

Several authors have used high pressure techniques to compress α- and/or β-silicon nitride. Apart from the above mentioned HIP and hot pressing techniques, methods for the generation of extremely high pressures ($p > 10\,\text{kbar}$) have been developed in the fields of earth sciences. In the 1950s to 1970s, the synthesis of diamond and c-BN was one of the few research fields outside the geoscience community, where these techniques were employed. In the past decades, an increasing trend towards utilisation of extreme pressures also in preparative inorganic chemistry and material science occurred. It is reflected by several recent review articles [323]. A main objective in the high pressure studies on silicon nitride was to obtain very dense ceramic bodies that do not contain any sintering additives and hence exhibit improved (thermo)mechanical properties. For example, Li et al. sintered amorphous silicon nitride nanopowders under pressures of 1–5 GPa [324]. Other researchers employed diamond anvil cells to determine the bulk modulus of α-Si_3N_4 up to 48 GPa [325] or measure its melting curve up to 37 GPa [326]. In none of these studies, a phase transformation was reported.

3.2.1. Discovery: DAC-syntheses

Spinel silicon nitride was first discovered by diamond anvil cell high pressure experiments which were aimed to synthesise a crystalline C_3N_4 phase. The underlying idea originated from reported attempts to synthesise β-C_3N_4 by gas phase processes using β-Si_3N_4 as a substrate for heteroepitactical growth [327] and the occurrence of $C_{3-x}Si_xN_4$-layers [134,177], where silicon substrates have been used for similar experiments. β-Si_3N_4 crystallites were used as seeds in order to initiate the crystallisation of an amorphous C/N precursor material which was generated by annealing triazido-s-triazine C_3N_{12} in a diamond anvil cell. Surprisingly, it was found that the seed crystals transformed into a novel cubic phase while the C/N matrix remained amorphous [328].

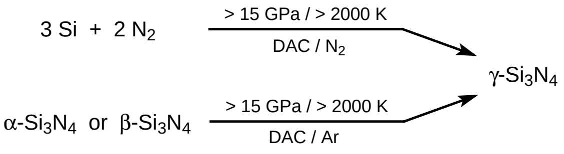

At the same time Zerr performed high pressure high temperature experiments in laser heated diamond anvil cells on elemental silicon in a nitrogen pressure medium as well as on the hexagonal α- and β-Si_3N_4 polymorphs. A thorough TEM investigation revealed the formation of spinel-Si_3N_4 [90].

Interestingly, in earlier studies no phase transformation was observed upon compressing α-Si_3N_4 to 48 GPa [325]. Suematsu et al. found that α-Si_3N_4 also survives HP/HT treatment at 4.9 GPa and 1600 °C and that the long known α-to-β-transformation requires not only heat but also the presence of a liquid phase in order to occur [326].

3.2.2. Nomenclature

As the spinel-type structure belongs to the cubic system, the new Si_3N_4 phase was initially given the symbol "c-Si_3N_4" [90]. The connotation to the most commonly used symbol for high-pressure boron nitride, c-BN,[1] was intended and c-Si_3N_4 was adopted in subsequent publications (see e.g. [89]). In the original works on the almost simultaneously discovered spinel nitrides of the heavier group 14 elements Ge and Sn, Leinenweber et al. used the prefix γ- for Ge_3N_4 [329], whereas Scotti et al. completely omitted the allocation of a prefix to determine the new Sn_3N_4 phase [330]. The nomenclature γ-M_3N_4 was also used in a highlight article on the novel group 14 element nitrides by Schnick [331] and at least in two other review articles [323e,332]. As the spinel modifications of many oxides and also oxide nitrides are traditionally indicated by γ (e.g. γ-Al_2O_3, γ-Fe_3O_4, γ-alon [333]), this appears to be more systematic. Consequently, this convention will be used preferentially throughout this review article. It should be noted however, that we initially hesitated to use the symbol γ because of an unconfirmed report on the synthesis of tetragonal silicon nitride back in 1986 [318] which would have been the third discovered polymorph in chronological order.

3.2.3. Structure

A comprehensive treatment of the spinel structure can be found in [334]. The general formulation of spinel compounds is AB_2X_4, space group *Fd*-3*m*. The structure is usually described as a (distorted) face-centred-cubic (fcc) array of anions X, located at 32e (Wyckoff-notation). The anion position is not entirely fixed by symmetry, but can deviate along the $\langle 1\,1\,1 \rangle$ direction, which gives rise to one free parameter, sometimes called "spinel parameter" and denoted with u. Only for $u = 1/4$ the anions are ideally cubic close-packed. In most cases however, there is a finite dilation, given by $u = (1/4) \pm \delta$. This has several important crystallographic implications, including changes in bond lengths, bond angles, interstice volumes and the symmetry of co-ordination polyhedra. In particular, the existence of u allows for a broad range of cations A, B with different sizes. The A cations are located within one eighth of the tetrahedral interstices and the B in one half of the octahedral interstices within the (distorted) fcc anion sublattice. In this particular case, Si atoms occupy both A and B sites. Hence, a more precise formulation for γ-Si_3N_4 is $Si^{[4]}[Si^{[6]}]_2N_4$. The six-fold co-ordination of silicon by nitrogen in γ-Si_3N_4, which previously was known only for some complex inor-

---

[1] c-BN is not the only high pressure polymorph of boron nitride: analogous to the existence of carbon in a cubic (diamond) and a hexagonal modification (lonsdaleite), there is also a hexagonal wurtzite-type *w*-BN, whilst the structure type of c-BN is sphalerite.

ganic anions [335] and oxide nitrides [336], was regarded as one of the most striking structural features at the time of its discovery. *Stishovite*, the corresponding high pressure polymorph of silicon *oxide* contains solely six-fold co-ordinated Si atoms. In the nitride γ-Si_3N_4, one third of the Si atoms remain in tetrahedral co-ordination, as in the low pressure polymorphs α- and β-Si_3N_4, but the co-ordination number of the nitrogen atoms is increased: While being in a trigonal planar configuration within the low pressure phases, the γ-phase has four-fold co-ordinated, i.e. sp^3-hybridized nitrogens, similar to the conditions in the ammonium-ion, $NH_4{}^+$. Compared with conventional oxide spinels, γ-Si_3N_4 and the other group 14 nitride spinels are unique in many regards.

While the binary oxide spinels based on transition metals, such as Fe_3O_4 or Fe_3S_4, still contain differently charged cation species ($Fe_3X_4 = Fe_2^{3+}X_3 \cdot Fe^{2+}X$, “2–3 spinels”) the electronic structure of the light main group elements does not allow different oxidation states, so that all sites will be occupied by ‘cations’ with a formal charge of +4 (‘4–4 spinels’). As a consequence, there is an absence of local electroneutrality: the tetrahedrally co-ordinated nitrogen ‘anion’ shares its formal charge of −3 with four surrounding silicon atoms of charge +4. This results in finite effective charges located at the $Si^{[4]}$ and $Si^{[6]}$ sites. Their formal magnitude can be calculated according to the simple electrostatic Pauling rule, resulting in $+1e$ at $Si^{[4]}$ and $-0.5e$ at $Si^{[6]}$. In reality, these charges will be somewhat lower due to redistribution of the electron density, but they will nevertheless remain of finite magnitude. An indication for a high electron density around the $Si^{[6]}$ site was found via ^{29}Si MAS-NMR by Sekine et al. (see Section 3.2.6.9). We can expect an intrinsic polarity to be a common feature among all spinel nitrides of Si, Ge and Sn and − if they exist[1]—also those of Ti, Zr, and Hf, as well as all their possible ternary and multinary solid solutions. The resulting ionic interactions will have important implications on the electronic structure of these compounds and their physical properties such as thermal expansion behaviour or thermal conductivity (see Section 3.2.6.6).

3.2.4. MAP-syntheses

The MAP technique allows compression of much larger sample amounts as compared to the DAC. Typical pressures up to 25 GPa and temperatures in excess of 2000 °C can be achieved [337,323a]. Due to the larger sample size the products may be characterised using XRD, FTIR or elemental analyses. These methods are essential in determining detailed information on the composition and structure of novel phases.

We synthesised γ-Si_3N_4 in a set of MAP-experiments (see Table 5). Two amorphous precursors namely silicon nitride-imide (Si_2N_2NH) and amorphous silicion nitride were used [338].

In the first MAP-experiment, the high temperature of about 2300 °C caused the silicon nitride to react with the capsule material. The γ-Si_3N_4-phase was successfully obtained from subsequent experiments at pressures of 13 GPa or higher. The fact that the β-modification was obtained at 10 GPa indicates (i) that β-Si_3N_4 and not α-Si_3N_4 is the thermodynamically stable modification for $p \leq 10$ GPa and (ii) that the phase boundary between the β- and the γ-phase lies within 10 and 13 GPa. This latter result agrees well with theoretical predictions valid for $T = 0$ K [90].

The morphology of the γ-Si_3N_4 differs significantly from the characteristic rod-like shape of β-Si_3N_4 crystallites (Fig. 8). Elemental analysis indicated an oxygen content of up to 12 wt.% in the cases where a platinum capsule surrounded by MgO was used as capsule material [338]. Element mappings of cross sections of the cylindrical samples were measured with electron probe microanalysis (EPMA). The data indicated that the oxygen content at the outer parts of the sample is much higher than in the centre. Therefore, it was concluded that oxygen diffused into the cylinder during the heat treatment. It was also shown that each of the γ-Si_3N_4-crystallites was surrounded by an oxide layer by dissolving the oxidised surface in HF followed by analysis of the silicon content in HF-solutions. An amorphous, most likely oxidic film was also detectable in HR-TEM investigations [338]. In order to decrease the contamination with oxygen, multiple encapsulation using molybdenum in com-

Table 5
Summary of a set of multi-anvil-press experiments performed at the Bayerisches Geoinstitut in Bayreuth (Germany) on the synthesis of spinel silicon nitride

Experiment no.	Precursor	Capsule material	Sample size Ø × h (mm)	Press	p_{max} (GPa)	T_{max} (°C)	t_{hold} (s)	Product
1	a-Si_3N_4	Re	1.6 × 2.9	Sumitomo	15	~2300	120	Reacts with Si_3N_4
2	Si_2N_2(NH)	Re	1.6 × 2.6	Hymag[a]	–	1800	60	c-Si_3N_4
3	a-Si_3N_4	Pt	1.6 × 2.6	Sumitomo[a]	–	–	–	c-Si_3N_4
4	Si_2N_2(NH)	–	2.0 × 3.7	–	10	–	–	β-Si_3N_4
5	–	–	1.6 × 2.7	–	15	–	120	c-Si_3N_4
6	–	Re	2.0 × 3.4	Zwick[b]	–	–	900	–
7	–	Pt/Mo	2.0 × 3.5	–	–	–	90	–
8	–	Pt/Mo/BN	–	–	–	–	–	–
9	a-Si_3N_4	–	–	–	–	–	–	–
10	Si_2N_2(NH)	–	–	–	13	1600	300	–

[a] Hymag and Sumitomo press, maximum load: 1000 t.
[b] Zwick press, maximum load: 5000 t.

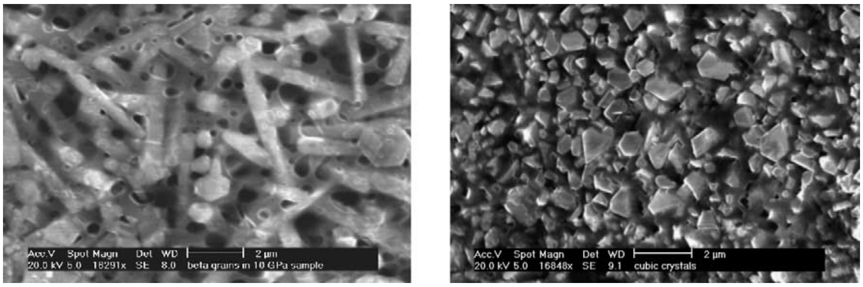

Fig. 8. (a) SEM image of the products obtained from MAP-experiment 4 (10 GPa, see Table 5): rod-like β-Si_3N_4 crystallites are formed in a porous amorphous matrix. (b) SEM image of the products obtained from MAP-experiment 2 (15 GPa): Si_3N_4-crystallites with distorted octahedral and hexagonal morphology are present. Nevertheless, an amorphous phase is also present.

bination with boron nitride was used for the high pressure experiments 7–10 (Table 5). The products contained much less oxygen compared to previous samples (<4 wt.%).

For a detailed structural analysis of the γ-Si_3N_4 powder, X-ray diffractograms were recorded and subjected to Rietveld-analyses. The data obtained by the former HR-TEM studies [90] were confirmed and refined by these examinations. The most important results are summarised in Table 6.

The multi-anvil technique was also chosen by other groups as a means for the HP/HT synthesis of γ-Si_3N_4. However, instead of amorphous precursors, the crystalline phases α- and β-Si_3N_4 were used as starting materials. Jiang et al. synthesised monolithic γ-Si_3N_4–samples, starting from a mixture of α- and β-Si_3N_4 powders [339]. Tanaka et al. employed a high purity β-Si_3N_4 powder with 0.5 wt.% oxygen content, in order to produce pure samples suitable for hardness measurements [340]. In both cases, an average grain size between 100 and 200 nm was reported.

In the experiments described above, based on amorphous Si/N precursors, only porous γ-Si_3N_4-products were obtained with crystallite sizes up to several micrometres. This is most likely due to the formation of gaseous side products, i.e. hydrogen, nitrogen and ammonia in the case of Si_2N_2NH, and/or the larger crystallisation-induced shrinkage.

Dense bodies, suitable for microhardness measurements were obtained in a subsequent and separate study in the system Si/Al/O/N [341], where a solid solution series $Si_{3-x}Al_xO_xN_{4-x}$ with β-Si_3N_4-structure (the so called β-sialons [333]) is known. These β-sialons were transformed into the respective spinel compounds (see Section 8.2).

Table 6
Summary of the structural data determined for spinel silicon nitride by X-ray powder diffraction and Rietveld-refinement [338,339,351]

Distance/angle	From [351]	From [339]
a_0 (Å)	7.7381(2)	7.7339(1)
Si_{tet}–N (Å)	1.8051(2) (4×)	1.7849(16)
Si_{oct}–N (Å)	1.8626(1) (6×)	1.8718(9)
Si_{oct}–Si_{oct} (Å)	2.7358(1) ($=a/\sqrt{8}$)	2.7343(1)
N–Si_{tet}–N (°)	109.47	109.47
N–Si_{oct}–N (°)	85.30(1)	n.n.
u[a]	0.25968(1)	0.2583(1)

The results of other authors deviate only slightly from each other (see also text).

[a] So called spinel or anion-parameter.

3.2.5. Shock synthesis

Shock-wave synthesis methods [342] can be subdivided into three classes: (i) so called “flyer-plate” or “impact”-experiments, where a shock wave is created due to the momentum of a projectile (flyer) that is shot onto the sample, (ii) shock-compressions or shock-compactions, which usually are based on an explosive charge, which is acting more or less directly on the material to be densified and (iii) detonative syntheses, where a precursor–explosive-mixture is detonated in a suitable vessel. All three techniques offer the opportunity to produce larger amounts of products. The disadvantages of shock wave experiments are obvious: The desired p–T-condition can only be perpetuated for a short time (∼1 ms). Besides, there are usually safety precautions and approval regulations to be taken into account. However, for a comprehensive characterisation of the spinel phase of silicon nitride it was very desirable to obtain larger amounts than are accessible by the multi-anvil-approach.

Shortly after the discovery of spinel silicon nitride, Sekine et al. obtained γ-Si_3N_4 in high yields by flyer plate shock wave experiments [343]. Sub-micrometre-powders of pure β-Si_3N_4 or a α-/β-Si_3N_4-mixture were blended with copper. Targets wrapped in copper- or platinum-hulls were impacted with steel- or platinum-projectiles [343a]. By variation of the projectile velocity between 1.5 and 2.1 km/s, peak pressures of 12–115 GPa and peak temperatures up to >3000 K were generated. The duration of these $p-T$-conditions was about 1 µs. The products were isolated by dissolving the copper in HNO_3 and were analysed with XRD and transmission electron microscopy as well as EDX. A maximum γ-Si_3N_4-yield of 80% was obtained at 50 GPa/2400 K. Decomposition of the silicon nitride was observed at still higher p- and T-values. The particle size of the synthesised γ-Si_3N_4 was determined to be 10–50 nm. Interestingly, it was first found that α-Si_3N_4 does not transform to the spinel phase under the same conditions [343]. The authors assumed a diffusionless (martensitic) transformation from β- to γ-Si_3N_4. Later, the same authors reported that α-Si_3N_4 can indeed be transformed and leads to a higher yield than β-Si_3N_4 under the same shock conditions [344].

In a further report of the same research group [343b] sintered dense β-Si_3N_4-discs (1 cm × 1.2 cm × 0.3 cm) were impacted with polycarbonate-, steel- and tungsten-projectiles in order to determine the Hugoniot-curve of β-Si_3N_4. In these experiments, the sample material was not recovered, but the onset of the $\beta \rightarrow \gamma$ transformation at 36 GPa was determined from shock velocity measurements. This much higher transition pressure compared to the static experiments is due to the low temperature of 460 K (at $p = 36$ GPa). A complete transformation into the high pressure phase was not observed even at the highest pressure of 150 GPa generated in the experiments, but a 100% conversion was extrapolated for $p_{\max} = 180$ GPa. However, according to recent calculations for this pressure range, a further high pressure modification should be formed, which is similar to the $CaTi_2O_4$-structure containing SiN_6-prisms as well as SiN_6-octahedra (see Section 3.4 on post-spinel phases).

The successful shock wave synthesis of spinel silicon nitride was a break-trough for a comprehensive characterisation of the novel phase (see below). However, the title “mass synthesis of cubic silicon nitride succeeded” in a press release in STA Today, a monthly magazine of the Science and Technology Agency of Japan, in June 2000 appears to be a little bit overstated [345]. Nevertheless, 2 years later in September 2002, Ito et al. from Nippon Oils and Fats (NOF) Corporation, Japan, reported on the shock synthesis of γ-Si_3N_4 powders in a multi-gram scale [346]. Applying an explosive compaction technique Ito and co-workers were able to convert up to 60% of α- or β-Si_3N_4 into the spinel phase. Pure γ-Si_3N_4 consisting of spherical agglomerates of nano-crystallites could be obtained by a two step acid treatment with HNO_3 and HF dissolving the copper and α-/β-Si_3N_4 [347]. The abrasive performance of the product was tested in lapping experiments in comparison to diamond powders.

Since shock wave experiments on Si_3N_4 date back to the 1980s, it is surprising that spinel silicon nitride was not discovered earlier. In 1980, Motomo and Setaka shock-compacted pre-compressed α-Si_3N_4 powders at dynamic pressures around 40 GPa using a flyer plate technique. The post-shock phase content varied between 87 and 100% β-Si_3N_4, depending on the nature of the starting powder [348]. The spinel phase was not detected. Flyer plate shock experiments were also reported by Hirai and Kondo in 1994 [349]. Nanocrystalline α-Si_3N_4 powders with mean crystallite sizes of ~70 nm were used as starting materials. The shock conditions were $p = 18$, 30, 40, 46, 50 and 60 GPa and $T \sim 700$, 1000, 1200, 1400, 1500 and 1700 K, respectively. No indications for an unknown phase were found. A summary of all successful syntheses approaches (including the static techniques) to γ-Si_3N_4 is given in Table 7.

3.2.6. *Properties of spinel silicon nitride*

In addition to the structural details of a novel crystalline phase it is also very interesting and useful to examine important physical properties. This is especially true for spinel silicon nitride since the low pressure phases α- and β-Si_3N_4 are used in several areas as structural and functional materials, as was already mentioned above (Section 3.2). Since its discovery in 1999, several studies have been focused on certain properties of γ-Si_3N_4. The results are summarised in the following paragraphs.

3.2.6.1. General properties. Spinel silicon nitride is a colourless solid, or slightly greyish powder if synthesised via shock wave techniques. Porous as well as dense samples have been synthesised by static DAC- and MAP-experiments. A thin amorphous layer was observed at the surface of γ-Si_3N_4 particles using high-resolution TEM [338]. It is assumed that this is an oxide-passivation layer which results from partial hydrolysis at the surface. A similar behaviour is well known from many other non-oxide compounds—especially silicon nitrides. The higher the surface area, i.e. the smaller the particles and the higher the open porosity, the higher the contamination with oxygen, if the material is handled in air. The oxide layer (or the oxygen content) in turn influences nearly all chemical and physical properties.

3.2.6.2. Hardness. The determination of the hardness of almost any material is a challenging task, since a large number of factors, which can influence the results, have to be taken into account. Hardness values of different materials can only be compared with each other, if they are measured under exactly identical conditions.

Nano-hardness measurements with MAP samples are summarised in Table 8 [350]. The examinations were performed with a modified AFM-device using loads between 3 and 5 mN. A cube-corner geometry diamond indentation tip was used. Due to the fact that the investigated γ-Si_3N_4-samples were polycrystalline, porous materials with crystallite sizes around 1 μm (as was evidenced by SEM-images), the obtained hardness values need to be critically considered, especially when they are compared with reference materials like single crystal c-BN or sapphire.

The results of the nano-hardness study show a large variation from measurement to measurement. This indicates that the sample is rather inhomogeneous, which was confirmed by SEM [350,351]. Nevertheless, a trend of decreasing hardness with increasing oxygen content could be identified. Extrapolation to estimate the hardness of oxygen-free γ-Si_3N_4 gave a maximum Vickers hardness value of HV = 43 GPa.

Further studies on the hardness of spinel nitride were reported in the literature. Jiang et al. [352] determined a mean value for the Vickers hardness of 35.31 GPa using a set of 40 indentations in a MAP-derived γ-Si_3N_4-sample, which was obtained from a crystalline precursor (see above) [339]. However, it has to be stressed that no load values were

Table 7
Overview of spinel silcon nitride synthesis reported in literature

Reference	Starting materials	Sample environment	Sample size (mm)	Pressure generation	$p_{\max}$ (GPa)	$T_{\max}$ (°C)	t^{T}_{hold} (s)	Result
[90]	Si, α-, β-, a-Si_3N_4	N_2	n.n.	DAC	15	1800	60–600	γ-Si_3N_4
[357]	a-Si_3N_4/a-B	N_2	n.n.	DAC	20	15–20 W (Nd:YAG laser)	n.n.	Nano-γ-Si_3N_4?/a-Si_3N_4
[339]	α-Si_3N_4/β-Si_3N_4	Pt	2.0 × 3.5	MAP	17 ± 0.5	1800	3600	γ-Si_3N_4 and unidentified phase
[340]	β-Si_3N_4	Pt	1.0 × 1.8	MAP	18	1800	1200	γ-Si_3N_4
[343]	β-Si_3N_4	Pt, Cu	n.n.	Flyer plate	12–115	(1–3) × 10^3	10^{-7} to 10^{-6}	β-Si_3N_4, nano-γ-Si_3N_4
[343]	β-Si_3N_4 (sintered bodies)	–	10 × 12 × 3	Flyer plate	28–150	187	10^{-7} to 10^{-6}	β-Si_3N_4, γ-Si_3N_4 (not recovered)

Table 8
Results of the nano-hardness study in [350]

Material	MAP-γ-Si_3N_4 (∼4 wt.% O)	MAP-γ-Si_3N_4 (∼14 wt.% O)	α-Al_2O_3-single crystal	c-BN-single crystal
Nano-hardness (GPa)	36 (8)	30 (9)	32 (2)	97 (3)

The numbers in brackets give the maximum deviation from the mean value. The oxygen content of the silicon nitride samples was determined with electron probe micro analysis (EPMA).

reported in this study. Tanaka et al. investigated a bulk MAP-γ-Si_3N_4-sample which was obtained from a very pure, crystalline starting material (see above) [340]. For the smallest load of 9.8 mN which was applied in this study, the authors report a hardness of 43 GPa. However, for a load of 981 mN a much lower value of ∼13 GPa was found. The strong load-hardness dependence determined in this report may be caused by a weak grain boundary phase.

In summary, it can be concluded that all the hardness values reported for spinel silicon nitride up to date deviate significantly from each other. Even within each study the variation of the determined values is relatively high. γ-Si_3N_4 is about twice as hard as α- and β-Si_3N_4. However, facing the minimum required pressure of 12 GPa for γ-Si_3N_4 and the extreme *macroscopic* hardness values of about 50 GPa that have been achieved for polycrystalline translucent c-BN at 'only' 7 GPa [353], it is obvious that favourable properties *in addition* to its hardness will determine whether spinel silicon nitride will ever become an industrially relevant material or remain a scientific curiosity.

3.2.6.3. Fracture toughness.

Indentation methods have been developed for the fracture mechanical analysis of advanced ceramics (see e.g. [354]) and are especially useful in cases where the achievable sample size prevents the application of more reliable methods, such as the single-edged notched beam or compact tension samples [355]. In the aforementioned work on polycrystalline translucent c-BN [353], an indentation method has been used to estimate the fracture toughness of the material. In spite of the fact that the synthesis of dense, polycrystalline γ-Si_3N_4 was reported [352,353], no indentation fracture toughness (K_{IC-ICL}) study on pure γ-Si_3N_4 has been published to the present day. In the case of the spinel-sialon γ-Si_2AlON_3, a mean K_{IC-ICL} of ∼4.6 MPa m$^{1/2}$ at indentation loads of 0.5 and 1.0 kg was found [341] (see also Section 8.2).

3.2.6.4. Elastic properties.

In contrast to the hardness and fracture toughness considered above, elastic moduli like the bulk modulus (or compressibility) B or the shear modulus G can be theoretically calculated. Initially, Kroll predicted a compressibility of $B_0(\gamma-Si_3N_4) = 300$ GPa and an elastic shear constant c_{44} of 340 GPa [90]. The analogous values for α- and β-Si_3N_4 were calculated to be $B_0(\beta-Si_3N_4) = 249$ GPa, $B_0(\alpha-Si_3N_4) = 227$ GPa and $c_{44}(\beta-Si_3N_4) = 150$ GPa. These results support the conclusion of the preceding section that the hardness of spinel silicon nitride is about a two times as high as that of the low pressure phases.

Mo et al. calculated a somewhat smaller value of $B_0(\gamma-Si_3N_4) = 280$ GPa and found that for a first derivative with respect to the pressure of $B'_0(\gamma-Si_3N_4) = 3.48$ [89]. Later, Kroll refined his investigations and estimated a shear modulus for polycrystalline spinel silicon nitride of $G_0(\gamma-Si_3N_4) = 261$ GPa [356]. Soignard et al. reported a shear modulus $G_0(\gamma-Si_3N_4) = 258$ GPa [357]. In this publication, a violation of the Cauchy-condition ($c_{44}/c_{12} > 1$) was found, which indicates a strong covalent bond characteristic for γ-Si_3N_4 as well as for other spinel nitrides. More recently, Kocer et al. estimated the bulk and shear modulus of γ-Si_3N_4 with ab initio calculations to be 311 and 349 GPa, respectively [358]. It is to be noted that this high latter value is based on the average of the tetragonal and rhombohedral shear moduli, while the above mentioned values of Kroll and Soignard et al. were an average of the Hashin–Shtrikman bounds.

The shock wave transformation experiments mentioned above were used for a first experimental determination of the elastic properties of γ-Si_3N_4. Fitting the Birch–Murnaghan-equation of state to the derived Hugoniot data, $B_0(\gamma-Si_3N_4) = 300 \pm 10$ GPa and $B'_0(\gamma-Si_3N_4) = 3.0 \pm 0.1$ were found. These results are based on the assumptions that the thermal coefficient of expansion α_V, the heat capacity C_V and the α−β-phase transformation energy ΔE are: $\alpha_V(\gamma-Si_3N_4) \sim \alpha_V(\beta-Si_3N_4) = 1.08\,10^{-5}\,K^{-1}$, $C_V(\gamma-Si_3N_4) \sim C_V(\beta-Si_3N_4) = 98.2$ J/(mol K) and $\Delta E(\beta-Si_3N_4 \rightarrow \gamma-Si_3N_4) \sim \Delta E(\alpha-\text{quartz} \rightarrow \text{stishovite}) = +821$ J/g. With the exception of the last value all results are close to the later experimentally determined data for spinel silicon nitride (see below).

Also static high pressure techniques were used to determine the bulk modulus of γ-Si_3N_4. Soignard et al. derived from DAC-investigations up to 35 GPa the following values: $B_0(\gamma-Si_3N_4) = 308 \pm 5$ GPa and $B'_0(\gamma-Si_3N_4) = 4.0 \pm 0.2$ [357].

Zerr et al. performed similar experiments up to 53 GPa and found: $B_0(\gamma-Si_3N_4) = 290 \pm 5$ GPa and $B'_0(\gamma-Si_3N_4) = 4.9 \pm 0.6$ [350]. The latter value is the highest reported so far for the first pressure derivative of the bulk modulus of γ-Si_3N_4. High values of B'_0 have also been reported for stishovite, the high-pressure modification of silicon oxide SiO_2 ($B'_0 = 5.3$) [359]. This gives evidence of a high anharmonic proportion of the interatomic potential around the octahedral silicon site. Also the larger thermal expansion coefficient of γ-Si_3N_4 is a consequence of this anharmonicity (see below).

Jiang et al. also determined the bulk modulus of γ-Si_3N_4 employing DAC-experiments. They reported the following data: $B_0(\gamma-Si_3N_4) = 317 \pm 11$ GPa and $B'_0(\gamma-Si_3N_4) = 2.3 \pm 2.1$ [360]. It should be stressed that for the latter value the reported deviation is almost as large as the absolute value. A very interesting part of Jiang's investigations is the Rietveld refinement of the diffraction data at high pressure, which provides a more detailed insight into the structural changes of the spinel under compression. As these structural refinements also revealed deviatoric strain above 20 GPa, induced by increasing shear gradients within a solid argon pressure medium, Jiang et al. decided to include only data that had been measured below this pressure. (If shear indeed has a significant influence on the determination of the compressibility of γ-Si_3N_4 by common methods, the investigations of Soignard and Zerr may have to be revised.) The structural refinements of Jiang et al. indicate that the SiN_4 tetrahedron is more compressible than the SiN_6 octahedron within γ-Si_3N_4. This corresponds to a decrease of the anion positional parameter with increasing pressure $\partial u/\partial p < 0$ which was also predicted by Ching et al. [361]. This phenomenon can be understood that upon pressurisation, the nitrogen sublattice starts approaching the ideal cubic packing arrangement at $u = 0.25$ (recall Section 3.2.3). This trend was confirmed by Jiang et al.'s own calculations: The polyhedral bulk moduli $B_0^{\mathrm{oct}} = B_0(SiN_6)$ and $B_0^{\mathrm{tet}} = B_0(SiN_4)$ were found to be 361 and 298 GPa, respectively. The bulk modulus of the spinel structure as a whole was calculated to be 328 GPa. This confirms that the simple average of the polyhedral moduli provides a good prediction for compressibility of the bulk—a fact that had been established previously for oxide spinels by Finger and colleagues [362] and Recio et al. [363].

From the previously mentioned bulk modulus of 290 GPa and the reduced elastic modulus E_r obtained from the load-displacement curves of the nanoindentation measurements, Zerr et al. calculated an estimate for the shear modulus [350]. The result, 148 ± 16 GPa, is more than 100 GPa lower than the theoretical predictions of around 260 GPa [356,357]. However, while the presence of a weak secondary phase such as silicon oxide was considered for the extrapolation to the possible microhardness of a dense, pure γ-Si_3N_4 material, the effect of this phase on the *elastic* response of the sample was not. Assuming that the entire 4% oxygen impurity is represented by amorphous silica, this would correspond to ~10 vol.% of SiO_2. Back-calculating to pure γ-Si_3N_4, it was found that the experimentally determined indentation elastic modulus of $E_r = 303$ GPa would support a shear modulus of up to 241 GPa ($\cong$ Poisson's ratio: $\nu = 0.18$). Final conclusions may be gained by measurements on sufficiently large γ-Si_3N_4 single crystals yet to be synthesised.

3.2.6.5. Thermal stability. The thermal stability of (ceramic) materials is a property which is very important for many applications. Shortly after the discovery of γ-Si_3N_4, first examinations with regard to the decomposition temperature were undertaken. The results of these experiments indicated that the spinel phase is stable at least up to 700 K [90]. Later, in two following studies, it was found that γ-Si_3N_4 is stable up to much higher temperatures.

Sekine and Mitsuhashi examined purified (low oxygen content), shock wave synthesised, γ-Si_3N_4 via DTA/TG with heating rates of 5 and 20 K/min under argon to 1480 and 1520 °C, respectively [364]. A back transformation into β-Si_3N_4 was found to start at ~1400 °C and the γ-to-β-Si_3N_4-enthalpy of transformation was determined to be -29.2 ± 3.5 kJ/mol. This indicates that the thermal stability is much better than that of the SiO_2 high pressure phase stishovite, which is converted into an amorphous phase at ~600 °C [365]. The observed transformation temperature is in the range of the c-BN/h-BN-equilibrium temperature (~1400 °C) [366,367] and also close to the temperature where diamond starts to convert thermally into graphite (~1500 °C) [368].

Jiang et al. investigated MAP-synthesised bulk-γ-Si_3N_4-sample with respect to the thermal stability *in air* at 1150, 1250, 1400 and 1600 °C for 0.5 h [339]. The colourless starting material contained significantly more oxygen as compared to the purified γ-Si_3N_4 used by Sekine. Black, cracked products were obtained. XRD-examinations proved that α- and β-Si_3N_4 are not detectable even after annealing at 1400 °C. At 1600 °C, both low pressure modifications were detectable by XRD in addition to the high pressure phase.

The reported results indicate that spinel silicon nitride is thermally stable up to temperatures, well above those typically occuring in cutting and grinding applications. It remains to be clarified which mechanisms lead to the decomposition and/or transformation of γ-Si_3N_4 and which phases are formed first. A direct, diffusion-less (martensitic) solid state reaction might occur, but dissolution-reprecipitation processes, which are well known for the α-to-β-Si_3N_4-transformation are also possible. Nevertheless, the back-transformation may proceed via more than one mechanism simultaneously.

3.2.6.6. Coefficient of thermal expansion. In order to determine the coefficient of thermal expansion α_{th}, the lattice parameter of γ-Si_3N_4 was measured at temperatures between 25 and 750 °C [351]. Independently and for almost identical temperature ranges of 20–800 °C, Jiang et al. [360] as well as Hintzen et al. (25–725 °C) [369] performed similar studies to determine α_{th}. The results correspond well with each other: while the coefficient of thermal expansion for β-Si_3N_4 [370] increases from 1 to $3 \times 10^{-6}\,\mathrm{K}^{-1}$ within the said temperature range (~300–1000 K), the corresponding values for γ-Si_3N_4 increase from 3 to $6.5 \times 10^{-6}\,\mathrm{K}^{-1}$ which is significantly higher. A recently published theoretical study supports these results [371]. These calculations resulted in $\alpha_{\mathrm{th}}(\gamma-Si_3N_4) = 3.3 \times 10^{-6}$ to $6.5 \times 10^{-6}\,\mathrm{K}^{-1}$ for $T = 300$–1000 K.

Table 9
Predicted thermodynamic properties of spinel Si_3N_4 (after [371])

Property	Symbol	Unit	At 300 K	At 1000 K
Heat capacity	c_p	J/(mol K)	92.72	166.95
Heat capacity	c_v	J/(mol K)	82.39	162.99
Entropy	S	J/(mol K)	−106.4	216.72
Helmholz energy	F	J/mol	−5.13	92.39
Grüneisen parameter	γ_{th}[a]	–	1.19	1.35
Thermal conductivity	λ_{th}	W/mK	60–70	–
Debye temperature	Θ_D[b]	K	1050–1100	

[a] The thermodynamic Grüneisen-parameter is a measure for the volume- and pressure-dependence of the lattice vibrations and for the force which is developed when the material is heated at p: constant definition, γ_{th}: $aVBc_v^{-1}$ [429].

[b] Maximum temperature at which higher vibrational frequencies are not yet activated.

3.2.6.7. Further thermal and thermodynamic properties. Based on a density functional theory approach and using experimentally determined values for the coefficient of thermal expansion α_{th} (see above) Hintzen et al. estimated further thermal and thermodynamic properties [371]. The results are summarised in Table 9.

So far there have been no experimental studies published on the determination of the properties listed in Table 9. For a deeper understanding of the physical properties of spinel silicon nitride and the relations with (chemical) structure and bonding parameters, experimental work would be desirable. The predicted thermal conductivity of γ-Si_3N_4 is significantly lower than the experimentally determined values for β-Si_3N_4 of >100 W/mK [370]. This property is very important for many practical applications.

3.2.6.8. Vibrational spectroscopic properties. The vibrational properties of spinel silicon nitride were experimentally investigated with FTIR- and Raman-spectroscopy as well as theoretically [90,339,371]. The FTIR-spectra show unusually strong variation from sample to sample. The Raman-spectra are in better agreement. Reason for these observations might be the varying oxygen content which is contained on the surface (as a passivation layer) and in the crystal lattice of each sample. In Table 10, the theoretically predicted vibrational modes are compared with the experimental Raman data.

3.2.6.9. NMR spectroscopic properties. In order to gain information about the NMR-spectroscopic properties of γ-Si_3N_4 it was attempted to use MAP-synthesised products for measuring ^{29}Si-nuclear magnetic resonance spectra [372]. Due to the relative small sample amount these experiments were not successful. Based on the shock wave synthesis of larger amounts of γ-Si_3N_4 it was possible to obtain ^{29}Si NMR data [373]. Two resonance signals were identified at -50.0 ± 0.2 and -225.0 ± 0.2 ppm, which can be assigned to the tetrahedrally and octahedrally co-ordinated Si-atoms. The chemical shift of the SiN_4-units correlates very well with the reported δ-values of −46.1 and −48.2 ppm for α-Si_3N_4 and −48.8 ppm for β-Si_3N_4 [373].

Table 10
Calculated and experimentally determined (via Raman spectroscopy) vibrational modes of spinel silicon nitride

Calculated vibrational modes [371]			Observed Raman signals	
Symmetry	Frequency (cm^{-1})	IR/Raman activity	[90]	[339]
T_{2u}	317			
T_{1u}	406 (410)	IR		
T_{2g}	415	R		
E_u	455			
T_{1g}	504			
E_{1g}	522	R	522 (vs)	522 (vs)
T_{1u}	619 (718)	IR		
T_{2u}	631			
T_{2g}	726	R	754 (w)	727 (m)
T_{1u}	729 (764)	IR		
E_u	775			
A_{2u}	782			
T_{1u}	819 (1030)	IR		
T_{2g}	840	R	864 (m)	845 (vs)
A_{2u}	946			
A_{1g}	972	R	979 (w)	979 (m)
–[a]	–	–	1034 (w)	1055 (m)

[a] No signals according to theory.

In contrast, the chemical shift of the SiN_6-units represents a record value, since all reported ^{29}Si NMR δ-values in the Si/C/N/O element system were found to be within the range from −10 ppm for SiC_4-units and −200 ppm for SiO_6-octahedral units in stishovite. The strong high field shift indicates an efficient, electromagnetic shielding of the Si-atoms. The ratio of the integrated signal intensities for the two resonances was 1:2 and corresponds very well with the SiN_4:SiN_6-ratio in the spinel structure.

3.2.6.10. Electronic properties. The electronic structure of a solid is the basis for almost all physical properties. Therefore, the experimental and theoretical examination and description of this structure is extremely important. Theoretical studies on this topic are discussed in Section 7 for binary and ternary phases. One of the most important figures is the band gap, which was predicted to be of direct character with a value of 3.45 eV for γ-Si_3N_4 [89]. This value is identical to the band gap of gallium nitride, a III–V-semiconductor, which is increasingly used for applications in optoelectronic devices such as LEDs and lasers (see e.g. [374]).

First attempts to determine the band gap of γ-Si_3N_4 were focused on measurements of the optical absorption edge. Direct and diffuse reflection techniques were used, which did not give any conclusive result [375]. Scattered light measurements on powdered samples indicated an absorption edge beyond the limits of the spectrometer, i.e. a band gap of $\Delta E > 5.2$ eV [375]. Transmission measurements in a DAC did not show a sharp absorption edge, but based on a thorough analysis of the absorption profile a preliminary value of 3.3 eV was determined [376].

3.3. Amorphous SiN_x

Amorphous silicon nitride phases may be prepared by several different synthetic routes. Bulk amounts are for example available by the diimide process, i.e. by reacting silicon tetrachloride with ammonia followed by annealing at temperatures below 1200 °C, where crystallisation is usually not observed. Other methods include polymer pyrolysis using perhydropolysilazanes (PHPS) as precursors or vapour phase deposition techniques (CVD and PVD) [321].

Amorphous silicon nitride (nano)powders have been used to fabricate sintered silicon nitride bodies. This may provide an opportunity to produce dense sintered α-Si_3N_4 which is usually not obtainable by classical sintering due to the α- to β-transformation [324].

It is well known that silicon nitride—just like silicon dioxide—is an insulating material. It is used in the form of coatings, which are usually deposited via gas-phase techniques, for electronic devices. A detailed discussion is provided, e.g. in [6,377] and will not be treated in this review.

3.4. Post-spinel nitrides

In addition to the spinel phase of silicon nitride discussed above, so called post-spinel phases have been investigated theoretically as well as experimentally. For these structures, co-ordination numbers for the (semi)metal atoms of ≥ 6 have to be taken into account [378]. For the case of silicon nitride, it was predicted by Kroll and von Appen [379] and Tatsumi et al. [380] that at pressures around 160 GPa—which are achievable in the laboratory only with maximum efforts—a phase with $CaTi_2O_4$-like structure should form, which contains SiN_6-prisms and SiN_6-octahedra. In a highlight article published in 1999 Schnick suggested Zr_3N_4 with a distorted Eu_3O_4-type structure and Mg_3NF_3 (defect NaCl) as post-spinel candidates [381]. Recent experimental studies with diamond anvil cells indicate that even at much lower pressures of 34 GPa and at room temperature a fourth crystalline Si_3N_4-phase is formed, which was named δ-Si_3N_4 [316]. The corresponding phase transformation was evidenced by a significant reduction of the number of Raman modes with respect to β-Si_3N_4 (at 38.2 GPa only 10 bands remain) and the appearance of new lines in the diffraction pattern. The crystal structure of δ-Si_3N_4 could not be unambiguously solved using XRD and TEM. A distorted tetragonal structure based on the high pressure modification of the mineral Willemite Zn_2SiO_4 (space group $I\bar{4}3d$) appears to be the best candidate (see also Section 2.4.3). In this case, all silicon atoms are four-co-ordinated by nitrogen. Consequently, δ-Si_3N_4 would *not* be a post-spinel phase rather than a metastable intermediate between β-Si_3N_4 and γ-Si_3N_4. The two remaining possible structures are tetragonal and orthorhombic. They would be more dense than γ-Si_3N_4 and hence post-spinel structures.

Other phases which were taken into closer consideration by Tatsumi et al. were calculated to be *less* dense than γ-Si_3N_4 at ambient conditions, which does not make them very likely candidates [380]. In both theoretical studies however, the $CaTi_2O_4$-type silicon nitride is the most dense phase and was calculated to have the lowest transformation pressure (Table 11).

It is interesting to compare these findings to a theoretical and experimental compression study on β-Ge_3N_4 by Dong et al. (see also Section 4) [382]. Compressing the homologous germanium nitride with β-Si_3N_4 structure to 38 GPa a symmetry reduction $P6_3/m \rightarrow P\underline{6} \rightarrow P3$ is predicted. Formation of a phase corresponding to the previously mentioned δ-Si_3N_4 was not observed, but the development of the Raman shifts of β-Ge_3N_4 and β-Si_3N_4 [383] under pressure are similar.

It seems that β-Ge_3N_4 is more stable than β-Si_3N_4 against compression. An equal trend was found for the wurtzite-to-rocksalt transformation of group 13 nitrides AlN and GaN: while wz−AlN → rs−AlN is reported to occur between 15 [384] and 20 GPa [385], both theoretical and experimental results give values between 31 and 50 GPa for GaN [386]. Corkill et al. pointed out that this is most likely caused by the repulsive potential of the core d-electrons of gallium and germanium, which are absent in the case of aluminium and silicon [387].

3.5. Silicon sub- and hypernitrides

Only very little is known about silicon subnitrides. Originally, Hengge [388] reported on the formation of $(Si_6N)_n$ phases. Kniep et al. [389] recently performed a thorough reexamination and a structure determination of a phase with the composition Si_2N. The material is obtained by a reaction

Table 11
Two sets of theoretically predicted silicon nitride post-spinel phases

Kroll and von Appen [379]				Tatsumi et al. [380]			
Structure type	Space group	V_0^{calc}/V_{spinel}	ΔE (eV/at.)	Structure type	Space group	V_0^{calc}/V_{spinel}	Δ*E* (eV/at.)
β-Si_3N_4	*P*6$_3$/*m*	1.256	−0.16	β-Si_3N_4	*P*6$_3$/*m*	1.26	−0.2
Ni_3Se_4	*C2/m*	0.986	0.27	K_2NiF_4	*I4/mmm*	1.12	1.5
$CaFe_2O_4$	*Pnma*	0.976	0.54	$SrPb_2O_4$, $(MgFe)_2SiO_4$	*Pba*, *Pbnm*	1.06, 1.03	0.2, 0.1
$CaTi_2O_4^*$	*Cmcm*	0.928	0.51	$CaTi_2O_4$	*Cmcm*	0.93	0.5
$p_{eq}(\gamma$-$Si_3N_4 \leftrightarrow *)$ (GPa)		160				210	

of calcium silicide with ammonium bromide:

$$CaSi_2 \rightarrow 4NH_4Br \xrightarrow{350\,^{\circ}C} Si_2N + 2CaBr_2 + 2NH_3 + 5H_2$$

This phase possess a layered structure and may be used as a filler or additive as well as a precursor for other silicon based ceramic materials. At 1000 °C, it forms silicon nitride and elemental silicon:

$$4Si_2N \xrightarrow[\text{Ar or } N_2]{1000\,^{\circ}C} \alpha/\beta{-}Si_3N_4 + 5Si$$

A binary crystalline silicon supernitride is not known, although amorphous nitrogen-rich SiN_x-phases may be formed in suitable CVD and PVD experiments (see Section 3.3). A hypothetical SiN_2-phase with a pyrite-type structure was recently examined by theoreticians [92].

4. Novel germanium nitrides

The germanium(IV) nitrides α-Ge_3N_4 and β-Ge_3N_4 with structures analogous to the corresponding silicon nitrides have been described in literature. Nevertheless, a germanium(II) nitride has been mentioned in papers published in the 1930s [390].

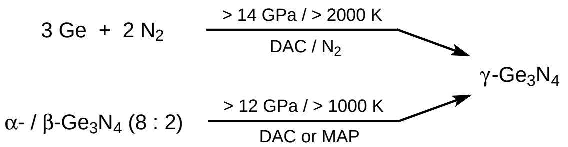

The synthesis of spinel Ge_3N_4 was realised independently at the same time by two research groups, who utilised diamond anvil cells [391,392] and MAP [391].

By analogy to the above described shock wave preparation of spinel silicon nitride it was also possible to generate spinel-Ge_3N_4 via this technique [393]. The static high pressure synthesis of γ-Ge_3N_4 was reproduced by a third group in order to analyse and compare the Raman spectra with the hexagonal α- and β-modifications [394]. In this study the phase transformation was also investigated theoretically. It seems that β-Ge_3N_4 is equally or even more stable against compression than β-Si_3N_4 (see Section 3.4).

5. Tin nitrides

Very few reports on tin nitride phases appeared in the literature. Non-stoichiometric SnN_x tin nitride films have been prepared via CVD [395] and PVD [396] and examined with respect to their electrical and optical characteristics. Compounds with the stoichiometries Sn_3N_2 and Sn_3N_4 were mentioned, but their structure, properties and even existence remained unclear [397].

In 1999, spinel-Sn_3N_4 was synthesised by Scotti et al. by reacting $SnBr_2$ or SnI_4 with potassium amide followed by annealing at 300 °C at ambient pressure [398]:

$$6SnBr_2 + 12KNH_2 \xrightarrow[NH_{3(l)}]{1\,bar/243\,K} \xrightarrow[2\text{–}5\text{ days}]{10^{-5}\,bar/573\,K} Sn_3N_4 + 3Sn + 12KBr$$

The side products KBr and tin were separated by washing with water and concentrated hydrochloric acid. Subsequently, the structure of the first crystalline tin nitride was determined using X-ray as well as neutron diffraction (spinel, space group $Fd3m$, $Z = 8$). A further bulk synthesis of γ-Sn_3N_4 is reported by Shemkunas et al., who employed a solid state metathesis reaction [399]:

$$3SnI_4 + 4Li_3N + xNH_4Cl \xrightarrow[623\,K]{2.5\,GPa} \gamma{-}Sn_3N_4 + 12LiI + xNH_4Cl$$

In this experiment, a piston–cylinder apparatus was used to create the elevated pressure and ammonium chloride acted as a moderator to lower the reaction temperature. Previous synthesis attempts without NH_4Cl led to the formation of tin metal. The γ-Sn_3N_4 produced by this method was reported to have an improved crystallinity with respect the products obtained by Scotti et al., possibly an effect of the high pressure conditions. The smaller lattice constant of $a = 9.0144(1)$ Å (compared to $a = 9.037$ Å determined by Scotti et al.) was attributed to this fact. With the lattice parameter of the third spinel nitride known, one can now recognise the systematic increase from γ-Si_3N_4 ($a = 7.738$ Å) to γ-Ge_3N_4 ($a = 8.213$ Å) further to γ-Sn_3N_4 ($a = 9.0144$ Å) as was to be expected. The high pressure-derived Sn_3N_4 samples exhibit four sharp Raman peaks located at 160, 416, 524, and 622 cm^{-1} and a relatively broad feature at 252 cm^{-1}, all corresponding to the five active modes predicted by theory and shifted towards lower frequencies with respect to those of γ-Ge_3N_4 as a consequence of the higher mass of Sn. The IR-spectrum exhibited only one absorption around 547 cm^{-1} that was assigned to the Sn–N T_{1u} stretching mode. Shemkunas at al. also point out that with hindsight, γ-Sn_3N_4 could be identified within some of the previously reported CVD and PVD layers.

6. Lead nitrides

Interestingly, although there are several binary lead phases known for non-metallic elements such as oxygen and sulphur, very little is known about the binary system Pb/N. This holds also true for the older literature published before 1970 and in the last century. While for many elements including tin (see above) binary phases have been reported, nothing had been published on lead-nitrogen compounds [400]. Later, two binary lead azide phases have been identified: α-$Pb(N_3)_2$ [401] and β-$Pb(N_3)_2$. However, although high pressure syntheses using diamond anvil cells have been attempted [402], to the best of our knowledge there is no lead nitride known to date.

7. Theoretical work on spinel nitrides

Theoretical calculations assisted the experimental work on spinel nitrides right from the beginning: Zerr et al. were able to show why spinel and not willemite II—type is the preferred structure type of Si_3N_4 at high pressures [90]. Shortly after the announcement of the first spinel nitride, several theoreticians focused their work on this new materials family. Binary solids (spinel-Si_3N_4 [89,90,105,358,403], spinel-C_3N_4 [89,105], spinel-Ti_3N_4 [404,105], spinel-Ge_3N_4 [105,382,394,403,405,406], spinel-Sn_3N_4 [105], spinel-Zr_3N_4 [105], spinel-Fe_3N_4 [407]) as well as ternary phases ($MM_2'N_4$ with M, $M' =$ C, Si, Ge, Sn, Ti, Zr) [105,403,404,408] were investigated. Before considering some of these results in more detail, it should be noted that recent experiments suggest that the regular high pressure polymorph of the heavy group 4 nitrides M_3N_4 (M = Zr, Hg) is not spinel-type ([410], see below). In a first work on γ-C_3N_4 and γ-Si_3N_4, Mo et al. found that the compressibility of γ-Si_3N_4 is significantly decreased in comparison to the low pressure modifications and predicted a direct electronic band gap energy $E_{gap} = 3.45\,eV$ that would be interesting for blue solid state emission and other optoelectronic applications [89]. Moreover, it was suggested that the necessary pressure for the formation of γ-Si_3N_4 could be decreased by doping with titanium [89]. Ab initio calculations indicate that spinel-Ti_3N_4, the hypothetical end member of this doping or exchange process, should be more stable than the defect-rocksalt structure previously assumed for this compound [404]. According to these calculations, spinel-Ti_3N_4 would be a semiconductor with a small direct band gap ($E_{gap} = 0.25\,eV$) [105,404]. For the solid solution, series γ-$Si[Si_{1-x}Ti_x]_2N_4$ metallic character is predicted for $x = 0.44$. Similar calculations for γ-Si_3N_4, γ-Ge_3N_4, γ-$SiGe_2N_4$, and γ-$GeSi_2N_4$ indicate that within these solids, E_{gap} could be adjusted between 1.85 and 3.45 eV, and the bulk modulus varies from 258 to 280 GPa. Assuming that the larger germanium atoms preferentially occupy the octahedral lattice sites, the authors point out that especially γ-$SiGe_2N_4$ could be an interesting synthesis target, because it had a high cohesive energy and a direct band gap of $E_{gap} = 1.85\,eV$. However, more recent theoretical results indicate that the occupation of tetrahedral sites is energetically favoured for the germanium atoms, instead of the silicon atoms [408]. HP/HT-experiments in the system Si–Ge–N suggested that γ-Si_3N_4 and γ-Ge_3N_4 are not totally miscible [409]: heating different mixtures of α-Si_3N_4 and β-Ge_3N_4, two *discrete* compositions with a non-integer Si:Ge ratio (i.e. γ-$(Si_xGe_{1-x})_3N_4$ with $x \approx 0.05$ and 0.6) emerged, *irrespective* of the initial ratio of the starting materials. Analysis of the X-ray patterns indicates that the Si^{4+}, normally considered to be the smaller ion, is strongly partitioned into the *octahedral* sites. Synthesis from a precursor with a homogeneous distribution of Si and Ge would be desirable in order to confirm these results.

Elaborate calculations on 20 different γ-$MM_2'N_4$-phases indicate that γ-$TiSi_2N_4$ and γ-$ZrTi_2N_4$ would be unstable. The remaining ternary nitride spinels are—at least with respect to decomposition into the binary spinels—predicted to be stable or metastable. One interesting aspect of these works is the prediction that E_{gap} and the electronic and optical properties vary considerably among these spinels and hence should be tailorable to discrete values by an exact control of the composition. Meanwhile it may be doubted if these calculations are of any relevance for possible applications: In 2002/2003, an experimental work by Zerr and Miehe showed that spinel is *not* the preferred structure type for the nitrogen-rich group 4 compounds: Heating Hf metal at 18 GPa and 2800 K in a DAC with nitrogen pressure medium yielded a novel hafnium(IV) nitride, Hf_3N_4 with thorium phosphide (Th_3P_4) structure [410]. Analogous syntheses of Zr_3N_4 were successful, and a subsequent theoretical investigation of the three thorium phosphide-type nitrides of Ti, Zr and Hf by Kroll predict interesting properties such as potential superconductivity [411]. The Th_3P_4 structure type exhibits an eight-fold co-ordination of the metal atoms by nitrogen, which itself is six-fold co-ordinated ($M^{[8]}/N^{[6]}$; average co-ordination number $N_c \approx 6.86$). The Th_3P_4-type nitrides are therefore significantly more dense than the corresponding spinels, where one-third of the metal atoms are in $M^{[4]}$ co-ordination ($N_c \approx 4.57$). As the regular group 4 mononitrides MN, M = Ti, Zr, Hf crystallise in the rocksalt structure and prefer a $M^{[6]}/N^{[6]}$ configuration, a high pressure modification with $N_c > 6$ is not surprising. It appears that while theoretical methods have grown to a high degree of precision in calculating the properties of a *particular* phase, efficient concepts for actually *predicting the structure type* of the most stable phase in a given system are still under development.

8. Multinary phases

8.1. Si/C/N

Numerous papers on the synthesis, structure and properties of ternary Si/C/N phases have been published [321,412]. A detailed consideration of these solids is beyond the scope of this review article. Badzian reviewed the structure and stability of silicon carbide nitrides, also making some side views on the binary C/N system [413]. According to his literature survey, Si/C/N materials are most commonly found to be amorphous, consisting either of random networks of SiN_4C_{4-x} tetrahedra or are dominated by short-range structural features of Si_3N_4 or SiC, respectively. Many materials synthesised by gas phase processes contain hydrogen as a fourth component, typically in the range of a few at.%, some as low as 0.9 at.%, and show a pronounced variation in thermal stability: some can be deposited at 1700 °C, whereas others decompose at 1400 °C to give Si_3N_4 and SiC.

In comparison to the binary C/N phases, materials in the ternary system Si/C/N and especially in the quaternary system Si/B/C/N may be interpreted as carbon nitrides which are stabilised by Si or Si and B atoms [414–416]. Doing so, the stability depends strongly on avoiding an agglomeration of N-atoms. Any formation of N–N bonds is the first step to the generation of the very stable N_2 molecules, which leads to the decomposition of the solid.

Extremely hard amorphous Si/C/N films with microhardnesses up to 6500 kg/mm^2 have been reported [417]. Crystalline and nanocrystalline Si/C/N phases were also synthesised. Studying the C insertion into α-Si_3N_4 by plasma-deposition, Badzian found a terminal concentration of 6% C. Given the well documented instability of C/N compounds, carbon obviously shows a pronounced preference to act as an *anion* within the Si/C/N system. This means that phases located at or close to the Si_3N_4–SiC tie line are, in general, expected to be more stable than those located between "C_3N_4" and Si_3N_4. Nevertheless, at least two crystalline examples of this type of Si/C/N phases exist: Synthesis and structure elucidation of SiC_2N_4, poly(silylcarbodiimide), Si[N=C=N]$_2$ and Si_2CN_4, silicon nitride carbodiimide, Si_2N_2[N=C=N], was reported in 1997 by Riedel et al. [418].

8.2. Oxide nitrides and sialons

In the quaternary system Si/Al/O/N and related multinary systems, numerous glasses and crystalline phases are known. In the past three decades, especially the so called α- and β-*sialons* have gained significant technological importance, similar to silicon nitride and silicon carbide ceramics [420]. The β-sialons can be formally derived by a coupled substitution of Si–N pairs versus Al–O within the β-Si_3N_4 structure, which gives rise to a solid solution series $Si_{3-x}Al_xO_xN_{4-x}$ [5c,419]. In a similar manner, the α-sialons are derived from α-Si_3N_4, but contain additional metal ions such as Li, Ca, Y or rare earth elements. The phase behaviour of the Si/Al/O/N-system has been examined extensively since the 1960s (see [420] and references therein). While in the vast majority of these publications, only temperature and composition were varied, until 1999 only one research group focused on the behaviour of sialons at high temperature *in combination* with high pressures in the GPa-regime. In the three studies reported, α- and β-sialons were pressurised up to 6 GPa and 1800 °C [421]. While the α-phase was observed to decompose in a complicated manner, forming β-sialon and other unidentified phases, the authors claim that the maximum substitution level x_{max} in β-$Si_{3-x}Al_xO_xN_{4-x}$ decreases dramatically with pressure.

Sekine et al. succeeded in synthesising the first spinel sialon via shock wave high pressure experiments [422]. Independently, we also found spinel sialon phases in the course of our MAP HP/HT experiments [341]. Four β-sialon starting materials were employed, namely β-$Si_{3-x}Al_xO_xN_{4-x}$ with $x = 1.0$, 1.1, 2.0 and 2.1. HP/HT experiments at $p \geq 13$ GPa/$T = 1800$ °C furnished the corresponding spinel sialons. These γ-$Si_{3-x}Al_xO_xN_{4-x}$ were structurally characterised in detail. The lattice parameter shows a linear increase with increasing Al–O-content starting from γ-Si_3N_4 [341,351]. First examinations of the mechanical properties using the Vickers method revealed that the novel ceramic materials are characterised by a hardness significantly higher than that of the low pressure sialon modifications (HV ∼28 GPa at 0.5–1 kg for γ-Si_2AlON_3). The fracture toughness, as determined by the indentation crack length method, was $K_{1c-ICL} = 4.6$ MPa m$^{1/2}$. This is in the upper range of α- and β-sialon ceramics, which have typically fracture toughnesses of 3–4.5 MPa m$^{1/2}$ [341]. Theoretical studies on γ-sialons have been published recently [423–425]. The experimental characterisation of functional properties and a detailed structure analysis (with respect to anion and cation distributions) remains a topic for future research.

Furthermore, numerous very interesting ternary and multinary phases with a large variety of structures have been prepared in the Si/Al/O/N and related element systems. These include, for example, the nitridosilicates examined by Schnick et al. [426]. However, even a very brief discussion on this topic would go beyond the scope of this review.

9. Summary and conclusions

In the past 15 years, numerous researchers have dealt with theoretical as well as experimental investigations of the nitrides of the lightest group 14 elements, the carbon nitrides. Many interesting crystalline phases with useful properties have been predicted to be metastable by several authors and are a promising target for preparative materials scientists and chemists. The majority of the experimental approaches are based on vapour phase deposition routes (CVD and PVD), which furnished many interesting, such as very hard and wear resistant, amorphous and (partially) crystalline coatings. Although there are various reports in the literature claiming the synthesis of a crystalline carbon(IV) nitride C_3N_4, none of the studies provides a comprehensive characterisation of a single phase material. A smaller but increasing part of the literature on carbon nitrides deals with bulk syntheses. Again, several interesting results have been obtained, but a crystalline C_3N_4 phase remains to be identified.

In 1999, three novel nitride phases of the heavier group 14 elements silicon, germanium and tin were discovered. These are the first examples of the new materials class of spinel nitrides. A large number of multinary spinel nitrides can possibly be prepared by high pressure techniques. Theoretical studies and the recent synthesis of the first spinels within the system Si/Al/O/N support this assumption.

The structure and materials properties of the binary spinel nitrides, especially γ-Si_3N_4, were investigated since its discovery. It turned out that this material is about twice as hard as the well known low pressure modifications of silicon nitride. Further hints for promising mechanical properties such as a high thermal stability have been found. Many interesting functional properties (e.g. a metal-to-insulator transition) depending on the solid solution composition, have been predicted theoretically for ternary and multinary phases containing transition elements in addition to Si.

Thus, in summary it can be stated that a fascinating new field in the area of nitrides has been discovered, which gives motivation for further studies dedicated to fundamental questions as well as the exploitation of the novel materials for industrial applications.

Acknowledgements

P. Kroll (Aachen, Germany) is gratefully acknowledged for many useful discussions and for providing the C_3N_4 structure images in Fig. 7. Our research was financially supported by the German Research Foundation (DFG, Bonn, Germany).

References

[1] K. Bewilogua, Sci. Technol. Appl. 52 (1996) 213.
[2] S. Matsumoto, E.-Q. Xie, F. Izumi, Diamond Relat. Mater. 8 (1999) 1175.
[3] T. Malkow, Mater. Sci. Eng. A292 (2001) 112.
[4] S. Muhl, J.M. Mendez, Diamond Relat. Mater. 8 (1999) 1809.
[5] (a) G. Petzow, M. Herrmann, Silicon nitride ceramics, in: M. Jansen (Ed.), Structure and Bonding, vol. 101, High Performance Non-Oxide Ceramics II, Springer-Verlag, Berlin, 2002, p. 47;
(b) M. Herrmann, H. Klemm, C. Schubert, Silicon nitride based hard materials, in: R. Riedel (Ed.), Handbook of Ceramic Hard Materials, Bd. 2, Wiley-VCH, Weinheim, 2000, Kapitel 6, p. 749;
(c) F.L. Riley, J. Am. Ceram. Soc. 83 (2000) 245.
[6] (a) Gmelin Handbook of Inorganic and Organometallic Chemistry, eighth ed., Silicon Suppl. vol. B4, System Si–N, Springer-Verlag, Berlin, 1989;
(b) Gmelin Handbook of Inorganic and Organometallic Chemistry, eighth ed., Silicon Suppl. vol. B5c, Silicon Nitride in Microelectronics and Solar Cells, Springer-Verlag, Berlin, 1991;
(c) Gmelin Handbook of Inorganic and Organometallic Chemistry, eighth ed., Silicon Suppl. vol. B5e, Non-Electronic Applications of Silicon Nitride, SiN_x:, SiN_x:H, Springer-Verlag Berlin, 1994.
[7] L. Escobar-Alarcon, J.E. Villarreal-Barajas, E. Camps, S. Muhl, E. Haro-Poniatowski, S. Romero, B. Salinas, Mater. Sci. Eng. B: Solid-State Mater. Adv. Technol. B90 (2002) 79.
[8] Z.B. Zhou, R.Q. Cui, Q.J. Pang, G.M. Hadi, Z.M. Ding, W.Y. Li, Solar Energy Mater. Solar Cells 70 (2002) 487.
[9] H. Sugimura, Y. Sato, N. Tajima, O. Takai, Surf. Coat. Technol. 142 (2001) 714.
[10] W. Kulisch, C. Popov, L. Zambov, New Diamond Front. Carbon Technol. 11 (2001) 53.
[11] H. Grueger, C. Kunath, PCT Int. Appl. WO 0369327 A1, 21.08.2003.
[12] B.L. Ivanov, L.M. Zambov, G.T. Georgiev, C. Popov, M.F. Plass, W. Kulisch, Chem. Vap. Deposit. 5 (1999) 265.
[13] S. Xu, S. Kumar, Y.A. Li, N. Jiang, S. Lee, J. Phys.: Condens. Matter 12 (2000) L121.
[14] M. Aono, S. Nitta, T. Iwasaki, H. Yokoi, T. Itoh, S. Nonomura, Mater Res. Soc. Symp. Proc.: Low-Dielectr. Const. Mater. V 565 (1999) 291.
[15] Z. Zhang, H. Guo, Y. Xu, W. Zhang, X. Fan, J. Mater. Sci. Lett. 18 (1999) 685.
[16] J. Wei, P. Hing, Z.Q. Mo, Wear 225–229 (1999) 1141.
[17] S. Miyake, Toraiborojisuto 44 (1999) 414 (Chem. Abstr. 131:91178).
[18] Y. Gu, Y. Zhang, X. Chang, Z. Tian, N. Chen, D. Shi, X. Zhang, L. Yuan, Sci. China, Ser. A: Math. Phys. Astron. 43 (2000) 185.
[19] A. Olszyna, A. Sokolowska, J. Konwerska-Hrabowska, M. Psoda, P. Pawlowski, Adv. Sci. Technol. 21 (1999) 35 (Diamond Films, Chem. Abstr. 132:57256).
[20] Y. Gu, Y. Zhang, X. Chang, Z. Tian, D. Shi, X. Zhang, L. Yuan, Wuli 28 (1999) 479 (Chem. Abstr. 132:67992).
[21] T. Komatsu, Jpn. Patent, JP 2000051678 A2, Chem. Abstr. 132:168348 (2000).
[22] J. Martin-Gil, F.J. Martin-Gil, M. Sarikaya, M. Qian, M. Jose-Yacaman, A. Rubio, J. Appl. Phys. 81 (1997) 2555.
[23] L. Hultmann, J. Neidhardt, N. Hellgren, H. Sjöström, J.-E. Sundgren, MRS Bull. 28 (2003) 194.
[24] D.Y. Zhong, G.Y. Zhang, S. Liu, E.G. Wang, Q. Wang, H. Li, X.J. Huang, J. Appl. Phys. 89 (2001) 5939.
[25] A. Karimi, R. Kurt, Surf. Eng. 17 (2001) 99.
[26] X.D. Bai, D. Zhong, G.Y. Zhang, X.C. Ma, S. Liu, E.G. Wang, Y. Chen, D.T. Shaw, Appl. Phys. Lett. 79 (2001) 1552.
[27] B. Schultrich, Fraunhofer Institut für Werkstoff und Strahltechnik (Germany), personal information.
[28] C.-M. Sung, M. Sung, Mater. Chem. Phys. 43 (1996) 1.
[29] W. Schnick, Angew. Chem. 105 (1993) 1649.
[30] C_3N_4 diamantähnlich?, Nachr. Chem. Tech. Lab. 41 (1993) 948 (in German).
[31] J. Haggin, Chem. Eng. News, 25 May 1992, p. 20.
[32] R. Riedel, Adv. Mater. 4 (1992) 759.
[33] P.H. Fang, J. Mater. Sci. Lett. 14 (1995) 536.
[34] V. Odintsov, V. Pepekin, International Annual Conference ICT on Pyrotechnics, vol. 26, 1995, p. 66/1; Chem. Abstr. 123 (1995) 344989.
[35] R.C. DeVries, Diamond Relat. Mater. 4 (1996) 1093.
[36] (a) M.-S. Wong, D. Li, Y.-W. Chung, W.D. Sproul, X. Chu, S.A. Barnett, Int. Patent WO 962591 A1 (1996) (Chem. Abstr. 125 (1996) 225879);
(b) T. Furutaki, O. Matsumoto, Jpn. Patent JP 07133103 A2 (1995) (Chem. Abstr. 123:91119);
(c) A. Tomyama, Jpn. Patent JP 0762543 A2 (1995) (Chem. Abstr. 122:320729);
(d) P.-H. Fang, US Patent US 5405515 A (1995) (Chem. Abstr. 122:294715);
(e) C.M. Lieber, C. Niu, Int. Patent WO 9502709 A2 (1995) (Chem. Abstr. 122:195036);
(f) E.E. Haller, M.L. Cohen, W.L. Hansen, Int. Patent WO 9116196 A1 (1991) (Chem. Abstr. 117:136369);
(g) H. Nishino, S. Ota, S. Morikawa, N. Inoue, T. Fujii, Jpn. Patent JP 10018040 A2;
(h) H. Nishino, S. Ota, N. Inoue, T. Fujii, Jpn. Patent JP 10008257 A2 (1998) (Chem. Abstr. 128:95741);
(i) Y. Utsumi, T. Imai, Jpn. Patent JP 09227298 A2 (1997) (Chem. Abstr. 127:241266);
(j) J. Martin Gil, F. Martin Gil, E. Moran Miguelez, M. Jose Yacaman, Span. Patent ES 2094084 A1 (1997) (Chem. Abstr. 127:180023);
(k) G.S. Tompa, US Patent US 5650201 A (1997) (Chem. Abstr. 127:170248);
(l) D.M. Teter, R.J. Hemley,.World Patent WO 9725273 A1 (1997) (Chem. Abstr. 127:163949);

(m) Y. Utsumi, T. Imai, A. Okamoto, Jpn. Patent JP 09184062 A2 (1997) (Chem. Abstr. 127:115649);
(n) Y. Utsumi, T. Imai, A. Okamoto, Jpn. Patent JP 09175900 A2 (1997) (Chem. Abstr. 127:98768);
(o) E. Baclez, B. Mutel, O. Dessaux, P. Goudmand, World Patent, WO 9710287 A1 (1997) (Chem. Abstr. 126:294421);
(p) J. Kouvetakis, M. Todd. US Patent US 566056 A (1997) (Chem. Abstr. 126:206816);
(q) E. Kamijo, Y. Tani, H. Ohara, M. Tsuijoka, Jpn. Patent JP 2000072415 A2 (2000) (Chem. Abstr. 132:182709);
(r) T. Komatsu, S. Fujiwara, Y. Kakudate, Jpn. Patent JP 2000064045 A2 (2000) (Chem. Abstr. 132:159273);
(s) M.L. Terranova, M. Rossi, V. Sessa, S. Piccirillo, World Patent WO 9961371 A2 (2000) (Chem. Abstr. 132:14676);
(t) K. Aizawa, S. Nita, Jpn. Patent JP 11238684 A2 (1999) (Chem. Abstr. 131:192127);
(u) T. Watanabe, Jpn. Patent JP 11229118 A2 (1999) (Chem. Abstr. 131:192977);
(v) D.M. Hemley, R.J. Hemley, World Patent WO 9725273 A1 (1997) (Chem. Abstr. 127:163949)

[37] (a) I.J. Kim, Kongkae Taeho Kongbo, Korean Patent KR 20000030382 (2000), A 20000605 (Chem. Abstr. 136:138484);
(b) H.-C. Shih, S.-L. Sung, S.-H. Tsai, US Patent, US 6346303 (2002) 12 pp., B1 20020212 (CAPLUS: 2002:114014);
(c) H. Ito, H. Saito, K. Kanda, Jpn. Kokai Tokkyo Koho JP 2002038269 (2002) 7 pp., A2 20020206 (Chem. Abstr. 136:142967);
(d) E. Miyamoto, H. Fukunaga, Y. Inagaki, Eur. Patent Appl. EP 1176469 (2002) 246 pp., A1 20020130 (Chem. Abstr. 136:142582);
(e) K. Kawamura, T. Karaki, K. Yamazaki, Jpn. Kokai Tokkyo Koho JP 2001318504 (2001) 13 pp., A2 20011116 (Chem. Abstr. 135:364497);
(f) J. Oba, Y. Kusano, K. Machida, Jpn. Kokai Tokkyo Koho JP 2001277249 (2001) 10 pp., A2 20011009 (Chem. Abstr. 135:273831);
(g) H. Maruyama, Jpn. Kokai Tokkyo Koho JP 2001276209 (2001) 5 pp., A2 20011009 (Chem. Abstr. 135:262320);
(h) T. Morita, Y. Nishizawa, Jpn. Kokai Tokkyo Koho JP 2001273625 (2001) 10 pp., A2 20011005 (Chem. Abstr. 135:282044);
(i) M. Tozaki, M. Ueda, M. Kobayashi, H. Okita, Jpn. Kokai Tokkyo Koho JP 2001254172 (2001) 8 pp., A2 20010918 (Chem. Abstr. 135:235249);
(j) T. Nonaka, K. Nagino, T. Arai, Jpn. Kokai Tokkyo Koho JP 2001167476 (2001) 10 pp., A2 20010622 (Chem. Abstr. 135:53581);
(k) R. Alexandrescu, V.G. Pugna, A. Crunteanu, S. Petcu, R. Cireasa, I. Morjan, D.C. Dumitras RO 115621 (2000) 5 pp., B1 20000428 (Chem. Abstr. 135:23446);
(l) L.G. Estella, I. Montero Herrero, F. Rueda Sanchez, Span. Patent ES 2138884 (2000) 7 pp., A1 20000116 (Chem. Abstr. 134:319838);
(m) V.S. Veerasamy, US 6222596 (2001) 27 pp., B1 20010424 (Chem. Abstr. 134:303115);
(n) Q. Fu, H. Zhu, C. Cao, H. Wang, J. Jiu, Chin. Patent CN 1256327 (2000) 7 pp., A 20000614 (Chem. Abstr. 134:135526);
(o) J. Karner, M. Pedrazzini, PCT Int. Appl WO 0104379 (2001) 25 pp., A1 20010118 (Chem. Abstr. 134:93670);
(p) S. Chooi, Y. Xu, M.S. Zhou, US Patent US 6165891 (2000) 10 pp., A 20001226 (Chem. Abstr. 134:64986);
(q) X. Chu, B. Zhang, PCT Int. Appl. WO 0072315 (2000) 19 pp., A1 20001130 (Chem. Abstr. 134:12626);
(r) G.-L. Chen, US Patent US 6136421 (2000), 6 Seiten, A 20001024 (Chem. Abstr. 133:304808);
(s) T. Kobayashi, Jpn. Kokai Tokkyo Koho JP 2000285437 (2000) 10 pp., A2 20001013 (Chem. Abstr. 133:316720);
(t) H. Ohara, Jpn. Kokai Tokkyo Koho, JP 2000246371 (2000) 6 pp., A2 20000912 (Chem. Abstr. 133:226287);
(u) K. Fuchigami, K. Wasumi, H. Nakai, J. Shinohara, Jpn. Kokai Tokkyo Koho JP 2000239845 (2000) 4 pp., A2 20000905 (Chem. Abstr. 133:201084);
(v) S. Miyake, S. Takeda, Jpn. Kokai Tokkyo Koho JP 2000219597 (2000) 11 pp., A2 20000808 (Chem. Abstr. 133:142846);
(w) J. Sato, Y. Ogimoto, K. Kojima, M. Hamamoto, H. Katayama, S. Sawamura, Jpn. Kokai Tokkyo Koho JP 2000207723 (2000) 7 pp., A2 20000728 (Chem. Abstr. 133:129077);
(x) H. Sjoestroem, Jpn. Kokai Tokkyo Koho JP 2000161371 (2000) 4 pp., A2 20000613 (Chem. Abstr. 133:21290);
(y) E. Kamijo, Y. Tani, H. Ohara, M. Tsujioka, Jpn. Kokai Tokkyo Koho JP 2000072415 (2000) 9 pp., A2 20000307 (Chem. Abstr. 132:182709);
(z) T. Komatsu, Jpn. Kokai Tokkyo Koho JP 2000051678 (2000) 4 pp., A2 20000222 (Chem. Abstr. 132:168348).

[38] A.Z. Zhuk, V.V. Milyavskii, T.I. Borodina, V.E. Fortov, Khimicheskaya Fizika 21 (2002) 41 (in Russian; Chem. Abstr. 138:59830).

[39] H.W. Roesky, H. Hofmann, Chemiker Zeitung 108 (1984) 231.

[40] See e.g.: D.N. Dhar, Chem. Rev. 67 (1967) 611.

[41] (a) N.S. Zefirov, D.I. Makhon'kov, Russ. Chem. Rev. 49 (1980) 337;
(b) E. Fischer, Z. Chem. 8 (1968) 281.

[42] (a) A. Weidinger, M. Waiblinger, B. Pietzak, T. Almeida Murphy, Appl. Phys. A 66 (1998) 287;
(b) B. Pietzak, M. Waiblinger, T. Almeida Murphy, A. Weidinger, M. Höhne, E. Dietel, A. Hirsch, Chem. Phys. Lett. 289 (1997) 259.

[43] N.V. Riggs, L. Radom, Aust. J. Chem. 38 (1985) 835.

[44] J.J. BelBruno, Chem. Phys. Lett. 270 (1997) 99.

[45] J.J. Belbruno, Z.-C. Tang, R. Smith, S. Hobday, Mol. Phys. 99 (2001) 957.

[46] E. Mayer, Monatsh. Chem. 101 (1970) 834.

[47] T. Sato, A. Narazaki, Y. Kawaguchi, H. Niino, G. Bucher, Angew. Chem. 115 (2003) 5364 (Angew. Chem. Int. Ed. 42 (2003) 5206).

[48] R.P. Subrayan, P.G. Rasmussen, Trends Polym. Sci. 3 (1995) 165.

[49] M.-H. Whangbo, R. Hoffmann, R.B. Woodward, Proc. R. Soc. Lond. A 366 (1979) 23.

[50] M.M. Labes, Mol. Cryst. Liq. Cryst. 171 (1989) 243.

[51] E. Ciganek, C.G. Krespan, J. Org. Chem. 33 (1968) 541.

[52] (a) J. Liebig, Ann. Pharm. (Lemgo Ger.) 10 (1834) 10;
(b) L. Gmelin, Ann. Pharm. Lemgo Ger. 15 (1835) 252.

[53] E.C. Franklin, J. Am. Chem. Soc. 44 (1922) 486.

[54] See e.g.: B.W. Nekrassow, Lehrgang der Anorganischen und Allgemeinen Chemie, VEB Verlag Technik, Berlin, 1956, p. 439.

[55] (a) J. Liebig, Ann. Chem. Pharm. 50 (1844) 337;
(b) J. Liebig, Ann. Chem. Pharm. 73 (1850) 257.

[56] P. Klason, J. Prakt. Chem. 33 (1886) 285.

[57] L. Pauling, J.H. Sturdivant, Proc. Natl. Acad. Sci. U.S.A. 23 (1937) 616.

[58] C.E. Redemann, H.J. Lucas, J. Am. Chem. Soc. 62 (1940) 842.

[59] H. May, J. Appl. Chem. 9 (1959) 340.

[60] A.I. Finkel'shtein, Z. Obshchei Khimii 31 (1961) 1132.

[61] L. Costa, G. Camino, J. Calorimet. Anal. Thermal Thermodyn. Chim. 17 (1986) 213.

[62] A.I. Finkel'shtein, N.V. Spiridonova, Russ. Chem. Rev. 33 (1964) 400.

[63] A.G. Koryakin, V.A. Gal'perin, A.N. Sarbaev, A.I. Finkel'shtein, Z. Organicheskoi Khimii 7 (1971) 972.

[64] N.I. Zhagrova, N.V. Spiridonova, A.I. Finkel'shtein, Z. Prikladnoi Spektroskopii 19 (1973) 153.

[65] N.I. Zhagrova, N.V. Spiridonova, A.I. Finkel'shtein, Z. Prikladnoi Khimii 48 (1975) 452.

[66] R.S. Hosmane, M.A. Rossman, N.J. Leonard, J. Am. Chem. Soc. 104 (1982) 5497.

[67] M. Shahbaz, S. Urano, P.R. LeBreton, M.A. Rossman, R.S. Hosmane, N.J. Leonard, J. Am. Chem. Soc. 106 (1984) 2805.

[68] A.M. Halpern, M.A. Rossman, R.S. Hosmane, N.J. Leonard, J. Phys. Chem. 88 (1984) 4324.

[69] M.A. Rossmann, N.J. Leonard, S. Urano, P.R. LeBreton, J. Am. Chem. Soc. 107 (1985) 3884.
[70] A.A. Grizik, G.P. Borodulenko, Tsvetnye Metally 45 (1972) 41 (Sov. J. Non-Ferrous Met. N.Y. (1972) 45).
[71] N.N. Nurakhmetov, B.A. Beremzhanov, A. Tashenov, R.Sh. Erkasov, Z. Obshchei Khimii 55 (1985) 1460 (J. Gen. Chem. USSR N.Y. (1985) 1300).
[72] G.I. Shtrempler, B. Murzubraimov, K. Rysmendeev, Z. Neorganicheskoi Khimii 27 (1982) 789 (Russ. J. Inorg. Chem. 27 (1982) 442).
[73] N.N. Nurakhmetov, B.A. Beremzhanov, A. Tashenov, R.S. Erkasov, Z. Neorganicheskoi Khimii 32 (1987) 13 (Russ. J. Inorg. Chem. 32 (1987) 6).
[74] M.L. Cohen, Phys. Rev. B 32 (1985) 7988.
[75] A.Y. Liu, M.L. Cohen, Science 245 (1989) 841.
[76] A.Y. Liu, M.L. Cohen, Phys. Rev. B 41 (1990) 10727.
[77] D.M. Teter, MRS Bull. Jpn. 98 (1998) 22.
[78] Y. Guo, W.A. Goddard III, Chem. Phys. Lett. 237 (1995) 72.
[79] T. Hughbanks, Y. Tian, Solid State Commun. 96 (1995) 321.
[80] (a) M. Mattesini, S.F. Matar, J. Etourneau, J. Mater. Chem. 10 (2000) 709;
(b) M. Mattesini, S.F. Matar, A. Snis, J. Etourneau, A. Mavromaras, J. Mater. Chem. 9 (1999) 3151.
[81] (a) J.E. Lowther, Phys. Rev. B 57 (1998) 5724;
(b) J.E. Lowther, Phys. Rev. B 59 (1999) 11683.
[82] F. Weich, J. Widany, Th. Fraunheim, Carbon 37 (1999) 545.
[83] B. Molina, L.E. Sansores, Mod. Phys. Lett. B 13 (1999) 193.
[84] A. Snis, S.F. Matar, Phys. Rev. B 60 (1999) 10855.
[85] D.M. Teter, R.J. Hemley, Science 271 (1996) 53.
[86] J. Ortega, O.F. Sankey, Phys. Rev. B 51 (1995) 2624.
[87] A.Y. Liu, R.M. Wentzcovich, Phys. Rev. B 50 (1994) 10362.
[88] I. Alves, G. Demazeau, B. Tanguy, F. Weill, Solid State Commun. 109 (1999) 697.
[89] S.-D. Mo, L. Ouyang, W.Y. Ching, I. Tanaka, Y. Koyama, R. Riedel, Phys. Rev. Lett. 83 (1999) 5046.
[90] A. Zerr, G. Miehe, G. Serghiou, M. Schwarz, E. Kroke, R. Riedel, H. Fueß, P. Kroll, R. Böhler, Nature 400 (1999) 340.
[91] P. Kroll, R. Hoffmann, J. Am. Chem. Soc. 121 (1999) 4698.
[92] R. Weihrich, V. Eyert, S.F. Matar, Chem. Pys. Lett. 373 (2003) 636.
[93] M. Mattesini, S.F. Matar, Phys. Rev. B: Condens. Matter Mater. Phys 65 (2002) 075110/1.
[94] (a) E. Kim, C. Chen, T. Köhler, M. Elstner, T. Frauenheim, Phys. Rev. Lett. 86 (2001) 652;
(b) E. Kim, C. Chen, T. Köhler, M. Elstner, T. Frauenheim, Phys. Rev. B: Condens. Matter Mater. Phys. 64 (2001) 094107/1.
[95] E. Sandre, C.J. Pickard, C. Colliex, Chem. Phys. Lett. 325 (2000) 53.
[96] M.C. Dos Santos, F. Alvarez, Braz. J. Phys. 30 (2000) 499.
[97] O.J. Ilegbusi, H. Song, J. Mater. Process. Manuf. Sci. 8 (2000) 34 (vol. date: 1999).
[98] S. Stafstrom, Appl. Phys. Lett. 77 (2000) 3941.
[99] E. Kim, C. Chen, Phys. Lett. A 282 (2001) 415.
[100] J.L. Corkill, M.L. Cohen, Phys. Rev. B 48 (1993) 17622.
[101] H. Yoa, W.Y. Ching, Phys. Rev. B 50 (1994) 11231.
[102] A. Reyes-Serrato, D.H. Galvan, I.L. Garzon, Phys. Rev. B 52 (1995) 6293.
[103] J.V. Badding, D.C. Nesting, Chem. Mater. 8 (1996) 535.
[104] S.F. Matar, M. Mattesini, C.R. Acad. Sci. Ser. IIc: Chim. 4 (2001) 255.
[105] W.Y. Ching, S.-D. Mo, I. Tanaka, M. Yoshiya, Phys. Rev. B 63 (2001) 064102/1.
[106] J.L. Zimmerman, R. Williams, V.N. Khabashesku, J.L. Margrave, Nanoletters 1 (2001) 731.
[107] See e.g.: R. Tenne, Chem. Eur. J. 8 (2002) 23.
[108] E. Hernandez, C. Goze, P. Bernier, A. Rubio, Appl. Phys. A: Mater. Sci. Process. A68 (1999) 287.
[109] M. Terrones, P. Redlich, N. Grobert, S. Trasobares, W.-K. Hsu, H. Terrones, Y.-Q. Zhu, J.P. Hare, C.L. Reeves, A.K. Cheetham, M. Rühle, H.W. Kroto, D.R.M. Walton, Adv. Mater. 11 (1999) 655.
[110] D.T. Vodak, K. Kim, L. Iordanidis, P.G. Rasmussen, A.J. Matzger, O.M. Yaghi, Chem. Eur. J. 9 (2003) 4197.
[111] R.Q. Zhang, K.S. Chan, R.S. Zhu, K.L. Han, Phys. Rev. B: Condens. Matter Mater. Phys. 63 (2001) 085419/1.
[112] R. Prasad, P. Chandra, J. Chem. Phys. 114 (2001) 1589.
[113] T. Fujii, J. Muraki, S. Arulmozhiraja, M. Kareev, J. Appl. Phys. 88 (2000) 5592.
[114] R.Q. Zhang, K.L. Han, R.S. Zhu, C.S. Lee, S.T. Lee, Chem. Phys. Lett. 321 (2000) 101.
[115] C.B. Gui, S.H. Yang, Z. Xiong, J.B. Hong, Acta Metall. Sin. (Engl. Lett.) 13 (2000) 145.
[116] Y.-G. Yoon, B.G. Pfrommer, F. Mauri, S.G. Louie, Phys. Rev. Lett. 80 (1998) 3388.
[117] J.A. Tossell, J. Magn. Reson. 127 (1997) 49.
[118] Z. Yong-Ping, G. You-Song, C. Chiang-Rang, T. Zhong-Zhou, S. Dong-Xia, Z. Xin-Gang, Y. Lei, Chin. Phys. 9 (2000) 545 (Chem. Abstr. 133:259537).
[119] G.-M. Rignanese, J.-C. Charlier, X. Gonze, Phys. Rev. B 66 (2002) 205416.
[120] M. Wibbelt, H. Kohl, Ph. Kohler-Redlich, Phys. Rev. B 59 (1999) 11739.
[121] P. Kroll, J. Solid State Chem. 176 (2003) 530.
[122] A. Greiner, Dissertation, TU Darmstadt, 1997 (in German).
[123] R. Riedel, E. Kroke, A. Greiner, A.O. Gabriel, L. Ruwisch, J. Nicolich, P. Kroll, Chem. Mater. 10 (1998) 2964.
[124] J. Kouvetakis, A. Bandari, M. Todd, B. Wilkens, N. Cave, Chem. Mater. 6 (1994) 811.
[125] P. Kroll, Personal information.
[126] E. Kroke, M. Schwarz, P. Kroll, E. Bordon, B. Noll, A. Norman, New J. Chem. 26 (2002) 508.
[127] (a) F. Weich, J. Widany, T. Frauenheim, Phys. Rev. Lett. 78 (1997) 3326;
(b) F. Weich, J. Widany, T. Frauenheim, Carbon 37 (1999) 545.
[128] (a) J.E. Lowther, Phys. Rev. B 57 (1998) 5724;
(b) J.E. Lowther, Phys. Rev. B 59 (1999) 11683.
[129] J.J. Cuomo, P.A. Leary, W. Reuter, D. Yu, M. Frisch, J. Vac. Sci. Technol. 16 (1979) 299.
[130] H.-X. Han, B.J. Feldman, Solid State Commun. 65 (1988) 921.
[131] T. Tomikawa, N. Fujita, Jpn. Patent JP 03240959 A2 (1991) (Chem. Abstr. 116:163119).
[132] J. Viehland, S. Lin, B.J. Feldman, K. Kilgore, M.T. Jones, Solid State Commun. 80 (1991) 597.
[133] Y. Chen, E.G. Wang, F. Chen, L. Guo, Mod. Phys. Lett. B 10 (1996) 567.
[134] L.C. Chen, C.Y. Yang, D.M. Bhusari, K.H. Chen, M.C. Lin, J.C. Lin, T.J. Chuang, Diamond Relat. Mater. 5 (1996) 514.
[135] H.W. Song, F.Z. Cui, X.M. He, W.Z. Li, H.D. Li, J. Phys. Condens. Matter 6 (1994) 6125.
[136] Y. Zhang, Z. Zhou, H. Li, Appl. Phys. Lett. 68 (1996) 634.
[137] P.H. Fang, Appl. Phys. Lett. 69 (1996) 136.
[138] A. Badzian, T. Badzian, Diamond Relat. Mater. 5 (1996) 1051.
[139] C. Niu, Y.Z. Lu, C.M. Lieber, Science 262 (1993) 334.
[140] J. Narayan, J. Reddy, N. Biunno, S.M. Kanetkar, P. Tiwari, N. Parikh, Mater. Sci. Eng. B 26 (1994) 49.
[141] Z.-M. Ren, Y.-C. Du, Z.-F. Ying, F.-M. Li, Y. Zhang, Mater. Res. Symp. Proc. 410 (1996) 313 (Chem. Abstr. 125:228695).
[142] K.M. Yu, M.L. Cohen, E.E. Haller, W.L. Hansen, A.Y. Liu, I.C. Wu, Phys. Rev. B 49 (1994) 5034.
[143] H. Sjoestroem, I. Ivanov, M. Johansson, L. Hultman, J.-E. Sundgren, S.V. Hainsworth, T.F. Page, L.R. Wallenberg, Thin Solid Films 246 (1994) 103.
[144] Y. Tian, X. Ren, D. Yu, J. He, S. Chen, J. Mater. Sci. Technol. 12 (1996) 312.

[145] S. Kumar, K.S.A. Butcher, T.L. Tansley, J. Vac. Sci. Technol. A 14 (1996) 2687.
[146] A. Fernandez, P. Prieto, C. Quiros, J.M. Sanz, J.-M. Martin, B. Vacher, Appl. Phys. Lett. 69 (1996) 764.
[147] L. Wan, R.F. Egerton, Thin Solid Films 279 (1996) 34.
[148] N. Axen, G.A. Botton, H.Q. Lou, R.E. Somekh, I.M. Hutchings, Surf. Coat. Technol. 81 (1996) 262.
[149] S. Veprek, J. Weidmann, F. Glatz, J. Vac. Sci. Technol. A 13 (1995) 2914.
[150] I. Gouzman, R. Brener, A. Hoffman, Thin Solid Films 253 (1994) 90.
[151] H. Xin, C. Lin, H. Xu, S. Zou, X. Shi, X. Wu, H. Zhu, P.L.F. Hemment, Sci. China, Ser. E: Technol. Sci. 39 (1996) 404 (Chem. Abstr. 126 (1997) 22060).
[152] D.-H. Lee, B. Park, J. Korean Phys. Soc. 29 (1996) 686 (Chem. Abstr. 126 (1997) 11716).
[153] Y.S. Gu, L.Q. Pan, X.R. Chang, Z.Z. Tian, J. Mater. Sci. Lett. 15 (1996) 1355.
[154] A.R. Merchant, D.G. McCulloch, D.R. McKenzie, Y. Yin, L. Hall, E.G. Gerstner, J. Appl. Phys. 79 (1996) 6914.
[155] X.W. Su, H.W. Song, F.Z. Cui, W.Z. Lee, H.D. Li, Surf. Coat. Technol. 84 (1996) 388.
[156] K. Ogata, J.F.D. Chubaci, F. Fujimoto, J. Appl. Pys. 76 (1994) 3791.
[157] S.L. Sung, T.G. Tsai, K.P. Huang, J.H. Huang, H.C. Shih, Jpn. J. Appl. Phys. Part 2 37 (1998) L148 (Chem. Abstr. 128:198753).
[158] T. Werninghaus, D.R.T. Zahn, E.G. Wang, Y. Chen, Diamond Relat. Mater. 7 (1998) 52.
[159] Y. Chen, L. Guo, E.G. Wang, J. Cryst. Growth 179 (1997) 515.
[160] D.W. Wu, W. Fan, H.X. Guo, M.B. He, X.Q. Meng, X.J. Fan, Solid State Commun. 103 (1997) 193.
[161] L.C. Chen, D.M. Bhusari, C.Y. Yang, K.H. Chen, T.J. Chuang, M.C. Lin, C.K. Chen, Y.F. Huang, Thin Solid Films 303 (1997) 66.
[162] H.K. Woo, Y. Zhang, S.T. Lee, C.S. Lee, Y.W. Lam, K.W. Wong, Diamond Relat. Mater. 6 (1997) 635.
[163] (a) A. Crunteanu, M. Charbonnier, M. Romand, F. Vasiliu, D. Pantelica, F. Negoita, R. Alexandrescu, Surf. Coat. Technol. 125 (2000) 301;
(b) A. Crunteanu, M. Charbonnier, M. Romand, J. Mugnier, C. Sandu, Appl. Surf. Sci. 168 (2000) 44.
[164] S. Mo, Y. Liu, Y. Yang, Y. Cheng, Guangpuxue Yu Guangpu Fenxi 19 (1999) 734 (Chem. Abstr. 132:211547).
[165] K. Fuchigami, H. Nakai, K. Wazumi, J. Shinohara, Ion Implantation Technolology 98, Int. Conf. Proc. 2, 12 (1999) 974 (Chem. Abstr. 132:173576).
[166] Y. Gu, Y. Zhang, Z. Duan, X. Chang, Z. Tian, D. Shi, L. Ma, X. Zhang, L. Yuan, Zhenkong Kexue Yu Jishu 19 (1999) 93 (Chem. Abstr. 132:211534).
[167] D. Shi, X. Zhang, L. Yuan, Y. Gu, Y. Zhang, Z. Duan, X. Chang, Z. Tian, Zhenkong Kexue Yu Jishu 19 (1999) 77 (Chem. Abstr. 132:211533).
[168] W. Zhang, Z.-H. Zhang, H.-X. Guo, Y. Xu, X.-J. Fan, Wuhan Univ. J. Nat. Sci. 4 (1999) 171 (Chem. Abstr. 132:82066).
[169] (a) Y.S. Gu, Y.P. Zhang, Z.J. Duan, X.R. Chang, Z.Z. Tian, D.X. Shi, L.P. Ma, X.F. Zhang, L. Yuan, Mater. Sci. Eng. A271 (1999) 206;
(b) Y.S. Gu, Y.P. Zhang, Z.J. Duan, X.R. Chang, Z.Z. Tian, N.X. Chen, C. Dong, D.X. Shi, X.F. Zhang, L. Yuan, J. Mater. Sci. 34 (1999) 3117.
[170] A. Crunteanu, R. Alexandrescu, S. Cojocaru, M. Charbonnier, M. Romand, F. Vasiliu, J. Phys. IV, 1, 9 (1999) 419 (Chem. Abstr. 132:40850).
[171] G. Beshkov, St. Georgiev, D.B. Dimitrov, P. Petrov, Thin Film Mater. Devices: Dev. Sci. Technol. Proc. Int. Sch. Condens. Matter Phys. 10 (1999) 551 (Chem. Abstr. 131:330070).
[172] D.J. Benard, C. Linnen, A. Harker, H.H. Michels, J.B. Addison, R. Ondercin, J. Phys. Chem. B 102 (1998) 6010.
[173] (a) S.F. Lim, A.T.S. Wee, J. Lin, D.H.C. Chua, K.L. Tan, J. Mater. Res. 14 (1999) 1153;
(b) S.F. Lim, A.T.S. Wee, J. Lin, D.H.C. Chua, C.H.A. Huan, Chem. Phys. Lett. 306 (1999) 53;
(b) S.F. Lim, A.T.S. Wee, J. Lin, D.H.C. Chua, Surf. Interface Anal. 28 (1999) 212.
[174] M. Trinquecoste, E. Daguerre, L. Couzin, J. Amiell, A. Derre, P. Delhaes, L. Ion, B. Held, Carbon 37 (1999) 457.
[175] Y. Cheng, Y. Wu, J. Chen, X. Qiao, C. Xie, Gongneng Cailiao 30 (1999) 200 (Chem. Abstr. 131:163544).
[176] L.P. Ma, Y.S. Gu, Z.J. Duan, L. Yuan, S.J. Pang, Thin Solid Films 349 (1999) 10.
[177] B. Mitu, G. Dinescu, E. Budianu, A. Ferrari, M. Balucani, G. Lamedica, A. Dauscher, M. Dinescu, Appl. Surf. Sci. 184 (2001) 96.
[178] W. Yu, G.B. Ren, S.F. Wang, L. Han, X.W. Li, L.S. Zhang, G.S. Fu, Thin Solid Films 402 (2002) 55.
[179] A. Yamazaki, S. Ohnita, Y. Watanabe, N. Kitazawa, Y. Nakamura, Surface Modification Technologies XIV, 2001, p. 624.
[180] A. Karimi, R. Kurt, Surface Modification Technologies XIV, 2001, p. 227.
[181] E. Walasek, S. Jonas, T. Stapinski, S. Kluska, A. Czyzewska, Key Eng. Mater. 206–213 (Pt. 1) (2002) 571 (Eur. Ceram. VII).
[182] (a) X.W. Liu, J.H. Lin, C.H. Tseng, H.C. Shih, Mater. Chem. Phys. 72 (2001) 258;
(b) X.W. Liu, C.H. Tseng, J.H. Lin, L.T. Chao, H.C. Shih, Surf. Coat. Technol. 135 (2001) 184.
[183] (a) C. Popov, M.F. Plass, L.M. Zambov, W. Kulisch, Surf. Coat. Technol. 142–144 (2001) 688;
(b) C. Popov, L.M. Zambov, M.F. Plass, W. Kulisch, Thin Solid Films 377–378 (2000) 156.
[184] J. Bulir, M.P. Delplancke-Ogletree, J. Lancok, M. Jelinek, C. Popov, A. Klett, W. Kulisch, Diamond Relat. Mater. 10 (2001) 1901.
[185] J. Qi, C.Y. Chan, I. Bello, C.S. Lee, S.T. Lee, J.B. Luo, S.Z. Wen, Surf. Coat. Technol. 145 (2001) 38.
[186] Y.-P. Zhang, Y.-S. Gu, H.-J. Gao, X.-F. Zhang, Wuli Xuebao 50 (2001) 1396 (in Chinese, Chem. Abstr. 135:230541).
[187] (a) J.-H. Ju, Y.-B. Xia, W.-L. Zhang, L.-J. Wang, W.-M. Shi, Z.-M. Huang, Z.-F. Li, G.-Z. Zeng, D.-Y. Tang, Yingyong Kexue Xuebao 19 (2001) 173 (in Chinese, Chem. Abstr. 135:248813);
(b) J. Ju, Y. Xia, W. Zhang, L. Wang, D. Tang, J. Non-Cryst. Solids 278 (2000) 213.
[188] Y. Zhang, Z. Tian, J. Univ. Sci. Technol. 7 (2000) 282.
[189] T. Ujvari, A. Toth, M. Mohai, J. Szepvolgyi, I. Bertoti, Solid State Ionics 141–142 (2001) 63.
[190] N.M.J. Conway, C. Godet, B. Equer, Mater. Res. Soc. Symp. Proc. 621 (2001) Q1.6.1.
[191] G.-H. Chen, X.-C. Wu, D.-Y. He, Wuji Cailiao Xuebao 16 (2001) 377 (in Chinese, Chem. Abstr. 135:8947).
[192] W. Kulisch, C. Popov, L. Zambov, J. Bulir, M.P. Delplancke-Ogletree, J. Lancok, M. Jeliinek, Thin Solid Films 377–378 (2000) 148.
[193] M.F. Plass, C. Popov, B. Ivanov, S. Mandl, M. Jelinek, L.M. Zambov, W. Kulisch, Appl. Phys. A: Mater. Sci. Process. 72 (2001) 21.
[194] Z. Han, Y. Zhang, Y. Tian, Y. Hu, Y. Kan, X. Zhang, Mater. Sci. Eng. B 78 (2000) 109.
[195] J. Wang, M.A.B. de Moraes, V. Baranauskas, S.F. Durrant, Thin Solid Films 377–378 (2000) 280.
[196] Y. Zhang, Y. Gu, X. Chang, Z. Tian, D. Shi, X. Zhang, L. Yuan, Cailiao Yanjiu Xuebao 14 (2000) 311 (in Chinese, Chem. Abstr. 134:60165).
[197] X. Wu, D. He, B. Wang, H. Yan, G. Chen, Rengong Jingti Xuebao 29 (2000) 275.
[198] Y. Gu, Y. Zhang, Y. Chang, Z. Tian, D. Shi, X. Zhang, L. Yuan, Rengong Jingti Xuebao 29 (2000) 234.
[199] G. Chen, Y. Zhang, H. Zhu, N. Yang, Rengong Jingti Xuebao 29 (2000) 224.

[200] D. Tanaka, Y. Ohkawara, N. Itoh, S. Ohshio, H. Ito, H. Saitoh, Jpn. J. Appl. Phys. Part 1 39 (7A) (2000) 4148.
[201] Y.-P. Zhang, Y.-S. Gu, X.-R. Chang, Z.-Z. Tian, D.-X. Shi, X.-F. Zhang, L. Yuan, Chin. Phys. 9 (2000) 545.
[202] X.W. Liu, S.H. Tsai, L.H. Lee, M.X. Yang, A.C.M. Yang, I.N. Lin, H.C. Shih, J. Vac. Sci. Technol. B 18 (2000) 1840.
[203] V. Krastev, P. Petrov, D. Dimitrov, G. Beshkov, C. Georgiev, I. Nedkov, Surf. Coat. Technol. 125 (2000) 313.
[204] P.Y. Tessier, R. Kre N'guessan, B. Angleraud, V. Fernandez, N. Mubumbila, G. Turban, Surf. Coat. Technol. 125 (2000) 295.
[205] E. D'Anna, M.L. De Giorgi, A. Luches, M. Martino, A. Perrone, A. Zocco, Thin Solid Films 347 (1999) 72.
[206] Y. Tani, Y. Aoi, E. Kamijo, Ion Implant. Technol. 98, Int. Conf. Proc. 2, 12 (1999), 791 (Chem. Abstr. 132:171545).
[207] (a) A.K.M.S. Chowdhury, D.C. Cameron, M.A. Monclus, Thin Solid Films 355–356 (1999) 85;
(b) A.K.M.S. Chowdhury, D.C. Cameron, M.S.J. Hashmi, J.M. Gregg, J. Mater. Res. 14 (1999) 2359.
[208] F.-R. Weber, H. Oechsner, Thin Solid Films 355–356 (1999) 73.
[209] N. Tajima, H. Saze, H. Sugimura, O. Takai, Jpn. J. Appl. Phys. part 2 38 (1999) L1131.
[210] (a) Y. Tani, Y. Aoi, E. Kamijyo, Adv. Sci. Technol.: Surf. Eng. 20 (1999) 211;
(b) Y. Tani, Y. Aoi, E. Kamijo, J. Phys. IV 9 (1999) 1131.
[211] (a) G.L. Chen, Y. Li, J. Lin, C.H.A. Huan, Y.P. Guo, Diamond Relat. Mater. 8 (1999) 1906;
(b) G.L. Chen, Y. Li, J. Lin, C.H.A. Huan, Y.P. Guo, Surf. Interface Anal. 28 (1999) 245;
(c) G.L. Chen, Y. Li, J. Lin, C.H.A. Huan, Y.P. Guo, J. Phys. D: Appl. Phys. 32 (1999) 195.
[212] Y. Peng, T. Ishigaki, S. Horinchi, Appl. Phys. Lett. 73 (1998) 3671.
[213] (a) M. Jelinek, W. Kulisch, M.P. Delplancke-Ogletree, V. Vorlicek, V. Studnicka, D. Chvostova, M. Trchova, J. Sobota, Diamond Relat. Mater. 8 (1999) 1857;
(b) M. Jelinek, Proc. SPIE: Int. Soc. Opt. Eng. 285 (2001) 4397.
[214] X.-C. Xiao, W.-H. Jiang, L.-X. Song, J.-F. Tian, X.-F. Hu, Chem. Phys. Lett. 310 (1999) 240.
[215] Y.G. Li, A.T.S. Wee, C.H.A. Huan, W.S. Li, J.S. Pan, Surf. Interface Anal. 28 (1999) 221.
[216] I. Gouzman, R. Brener, A. Hoffman, J. Vac. Sci. Technol. A 17 (1999) 411.
[217] J. Wei, P. Hing, Z.Q. Mo, Surf. Interface Anal. 28 (1999) 208.
[218] J.-J. Wu, T.-R. Lu, C.-T. Wu, T.-Y. Wang, L.-C. Chen, K.-H. Chen, C.-T. Kuo, T.-M. Chen, Y.-C. Yu, C.-W. Wang, E.-K. Lin, Diamond Relat. Mater. 8 (1999) 605.
[219] D.-W. Wu, D.-J. Fu, X.-W. Mao, M.-S. Yie, Y.-G. Peng, X.-J. Fan, Wuli Xuebao 48 (1999) 904 (Chem. Abstr. 131:105563).
[220] P.-N. Wang, Z. Guo, X.-T. Ying, J.-H. Chen, X.-M. Xu, F.-M. Li, Phys. Rev. B 59 (1999) 13347.
[221] T. Hayashi, A. Matsumuro, M. Muramatsu, M. Kohzak, Adv. Sci. Technol.: Surface Eng. 20 (1999) 541.
[222] G. Fu, W. Yu, S.F. Wang, L. Zhang, X.W. Li, Proc. SPIE: Int. Soc. Opt. Eng. 201 (2001) 4602.
[223] C. Fernandez-Ramos, J.C. Sanchez-Lopez, M. Belin, C. Donnet, L. Ponsonnet, A. Fernandez, Diamond Relat. Mater. 11 (2002) 169.
[224] D.F. Wang, K. Kato, Wear 252 (2002) 210.
[225] S.-I. Aoqui, T. Ohshima, T. Ikegami, K. Ebihara, Sci. Technol. Adv. Mater. 2 (2001) 533.
[226] G. Fanchini, A. Tagliaferro, G. Messina, S. Santangelo, A. Paoletti, A. Tucciarone, J. Appl. Phys. 91 (2002) 1155.
[227] M. Akiyama, I. Alexandrou, M. Chhowalla, G.A.J. Amaratunga, J. Mater. Sci. 36 (2001) 5397.
[228] (a) Y. Setsuhara, Y. Takaki, S. Miyake, M. Kumagai, Y. Sakawa, T. Shoji, Trans. JWRI 30 (2001) 511;
(b) Y. Setsuhara, Y. Sakawa, T. Shoji, M. Kumagai, S. Mikaye, Surf. Coat. Technol. 142–144 (2001) 874.
[229] S.P. Lee, J.B. Kang, Microchem. J. 70 (2001) 239.
[230] F. Le Normand, J. Hommet, T. Szorenyi, C. Fuchs, E. Fogarassy, Phys. Rev. B 64 (2001) 235416/1.
[231] P. Hammer, F. Alvarez, Thin Solid Films 398–399 (2001) 116.
[232] G.-S. Fu, W. Yu, S.-F. Wang, X.-W. Li, L.-S. Zhang, L. Han, Wuli Xuebao 50 (2001) 2263 (in Chinese, Chem. Abstr. 136:106182).
[233] (a) Y.H. Cheng, B.K. Tay, S.P. Lau, X. Shi, X.L. Qiao, J.G. Chen, Y.P. Wu, C.S. Xie, Appl. Phys. A: Mater. Sci. Process. 73 (2001) 341;
(b) Y.H. Cheng, B.K. Tay, S.P. Lau, X. Shi, X.L. Qiao, Z.H. Sun, J.G. Chen, Y.P. Wu, C.S. Xie, Diamond Relat. Mater. 10 (2001) 2137;
(c) Y.H. Cheng, Z.H. Sun, B.K. Tay, S.P. Lau, X.L. Qiao, J.G. Chen, Y.P. Wu, C.S. Xie, Y.Q. Wang, D.S. Xu, S.B. Mo, Y.B. Sun, Appl. Surf. Sci. 182 (2001) 32.
[234] G. Soto, E.C. Samano, R. Machorro, M.H. Farias, L. Cota-Araiza, Appl. Surf. Sci. 183 (2001) 246.
[235] W. Shi, J.D. Wu, J. Sun, H. Ling, Z.F. Ying, X.M. Ding, Z.Y. Zhou, F.M. Li, Appl. Phys. A: Mater. Sci. Process. 73 (2001) 605.
[236] N. Hellgren, N. Lin, E. Broitman, V. Serin, S.E. Grillo, R. Twesten, I. Petrov, C. Colliex, L. Hultman, J.-E. Sundgren, J. Mater. Res. 16 (2001) 3188.
[237] L.F. Niu, S.J. Zhang, D.J. Li, J.K. Zhang, S.G. Yang, Z. Tian, Z.G. Huang, H.L. Zhang, J. Adhes. Sci. Technol. 15 (2001) 1121.
[238] Th. Malkow, I. Arce-Garcia, A. Kolitsch, D. Schneider, S.J. Bull, T.F. Page, Diamond Relat. Mater. 10 (2001) 2199.
[239] J. Bell, Z. Chen, A. Olofinjana, Diamond Relat. Mater. 10 (2001) 2184.
[240] T. Szorenyi, J.-P. Stoquert, J. Perriere, F. Antoni, E. Fogarassy, Diamond Relat. Mater. 10 (2001) 2107.
[241] Y. Aoi, K. Sakurada, K. Ono, E. Kamijo, Key Eng. Mater. 206–213 (2002) 531.
[242] J. Bulir, M. Jelinek, J. Lancok, M. Trchova, K. Jurek, Proc. SPIE: Int. Soc. Opt. Eng. 261 (2001) 4430.
[243] M. Lejeune, O. Durand-Drouhin, K. Zellama, M. Benlahsen, Solid State Commun. 120 (2001) 337.
[244] J. Ning, Y. Lu, H. Zhai, Y. Feng, Y. Wang, Surf. Coat. Technol. 145 (2001) 71.
[245] C. Jama, A. Al Khawwam, A-S. Loir, P. Goudmand, O. Dessaux, L. Gengembre, J. Grimblot, Surf. Interface Anal. 31 (2001) 815.
[246] A. De Graaf, E. Aldea, G. Dinescu, M.C.M. Van De Sanden, Plasma Sources Sci. Technol. 10 (2001) 524.
[247] G. Dinescu, A. De Graaf, E. Aldea, M.C.M. Van De Sanden, Plasma Sources Sci. Technol. 10 (2001) 513.
[248] A. Laskarakis, S. Logothetidis, M. Gioti, Phys. Rev. B: Condens. Matter Mater. Phys. 64 (2001) 125419/1.
[249] O. Bohme, S. Yang, D.G. Teer, J.M. Albella, E. Roman, J. Vac. Sci. Technol. A 19 (2001) 2578.
[250] O. Takai, N. Tajima, H. Saze, H. Sugimura, Surf. Coat. Technol. 142–144 (2001) 719.
[251] Z. Hubicka, M. Sicha, L. Pajasova, L. Soukup, L. Jastrabik, D. Chvostova, T. Wagner, Surf. Coat. Technol. 142–144 (2001) 681.
[252] P. Cao, W.T. Zheng, Z. Jiang, Z. Jin, Z. Mu, C. Dong, Mater. Chem. Phys. 72 (2001) 93.
[253] K. Isao, W. Xu, T. Fujimoto, Surf. Interface Anal. 32 (2001) 74.
[254] B.B. Nayak, B.S. Acharya, S.R. Mohanty, T.K. Borthakur, H. Bhuyan, Surf. Coat. Technol. 145 (2001) 8.
[255] H. Ohta, A. Matsumuro, Y. Takahashi, Mater. Res. Soc. Symp. Proc. 647 (2001) 11.8/1.
[256] D.L. Yu, Y.J. Tian, J.L. He, F.R. Xiao, T.S. Wang, D.C. Li, L. Li, G. Zheng, O. Yanagisawa, J. Cryst. Growth 233 (2001) 303.
[257] O. Durand-Drouhin, M. Lejeune, M. Clin, J. Henocque, Mater. Sci. Semicond. Process. 4 (2001) 335.
[258] J.P. Zhao, Z.Y. Chen, T. Yano, T. Ooie, M. Yoneda, J. Sakakibara, Appl. Phys. A: Mater. Sci. Process. 73 (2001) 97.
[259] C.-T. Kuo, J.-Y. Wu, T.-R. Lu, Mater. Chem. Phys. 72 (2001) 251.
[260] Y.-A. Li, S. Xu, H.-S. Li, W.-Y. Luo, J. Mater. Sci. Lett. 17 (1998) 31.

[261] X.-M. He, W.-Z. Li, H.-D. Li, J. Mater. Res. 12 (1997) 1595.

[262] P. Prieto, C. Quiros, E. Elizalde, A. Fernandez, J.M. Martin, J.M. Sanz, Nucl. Instrum. Methods Phys. Res. Sect. B 122 (1997) 534.

[263] J.Q. Xie, Y. Zheng, J.Y. Feng, Nucl. Instrum. Methods Phys. Res. Sect. B 122 (1997) 239.

[264] R. Alexandrescu, F. Huisken, G. Pugna, A. Crunteanu, S. Petcu, S. Cojocaru, R. Cireasa, I. Morjan, Appl. Phys. A: Mater. Sci. Process. A65 (1997) 207.

[265] W. Lu, K. Komvopoulos, P. Patsalas, C. Charitidis, M. Hioti, S. Logothetidis, Surf. Coat. Technol. 168 (2003) 12.

[266] D.L. Yu, J.L. He, S.M. Liu, D.C. Li, Y.J. Tian, J. Mater. Sci. 38 (2003) 1471.

[267] J. Wie, J. Appl. Phys. 92 (2002) 6525.

[268] I. Zergioti, I. Alexandrou, A. Sfounis, G.A.J. Amaratunga, C. Fotakis, M. Velegrakis, Appl. Surf. Sci. 197–198 (2002) 387.

[269] H. Gruger, D. Selbmann, E. Wolf, A. Leonhardt, J. Mater. Sci. 32 (1997) 2849.

[270] S. Matsumoto, K.K. Chattopadhyay, M. Mieno, T. Ando, J. Mater. Res. 13 (1998) 180.

[271] S. Lopez, H.M. Dunlop, M. Benmalek, G. Tourillon, M.-S. Wong, W.D. Sproul, Surf. Interface Anal. 25 (1997) 315.

[272] C.W. Ong, X.-A. Zhao, Y.C. Tsang, C.L. Choy, P.W. Chan, J. Mater Sci. 32 (1997) 2347.

[273] Final report of BMBF-project “Herstellung, Struktur und Eigenschaften von C-N-Schichten”, project no.: 03N5002, Bonn, 1998.

[274] see e.g. A. Badzian, T. Badzian, W.D. Drawl, R. Roy, Diamond Relat. Mater. 7 (1998) 1519.

[275] A. Badzian, T. Badzian, R. Roy, W. Drawl, Thin Solid Films 354 (1999) 148.

[276] Z. Gong, E.G. Wang, C. Xu, Y. Chen, Thin Solid Films 348 (1999) 114.

[277] M.R. Wixom, J. Am. Ceram. Soc. 73 (1990) 1973.

[278] T. Sekine, H. Kanda, Y. Bando, M. Yokohama, K. Hojou, J. Mater. Sci. Lett. 9 (1990) 1376.

[279] L. Maya, D.R. Cole, E.W. Hagaman, J. Am. Ceram. Soc. 74 (1991) 1686.

[280] M. Todd, J. Kouvetakis, T.L. Groy, D. Chandrasekhar, D.J. Smith, P.W. Deal, Chem. Mater. 7 (1995) 1422.

[281] H. Sjostrom, M. Stafstrom, J.E. Sundgren, Phys. Rev. Lett. 76 (1996) 2205.

[282] D.-W. Wu, M.-B. He, H.-X. Guo, H.-L. Luo, Z.-H. Zhang, D.-J. Fu, X.-J. Fan, Wuli Xuebao 46 (1997) 530 (Chem. Abstr. 127:310499).

[283] H. Montigaud, B. Tanguy, G. Demazeau, S. Courjault, M. Birot, J. Dunogues, C.R. Acad. Sci. Paris Ser. II b, 325 (1997) 229.

[284] M. Kawaguchi, K. Nozaki, Chem. Mater. 7 (1995) 257.

[285] M. Kawaguchi, Y. Tokimatsu, K. Nozaki, Y. Kaburagi, Y. Hishiyama, Chem. Lett. (1997) 1003.

[286] T.-R. Lu, C.T. Kuo, T.M. Chen, Thin Solid Films 308–309 (1997) 126.

[287] J. McMurran, J. Kouvetakis, D.C. Nesting, J.L. Hubbard, Chem. Mater. 10 (1998) 590.

[288] D.C. Nesting, J. Kouvetakis, J.V. Badding, Beitrag zum Tagungsband, in: The 5th NIRIM International Symposium on Advanced Materials (ISAM’98), Tsukuba, Japan, 1–5 March 1998.

[289] V. Iota, C.S. Yoo, H. Cynn, Science 283 (1999) 1510.

[290] Q. Fu, C.-B. Cao, H.-S. Zhu, J. Mater. Sci. Lett. 18 (1999) 1485.

[291] H. Montigaud, B. Tanguy, G. Demazeau, I. Alves, M. Birot, J. Dunogues, Mater. Sci. Forum 325–326 (2000) 31.

[292] H.A. Ma, X.P. Jia, L.X. Chen, P.W. Zhu, M.L. Guo, X.B. Guo, Y.D. Wang, S.Q. Li, G.T. Zhou, G. Zhang, P. Bex, J. Phys.: Cond. Matter 14 (2002) 11269.

[293] S. Courjault, B. Tanguy, G. Demazeau, C.R. Acad. Sci. Ser. IIc: Chim. 2 (1999) 487 (Chem. Abstr. 132:102038).

[294] Q. Fu, J.-T. Jiu, H. Wang, C.-B. Cao, H.-S. Zhu, Chem. Phys. Lett. 301 (1999) 87.

[295] (a) Q. Lu, C. Cao, C. Li, J. Zhang, H. Zhu, X. Kong, X. Duang, J. Mater. Chem. 13 (2003) 1241;
(b) Q. Lu, C. Cao, H. Zhu, Chin. Sci. Bull. 48 (2003) 519;
(c) Q. Lu, C.CaoJ. Zhang, C. Li, H. Zhu, Chem. Phys. Lett. 372 (2003) 469.

[296] Y.-J. Bai, B. Lu, Z.-G. Liu, L. Li, D.-L. Cui, X.-G. Xu, Q.Q.-L. Wang, J. Cryst. Growth 247 (2003) 505.

[297] V.P. Dymont, E.M. Nekrashevich, I.M. Starchenko, Dokl. Nats. Akad. Nauk Belarusi 43 (1999) 48 (Chem. Abstr. 132:155459).

[298] N.N. Thadhani, Adv. Sci. Technol. 15 (Part C) (1999) 407.

[299] Y. Fahmy, T.D. Shen, D.A. Tucker, R.L. Spontak, C.C. Koch, J. Mater. Res. 14 (1999) 2488.

[300] M.D. Alcala, J.C. Sanchez-Lopez, C. Real, A. Fernandez, P. Matteazzi, Diamond Relat. Mater. 10 (2001) 1995.

[301] (a) L.-W. Yin, M.-S. Li, Y.-X. Liu, J.-L. Sui, J.-M. Wang, J. Phys.: Cond. Matter 15 (2003) 309;
(b) L.-W. Yin, M.-S. Li, G. Luo, J.-L. Sui, J.-M. Wang, Chem. Phys. Lett. 369 (2003) 483.

[302] L.-W. Yin, Y. Bando, M.-S. Li, Y.-X. Liu, Y.-X. Qi, Adv. Mater. 15 (2003) 1840.

[303] N. Khabashesku, J. Zimmerman, J. Margrave, Chem. Mater. 12 (2000) 3264.

[304] N. Khabashesku, N. Valery, J. Margrave, Adv. Eng. Mater. 4 (2002) 671.

[305] Z. Zhang, K. Leinenweber, M. Bauer, L.A.J. Garvie, P.F. McMillan, G.H. Wolf, J. Am. Chem. Soc. 123 (2001) 7788.

[306] K.P. Burdina, N.B. Zorov, O.V. Kravchenko, Y.Y. Kuzyakov, J.I. Kim, S.A. Kulinich, Mendeleev Commun. (2000) 207.

[307] V.P. Dymont, I. Smurov, Mater. Sci. Eng. B 82 (2001) 39.

[308] E.G. Gillan, Chem. Mater. 12 (2000) 3906.

[309] E. Kroke, M. Schwarz, V. Buschmann, G. Miehe, H. Fueß, R. Riedel, Adv. Mater. 11 (1999) 158.

[310] (a) E. Ott, E. Ohse, Chem. Ber. 54 (1921) 179;
(b) J. Köhler, E. Meyer, Explosivstoffe, eighth ed., VCH, Weinheim, 1995.

[311] M. Schwarz, diploma thesis, TU Darmstadt, 1998 (in German).

[312] A. Andreyev, M. Akaishi, Koatsuryoku no Kagaku to Gijutsu 10 (2000) 169.

[313] A. Andreyev, M. Akaishi, D. Goldberg, Chem. Phys. Lett. 372 (2003) 635.

[314] (a) T. Komatsu, T. Nakamura, J. Mater. Chem. 11 (2001) 474;
(b) T. Komatsu, J. Mater. Chem. 11 (2001) 799;
(c) T. Komatsu, J. Mater. Chem. 11 (2001) 802.

[315] (a) Gmelin Handbook of Inorganic Chemistry, eighth ed., Silicon Suppl. vol. B3, System Si-C, Springer, Verlag-Berlin, 1986;
(b) W.D.G. Boecker, cfi/Ber. DKG 5 (1997) 244;
(c) K.A. Schwetz, Silicon carbide based hard materials, in: R. Riedel (Ed.), Handbook of Ceramic Hard Materials, Bd. 2, Wiley-VCH, Weinheim, 2000, p. 683.

[316] A. Zerr, Phys. Stat. Sol. (b) 227 (2001) R4.

[317] Y. Cai, A. Zimmermann, S. Prinz, F. Aldinger, J. Mater. Res. 17 (2002) 2765;
(b) Y. Cai, A. Zimmermann, S. Prinz, S. Krämer, F. Philipp, W. Sigle, F. Aldinger, Phil. Mag. Lett. 82 (2002) 553;
(c) Y. Cai, A. Zimmermann, S. Prinz, F. Aldinger, Phys. Stat. Sol. (b) 231 (2002) R4.

[318] S. Saha, M.A. Hossian, M.A. Quader, J. Bangladesh, Acad. Sci. 10 (1986) 13.

[319] A.W. Weimer (Ed.) Carbide, Nitride and Boride Materials, Synthesis and Processing, Chapman & Hall, London, 1997.

[320] B.W. Sheldon, S.C. Danforth (Eds.), Silicon-Based Structural Ceramics: Ceramic Transactions, vol. 42, The American Ceramic Society, 1994.

[321] E. Kroke, Y.-L. Li, C. Konetschny, E. Lecomte, C. Fasel, R. Riedel, Mater. Sci. Eng. R 26 (2000) 97.

[322] J.G. Heinrich, F. Aldinger (Eds.) Ceramic Materials and Components for Engines, Wiley-VCH, Weinheim, 2001.

[323] (a) E. Kroke, Angew. Chem. Int. Ed. 41 (2002) 77;
(b) J.S. Schilling, J. Phys. Chem. Solids 59 (1998) 553;

(c) J.S. Schilling, Hyperfine Interact. 128 (2000) 3;
(d) P.F. McMillan, Curr. Opin. Solid State Mater. Sci. 4 (1999) 171;
(e) J.V. Badding, Annu. Rev. Mater. Sci. 28 (1998) 631;
(f) R.J. Hemley, Annu. Rev. Phys. Chem. 51 (2000) 763;
(g) P.F. McMillan, Nat. Mater. 1 (2002) 19.

[324] Y.-L. Li, Y. Liang, F. Zheng, X.-F. Ma, S.-J. Cui, J. Mater. Res. 15 (2000) 988.

[325] M. Kruger, J.H. Nguyen, Y.M. Li, W.A. Caldwell, M.H. Manghnani, R. Jeanloz, Phys. Rev. B 55 (1997) 3456.

[326] H. Suematsu, M. Mitomo, T.E. Mitchell, J.J. Petrovic, O. Fukunaga, N. Ohashi, J. Am. Ceram. Soc. 80 (1997) 615.

[327] W. Dawai, F. Djun, G. Huaixi, Z. Zhihong, M. Xianquan, F. Xiangung, Phys. Rev. B 56 (1997) 4949.

[328] G. Serghiou, G. Miehe, M. Schwarz, E. Kroke, R. Riedel, Unpublished results.

[329] K. Leinenweber, M. O'Keeffe, M. Somayazulu, H. Hubert, P.F. McMillan, G.H. Wolf, Chem. Eur. J. 5 (1999) 3076.

[330] N. Scotti, W. Kockelmann, J. Senker, S. Trassel, H. Jacobs, Z. Anorg. Allg. Chem. 625 (1999) 1435.

[331] W. Schnick, Angew. Chem. Int. Ed. 38 (1999) 3309.

[332] J. Haines, J.M. Léger, G. Bocquillon, Annu. Rev. Mater. Res. 31 (2001) 1.

[333] R. Metselaar, J. Eur. Ceram. Soc. 18 (1998) 183.

[334] K.E. Sickafus, J.M. Wills, J. Am. Ceram. Soc. 82 (1999) 3279.

[335] (a) W. Heininger, R. Stucka, G. Nagorsen, Z. Naturforsch. B 41 (1986) 702;
(b) W. Heininger, K. Polborn, G. Nagorsen, Z. Naturforsch. B 43 (1988) 875.

[336] K. Köllisch, W. Schnick, Angew. Chem. Int. Ed. 38 (1999) 3309.

[337] See http://www.bgi.uni-bayreuth.de/, European Facility for High-Pressure Research.

[338] M. Schwarz, G. Miehe, A. Zerr, E. Kroke, B. Poe, H. Fuess, R. Riedel, Adv. Mater. 12 (2000) 883.

[339] J.Z. Jiang, K. Stahl, R.W. Berg, D.J. Frost, T.J. Zhou, P.X. Shi, Europhys. Lett. 51 (2000) 62.

[340] I. Tanaka, F. Oba, T. Sekine, E. Ito, A. Kubo, J. Mater. Res. 17 (2002) 731.

[341] M. Schwarz, G. Miehe, A. Zerr, E. Kroke, M. Heck, B. Thybusch, B.T. Poe, I.-W. Chen, R. Riedel, Angew. Chem. Int. Ed. 41 (2002) 789 (Angew. Chem. 114 (2002) 804).

[342] (a) J.R. Asay, M. Shahinpoor (Eds.), High-Pressure Shock Compression of Solids, Springer, New York, 1993;
(b) R.A. Graham, Solids under High-Pressure Shock Compression, Springer, New York, 1993 and literature cited there;
(c) L. Davison, Y. Horie, T. Sekine (Eds.), Shock Compression of Solids V: Shock Chemistry with Applications to Meteorite Impacts, Springer-Verlag, New York, 2003.

[343] (a) T. Sekine, H. He, T. Kobayashi, M. Zhang, F. Xu, Appl. Phys. Lett. 76 (2000) 3706;
(b) H. He, T. Sekine, T. Kobayashi, H. Hirosaki, I. Suzuki, Phys. Rev. B 62 (2000) 11412.

[344] T. Sekine, J. Am. Ceram. Soc. 85 (2002) 113.

[345] See http://www.mext.go.jp/english/news/2000/07/s000702.htm.

[346] K. Ito, Oral presentation on the First International Workshop on Spinel Nitrides and Related Materials, Rüdesheim, Germany, 2002.

[347] T. Sekine, T. Yajima, K. Takahashi, K. Ito, Jpn. Patent Appl. JP 2002-179412a.

[348] M. Mitomo, N. Setaka, J. Mater. Sci. Lett. 16 (1981) 851.

[349] H. Hirai, K. Kondo, J. Am. Ceram. Soc. 77 (1994) 487.

[350] A. Zerr, M. Kempf, M. Schwarz, E. Kroke, M. Göken, R. Riedel, J. Am. Ceram. Soc. 85 (2002) 86.

[351] M. Schwarz, Dissertation, TU Darmstadt, 2003.

[352] J.Z. Jiang, F. Kragh, D.J. Frost, K. Ståhl, H. Lindelov, J. Phys.: Condens. Matter 13 (2001) L515.

[353] T. Taniguchi, M. Akaishi, S. Yamaoka, J. Am. Ceram. Soc. 79 (1996) 547.

[354] R.F. Cook, G.M. Pharr, J. Am. Ceram. Soc. 73 (1990) 787.

[355] B. Sherman, Adv. Eng. Mater 1 (1999) 161.

[356] P. Kroll, B. Eck, R. Dronskowski, Adv. Mater. 12 (2000) 307.

[357] E. Soignard, M. Somayazulu, J. Dong, O.F. Sankey, P.F. McMillan, J. Phys.: Condens. Matter 13 (2001) 557.

[358] C. Kocer, N. Hirosaki, S. Ogata, Phys. Rev. B Condes. Mater. 67 (2003) 035210/1.

[359] B. Li, S.M. Rigden, R.C. Liebermann, Phys. Earth Planet. Interiors 96 (1996) 113.

[360] J.Z. Jiang, H. Lindelov, L. Gerward, K. Ståhl, J.M. Recio, P. Mori-Sanchez, S. Carlson, M. Mezouar, E. Dooryhee, A. Fitch, D.J. Frost, Phys. Rev. B 65 (2002) 16202.

[361] W.Y. Ching, S.-D. Mo, L. Ouyang, Phys. Rev. B 64 (2001) 245110 (1–7).

[362] L.W. Finger, R.M. Hazen, A. Hofmeister, Phys. Chem. Miner. 215–220 (1986) 13.

[363] J.M. Recio, R. Franco, A. Martín Pendás, M.A. Blanco, L. Pueyo, Phys. Rev. B 63 (2001) 184101.

[364] T. Sekine, T. Mitsuhashi, Appl. Phys. Lett. 79 (2001) 2719.

[365] M. Grimsditch, S. Popova, V.V. Brazhkin, R.N. Voloshin, Phys. Rev. B 50 (1994) 12984.

[366] M. Akaishi, T. Satoh, M. Ishii, T. Taniguchi, S. Yamaoka, J. Mater. Sci. Lett. 12 (1993) 1883.

[367] V.L. Solozhenko, V.Z. Turkevich, W.B. Holzapfel, J. Phys. Chem. Solids 103 (1999) 2903.

[368] T. Evans, P.F. James, Proc. R. Soc. Lond. A277 (1964) 260.

[369] H.T.J.M. Hintzen, M.M.R.M. Hendrix, H.J. Wondergem, C. Fang, T. Sekine, G. de With, J. Alloy. Compd. 351 (2003) 40.

[370] R.J. Bruls, H.T. Hintzen, G. de With, R. Metselaar, J.C. van Miltenburg, J. Phys. Chem. Solids 62 (2001) 783.

[371] C.M. Fang, G.A. Wijs, H.T. Hintzen, G. de With, J. Appl. Phys. 93 (2003) 5175.

[372] K. MacKenzie, E. Kroke, M. Schwarz, R. Riedel, Unpublished results.

[373] T. Sekine, M. Tansho, S. Kanzaki, Appl. Phys. Lett. 78 (2001) 3050.

[374] (a) J.L. Pankove, T.D. Moustakis, T.D. Moustakas, Gallium Nitride, Academic Press, New York, 1999;
(b) S. Nakamura, G. Fasol, S.J. Pearton, The Blue Laser Diode: The Complete Story, second ed., Springer-Verlag, Telos, 2000.

[375] E. Kroke, M.Schwarz, S. Karg, R. Schmechel, Unpublished results.

[376] A. Zerr, M. Schwarz, R. Schmechel, R. Kolb, H. von Seggern, R. Riedel, Acta Cryst. A 58 (Suppl.) (2002) C47.

[377] K.B. Sundaram, Silicon Nitride and Silicon Dioxide Thin Insulating Films, The Electrochemical Society, 1999.

[378] A.F. Wells, Structural Inorganic Chemistry, Clarendon Press, Oxford, 1975, Table 13.9, p. 490.

[379] P. Kroll, J. von Appen, Phys. Stat. Sol. (b) 226 (2001) R6.

[380] K. Tatsumi, I. Tanaka, H. Adachi, F. Oba, T. Sekine, J. Am. Ceram. Soc. 85 (2002) 7.

[381] W. Schnick, Angew. Chem. Int. Ed. 38 (1999) 3309.

[382] J. Dong, O.F. Sankey, S.K. Deb, G. Wolf, P.F. McMillan, Phys. Rev. B 61 (2000) 11979.

[383] A. Zerr, G. Miehe, G. Serghiou, M. Schwarz, E. Kroke, R. Riedel, R. Boehler, A new cubic silicon nitride phase, in: M.H. Manghnani, W.J. Nellis, M.F. Nicol (Eds.), Science and Technology of High Pressure, Proceedings of AIRAPT-17, Universities Press, Hyderabad, India, 2000, p. 914.

[384] H. Vollstädt, E. Ito, M. Akaishi, S. Akimoto, O. Fukunaga, Proc. Jpn. Acad. 66B (1990) 7.

[385] S. Uehara, T. Masamoto, A. Onodera, M. Ueno, O. Shimomura, K. Takemura, J. Phys. Chem. Solids 58 (1997) 2093.

[386] S. Limpijumnong, R.L. Lambrecht, Phys. Rev. Lett. 86 (2001) 91.

[387] J.L. Corkill, A. Rubio, M.L. Cohen, J. Phys.: Condens. Matter 6 (1994) 963.

[388] E. Hengge, Z. Anorg. Allg. Chem. 315 (1962) 298.

[389] (a) R. Kniep, J. Haberecht, World Patent WO02/096799A2 (2002);
(b) J. Haberecht, R. Ramlau, H. Borrmann, R. Kniep, Neue Untersuchungen zur Bildung und Charakterisierung von "Si_3N" 10,

Vortragstagung der GDCh-Fachgruppe Festkörperchemie, Münster, 2000;
(c) R. Kniep, Oral presentation on the First International Workshop on Spinel Nitrides and Related Materials, Rüdesheim, Germany, 2002.
[390] H. Bitterer (Ed.), Gmelins Handbuch der anorganischen Chemie, eighth ed., Germanium-Ergänzungsband, System No. 45, VCH, Weinheim, 1958, p. 507.
[391] K. Leinenweber, M. O'Keeffe, M. Somayazulu, H. Hubert, P.F. McMillan, G.H. Wolf, Chem. Eur. J. 5 (1999) 3076.
[392] G. Serghiou, G. Miehe, O. Tschauner, A. Zerr, R. Boehler, J. Chem. Phys. (1999) 4659.
[393] H. He, T. Sekine, T. Kobayashi, K. Kimoto, J. Appl. Phys. 90 (2001) 4403.
[394] S.K. Deb, J. Dong, H. Hubert, P.F. McMillan, O.F. Sankey, Solid State Commun. 114 (2000) 137.
[395] N. Takahashi, K. Terada, T. Takahashi, T. Nakamura, W. Inami, Y. Kawata, J. Electron. Mater. 32 (2003) 268.
[396] T. Lindgren, M. Larsson, S.-E. Lindquist, Solar Energy Mater. Solar Cells 73 (2002) 377.
[397] M. Becke (Ed.), Gmelins Handbuch der anorganischen Chemie, eighth ed., "Zinn", Part C1, VCH, Weinheim, 1972, p. 144.
[398] N. Scotti, W. Kockelmann, J. Senker, S. Traßel, H. Jacobs, Z. Anorg. Allg. Chem. 625 (1999) 1435.
[399] M.P. Shemkunas, G.H. Wolf, K. Leinenweber, W.T. Petuskey, J. Am. Ceram. Soc. 85 (2002) 101.
[400] H. Bitterer (Ed.), Gmelins Handbuch der anorganischen Chemie, eighth ed., "Blei", Part C3, VCH, Weinheim, 1970.
[401] C.H. Choi, H.P. Boutin, Acta Cryst. B25 (1969) 982.
[402] A. Zerr, Personal information.
[403] W.Y. Ching, S.-D. Mo, L. Ouyang, Phys. Rev. B. 63 (2001) 245110/1.
[404] W.Y. Ching, S.-D. Mo, L. Ouyang, I. Tanaka, M. Yoshiya, Phys. Rev. B 61 (2000) 10609.
[405] B. Molina, L.E. Sansores, Int. J. Quant. Chem. 80 (2000) 249.
[406] J.E. Lowther, Phys. Rev. B 62 (2000) 5.
[407] (a) Y.-N. Xu, P. Rulis, W.Y. Ching, J. Appl. Phys. 91 (2002) 7352;
(b) W.Y. Ching, Y.-N. Xu, P. Rulis, Appl. Phys. Lett. 80 (2002) 2904.
[408] J. Dong, J. Deslippe, O. Sankey, E. Soignard, P.F. McMillan, Phys. Rev. B: Condens. Matter 67 (2003) 094104/1.
[409] E. Soignard, M. Somayazulu, H.K. Mao, J.-J. Dong, O.F. Sankey, P.F. McMillan, Solid State Commun. 120 (2001) 237.
[410] A. Zerr, G. Miehe, R. Riedel, Nat. Mater. (2003) 185–189.
[411] P. Kroll, Phys. Rev. Lett. 90 (2003) 125501.
[412] J. Bill, T.W. Kamphowe, A. Muller, T. Wichmann, A. Zern, A. Jalowieki, J. Mayer, M. Weinmann, J. Schuhmacher, K. Muller, J. Peng, H.J. Seifert, F. Aldinger, Appl. Organomet. Chem. 15 (2001) 777.
[413] A. Badzian, J. Am. Ceram. Soc. 85 (2002) 16.
[414] H.-P. Baldus, M. Jansen, Angew. Chem. 109 (1997) 338 (Review).
[415] H.J. Seifert, F. Aldinger, Struct. Bonding: High Performance Non-Oxide Ceram. I (Berlin, Germany) 101 (2002) 1 (Review).
[416] M. Jansen, B. Jaeschke, T. Jaeschke, Struct. Bonding: High Performance Non-Oxide Ceramics I (Berlin, Germany) 101 (2002) 137.
[417] A.G. Varlamov, in: Y. Pauleau, P.B. Barna (Eds.), Protective Coatings and Thin Films, Kluwer Academic Publishers, Dordrecht, The Netherlands, 1997, p. 89.
[418] R. Riedel, A. Greiner, G. Miehe, W. Dressler, H. Fuess, J. Bill, F. Aldinger, Angew. Chem. Int. Ed. 36 (1997) 603.
[419] R. Riedel, Angew. Chem. 114 (2002) 2721.
[420] (a) T. Ekström, M. Nygren, J. Am. Ceram. Soc. 75 (1992) 259;
(b) I.-W. Chen, R. Shuba, in: Encyclopedia of Materials: Science and Technology, Elsevier, Amsterdam, 2001, p. 8471;
(c) C.B. Raju, S. Verma, M.N. Sahu, P.K. Jain, S. Choudary, Indian J. Eng. Mater. Sci. 8 (2001) 36;
(d) F.L. Riley, J. Am. Ceram. Soc. 83 (2000) 246.
[421] (a) M. Haviar, H. Herbertsson, J. Mater. Sci. Lett. 11 (1992) 179;
(b) M. Haviar, H. Herbertsson, J. Mater. Sci. Lett. 12 (1993) 1888;
(c) M. Haviar, Z. Lences, H. Herbertsson, J. Mater. Sci. Lett. 16 (1997) 236.
[422] T. Sekine, H. He, T. Kobayashi, M. Tansho, K. Kimoto, Key Eng. Mater. 237 (2003) 49.
[423] L. Ouyang, W.Y. Ching, Appl. Phys. Lett. 81 (2002) 229.
[424] K. Tatsumi, I. Tanaka, H. Adachi, M. Yoshiya, Phys. Rev. B: Condens. Matter 66 (2002) 165210/1.
[425] J.E. Lowther, M. Schwarz, E. Kroke, R. Riedel, J. Solid Sate Chem. 176 (2003) 549.
[426] (a) W. Schnick, T. Schlieper, H. Huppertz, K. Köllisch, M. Orth, R. Bettenhausen, B. Schwarze, R. Lauterbach, Phosphorus Sulphur Silicon Rel. Elem. 124–125 (1997) 163;
(b) W. Schnick, H. Huppertz, Chem. Eur. J. 3 (1997) 679.
[427] Chemical Abstracts Service (CAS), Online search in the Registry File on 14 September 2003 (search for single component binary compounds).
[428] Inorganic Crystal Structure Database (ICSD), February 2003.
[429] L. Vocaldo, J.P. Poirer, G.D. Price, Am. Mineralogist 85 (2000) 390.
[430] A.P. Purdy, C.F. George, Organometallics 14 (1995) 1076.